MONASH University

NUMERICAL INVESTIGATION OF PARTICLE SEGREGATION IN SANDPILE AND VIBRATED SYSTEMS

BY

Dizhe Zhang

A thesis submitted for the degree of

Doctor of Philosophy

At Monash University in 2019

LABORATORY FOR SIMULATION AND MODELLING OF PARTICULATE SYSTEMS, DEPARTMENT OF CHEMICAL ENGINEERING,

MONASH UNIVERSITY, CLAYTON, VIC 3800, AUSTRALIA

COPYRIGHT NOTICE

This page is intentionally blank

ABSTRACT

Granular matters are widely used in various industries, including food, metallurgy, pharmaceuticals, agricultural, and chemical industries. A common problem for handling granular materials is the segregation that might significantly affect the process efficiency. Segregation is majorly caused by particle property difference including particle size, density and shape. In the past decades, great amounts of efforts have been made to understand the underlying segregation mechanisms. But to date, there are still many questions remaining unanswered for the segregation phenomenon. This thesis presents a comprehensive study of the segregation phenomenon with the help of DEM. Specifically, the study mainly focuses on the segregation happening in two most fundamental processes, piling process and vibrated systems. Four specific components are included to construct a comprehensive investigation of the segregation in these two processes.

Piling process is the most fundamental granular handling process in industries. One of the striking features affecting stockpiles properties are the internal patterns formed by the stratification and segregation processes. Based on the DEM simulations with binary spherical particles of different sizes, it was found that the void-filling mechanism can trigger the stratification and segregation by differentiating the motions of particles with different sizes. The associated

parameter studies were also conducted, and it was concluded that larger size ratio, lower injection height and smaller mass ratio can significantly strengthen the void-filling processes which will further intensify the segregation.

The effect of particle shape on sandpile segregation was further examined by use of ellipsoids. The binary mixtures adopted in the DEM simulations are of two typical types, ellipsoids with different sizes but same shape, and ellipsoids of different shapes but same equivalent size. It was found that a “static avalanche” mechanism dominated the segregation phenomenon. This mechanism illustrates that pre-piled ellipsoids tend to maintain their positions instead of reconstructing the local pattern with upcoming particles. Considering the exact shape effects, it was concluded that less spherical mixtures can result in worse flowability which will consequently weaken the segregation phenomenon.

For vibration-induced segregation, Brazil Nut effect was first investigated, focusing the rising behavior of single large particle under diffident input vibration conditions such as amplitude and frequency. A phase diagram against the vibration conditions were constructed, and it was found that segregation only occurs within a special range of vibration frequency under fixed vibration amplitude. The particle size ratio is also important as it was found that larger size ratio can induce stronger segregation. Considering the effect of intruder shape, it was concluded that the shape of intruder cannot significantly affect the overall bed behavior while

the initial orientation of the ellipsoidal intruder can directly influence its rising time.

The vibration-induced segregation was further studied with cases containing more than one large particles. It was found that the introduction of more large particles significantly extended the range of vibration conditions needed for segregation to be observed. Moreover, a comprehensive study on the particle shape has been made and it was found that the particle shape can influence the segregation behavior by affecting the small particles' percolation behavior.

DECLARATION

This thesis contains no material which has been accepted for the award of any other degree or diploma at any university or equivalent institution and that, to the best of my knowledge and belief, this thesis contains no material previously published or written by another person, except where due reference is made in the text of the thesis.

Signature: ……

Print Name: ……..

Date: ……..

This page is intentionally blank

ACKNOWLEDGEMENTS

I would like to express my sincere gratitude to my research supervisors, Dr Zongyan Zhou and Prof. Aibing Yu, for offering me the opportunity to work on this project and unconditional help during the research. I wish to thank Dr Zongyan Zhou for teaching me how to do scientific research, and for his wise guidance and extraordinary inspiration. This work would not be possible without his help and strong support.

I am very grateful to Australian Research Council and BlueScope Steel for the financial support, and the NCI National Facility for the support in computation. I also wish to thank Monash University, for providing me with the tuition fee scholarship.

I would like to thank my friends and colleagues in SIMPAS (Lab for Computer Simulation and Modelling of Particulate Systems) for providing me with a great deal of help in my studies and fantastic life in Melbourne. I am also grateful to the staffs in the Department of Chemical Engineering at Monash University for their various help during my PhD study.

Thanks also to my parents and my friends for their unconditional love, encouragement and strong support over the past few years.

This page is intentionally blank

TABLE OF CONTENTS

LIST OF FIGURES

Chapter 1 Introduction

1.1 Backgrounds

Granular matters such as particulate materials, powders, grains and bulk solids are widely used in both nature and industry. A better understanding of them will help to optimize various industrial processes, for example the stockpiling and mixing processes in food, pharmaceutical and steel making industries. In recent years, a great amount of work has been done on granular matters to investigate their effects on many industrial issues, of which the segregation issue has been put lots efforts on.

Particle segregation is the phenomenon that dissimilar granular matters tend to segregate when they are mixed together by flowing, shaking or vibrating (Ottino and Khakhar 2000). Sandpile segregation is the most fundamental free surface segregation which demonstrates the granular matters' self-motivated segregation behavior. And vibration-induced segregation can represent the granular segregation with outside motivation. Both of these two phenomena are widely observed in various industries and can cause many practical issues. Therefore in this thesis, in order to better understand the segregation phenomenon in a fundamental view, the research will be mainly conducted in respect to segregation in stockpiles and vibrated systems.

For stockpile segregation, many researchers have investigated the pattern formation and pressure distribution of particulate heaps based on experiments

and simulations. General segregation describes the phenomenon that larger particles tend to segregate at the sided bottom area while small particles can accumulate at the center. It was found that this segregation feature is basically dominated by various particle properties (Lumay et al. 2013) and charging methods (Drahun and Bridgwater 1983). Several basic mechanisms have been proposed to interpret this phenomenon, including percolation, sieving and angle of repose. Stratification as a special case of segregation has also been studied by different researchers. It describes a specific pattern that particles with different physical properties stratified into different layers during the formation of stockpiles. This phenomenon was first investigated using particles of different shapes and it was found that the phenomenon was triggered by difference in repose angles (Makse et al. 1997, Makse 1998, Makse and Herrmann 1998, Cizeau et al. 1999). Recently, Benito et al. (2014) conducted physical experiments to study the pile segregation, and it was claimed that stratification could also be observed with spherical particles.

For vibration-induced segregation, it is also called Brazil-nut effect as it describes the phenomenon that large particles tend to rise within bulk solids of small particles with input vibrations. Previous researches have focused on investigating the triggering mechanisms together with vibration conditions and particle properties (Ahmad and Smalley 1973, Rosato et al. 1986, Rosato et al. 1987, Cooke et al. 1996, Lan and Rosato 1997, Rosato et al. 2002). It was found that vibration

conditions can affect the mechanisms triggering the segregation and differences in particle properties are essential for segregation to occur. Schroter et al. (2006) summarized the physical mechanisms into convection, thermal diffusion and geometric effects, and they also identified the reverse Brazil-nut effect.

As the stockpile segregation and vibration-induced segregation are both industrial issues, experimental and simulating conditions must be set proper to reproduce the real phenomena. Considering the pros and cons of experimental and numerical studies, physical experiments are able to redraw the real flow patterns by using materials and devices comparable to industrial cases, but the computational simulations can demonstrate the force and velocity profiles inside the stockpile which can help to study the inner physics or mechanisms. DEM simulation is a typical and well-accepted method to conduct fundamental studies. It can provide macroscopic information as well as the microscopic profiles within the particle bed. The disadvantage of DEM is that it is largely limited by computational facilities and large-scale computation may cause extreme long time which may not be applicable.

1.2 Research objectives

The general objective of this thesis is to obtain a better understanding of the segregation phenomena occur in stockpiles and vibrated systems with the help of an ellipsoidal DEM model. The detailed objectives are listed below:

1) Review the previous researches related to stockpile segregation and vibration-induced segregation, and understand the proposed physical mechanisms and associated parameter studies. Identify the key gaps based on the previous studies.

2) Propose the mechanism to interpret the stratification and segregation in stockpiles together, and include the cases with spherical cases. Examine the effects of particle size and other charging related parameters.

3) Comprehensively study the effects of shape on size segregation in stockpiles. Explain the reason of shape effects and obtain the results for shape segregation regardless of size difference.

4) Explore the vibration-induced segregation with single large intruder by DEM simulations. Construct a phase diagram in respect to the vibration amplitude and vibration frequency, and explain the vibration effects through microscopic studies. Examine the effects of particle size and intruder shape associated with the vibration conditions.

5) Extend the study of vibration-induced segregation to cases with multiple intruders. Study the effects of intruder numbers together with the vibration conditions and explain the difference compared to single intruder cases. Comprehensively study the shape effects considering the shape of small particles and large intruders separately, explain the effects from both

macroscopic and microscopic views.

1.3 Thesis outline

Based on the previous researches and the several basic objectives above, this thesis is divided into 7 chapters and the outline of each chapter is listed below:

Chapter 1 introduces the general backgrounds about granular segregation occurring in piling process and vibrated systems.

Chapter 2 gives a comprehensive review of the related work that has been done over the past few decades. Several research areas have been mainly reviewed, including basic concepts of segregation, discrete element method, segregation in piling processes, and vibration-induced segregation.

Chapter 3 will mainly discuss the sandpile segregation and stratification with spherical particles. Void-filling mechanism has been further interpreted which can explain the two phenomena together. The associated parameter studies are also conducted including the effects of size ratio, injection height, mass ratio and friction coefficients.

Chapter 4 will discuss the simulations of ellipsoids with the help of an ellipsoidal DEM model. Two types of granular mixtures have been adopted to understand the shape effects. The first one considers the binary mixture of particles with same shape but different sizes, while the other one considers the binary mixture of

particles with different shapes but same size. Therefore the shape effects can be well studied associated with the general size segregation.

Chapter 5 will mainly discuss vibration-induced segregation with binary mixture containing single large particle. As there is only one large particle, the overall bed property will be mainly decided by small particles. Then it can offer a clearer view on the rising pattern of the single intruder. Vibration conditions including vibration amplitude and frequency are well studied with a phase diagram to predict the occurrence of segregation phenomenon. And other parameters including particle size and shape are also investigated which can help understand the real cause of the intruder's rising behavior.

Chapter 6 will upgrade the single intruder cases to vibrated systems containing multiple large intruders. The vibration conditions will be further studied associated with the effects of intruder numbers. On the other hand, the effects of shape will be comprehensively studied considering both the shape of small particles and the shape of large intruders.

Chapter 7 gives an overview of the conclusions obtained from the whole work, and the current limitations with possible further study areas are also discussed.

Chapter 2 Literature review

2.1 Introduction

Particles are major material types observed both in nature and daily life. Many industries have involved large quantities of particles within manufacturing and transporting procedures. As particles are playing an increasingly significant role, a better understanding of particles behavior in both macro and micro views is of great importance.

In recent decades, the advancing in modern science has given rise to the development of particle technology. As one of the most important particle issues, segregation is playing a rather important part in scientific study of particle technology. Lots of research techniques have been applied to scientifically investigate the granular segregation, of which the most important two research methods are physical experiments and numerical simulations. The application of these two methods have cohesively fulfilled the understanding of this granular behavior.

This chapter is divided into 3 parts. In the first part, the basic concepts and fundamental understanding of the segregation phenomenon will be introduced. In the next two parts, the previous researches on stockpile segregation and vibration-induced segregation will be comprehensively reviewed, respectively.

2.2 Basic concepts about granular segregation

2.2.1 Basic mechanisms

The mechanisms of segregation have been studied by different researchers from various views including microscale particle behavior, geometry of reactors, motivating setups and many others. Among all the different interpretations of particle segregation, the triggering factor that makes the segregation occur is the difference of particle properties. Williams (1963, 1967, 1968, 1976) introduced this idea in the study of different types of segregation, it was highlighted that while difference in particle properties can give rise to particle segregation, difference in particle size plays the most important role rather than density, shape, and resilience. Other researchers also fulfilled the parameter study in the last several decades, and this will be further reviewed in other chapters.

Other than considering the difference in physical properties, other researchers extended the research to the fundamental moving patterns inside the segregation behavior. Brown (1939) stated that the segregation of granular materials can be basically divided into two types: free surface segregation, and vibration induced segregation. Drahun and Bridgewater (1983) then studied free surface segregation based on physical experiment. They poured particles onto a rectangular bed which made the particles form a two-dimensional heap. Several parameters including particle shape, size ratio, and density were studied. It was

stated in this research that free surface segregation was triggered by avalanching, inter-particle percolation and particle migration. Another type considers segregation triggered by input vibrations, Williams and Shields (1967) are the first to study particle segregations in a vibrated bed. By conducting physical experiments, they interpreted the vertical segregation patterns of a two-component mixture inside a vibrated channel. It was stated in their research that the direction of vibration was the key factor influencing the amount of segregation, but they didn't give a clear description about the mechanism triggering the vertical segregation. Considering the mechanisms, Huerta and Ruiz-Suarez (2004) tried to give a final explanation onto this phenomenon after several decades of debates, they stated that the vibration-induced segregation is a result of a combination of three mechanisms that inertia, convection and fluidization will cohesively stimulate the behavior under different vibration circumstances.

Ignoring the segregation patterns, the major inside mechanisms of all kinds of segregation have been reviewed by various researchers in the past decades. Based on the work of Mosby (1996), Silva (1997), Salter et al. (2000), and Silva et al. (2000) summarized thirteen mechanisms that can be used to explain different regimes of granular segregation. These mechanisms are: trajectory, air current, rolling, sieving, impact, embedding, angle of repose, push-away, displacement, percolation, fluidization, agglomeration, and concentration driven displacement. But as a specific segregation phenomenon can sometimes the result of several

different mechanisms, Tang and Puri (2004) introduced a new method of classification which highlights several independent mechanisms that individually influence the particles behavior. From his work, based on the role of particle size in the segregation mechanisms, the previous thirteen mechanisms are further divided into four types: trajectory segregation, sieving segregation, fluidization segregation, and agglomeration segregation. Figure 2-1 shows the exact patterns of these four mechanisms.

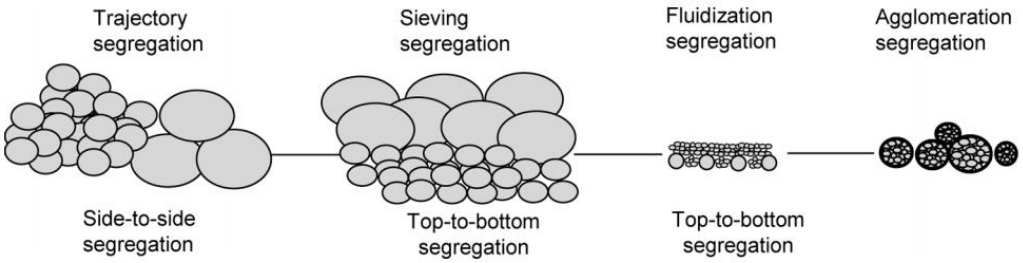

Figure 2-1 Four primary segregation patterns (Tang and Puri 2004)

Side-to-side segregation interprets the segregation pattern that different particles tend to segregate to different direction in horizontal coordinates. It is basically caused by the difference in particle size, shape and density, which differs the moving patterns of different particles. Tang and Puri (2004) believe that trajectory segregation is the key mechanism dominating this type of segregation, and this trajectory theory also contains rolling, embedding, angle of repose, push-away as its special cases.

Trajectory segregation can also be called “inertial segregation”. As shown in Figure

2-2, trajectory segregation describes the nature that larger particles tend to be affected less when air flow is introduced in free fall circumstances. Williams (1976) gave a more detailed explanation on this mechanism. He stated that under the same fluid viscosity conditions, if the large particle is twice larger than the small one, the large particle will therefore travel four times further than the small one. Rolling (shown in Figure 2-3a) also highlights the motion of larger particles that during the formation of heaps, larger particles tend to simply roll down on the top of the free surface which results in the segregation of large particles. The angle of repose mechanism is another one largely observed in heap formation. Other than focusing on the size or density of the particles, this mechanism describes that for particles with different shapes, the difference in angle of repose will cause particles with lower angle of repose to flow over particles with larger ones. This will further results in them to flow down to the heap edge which form the side-to-side segregation pattern, as shown in Figure 2-3c. Different from rolling and angle of repose, embedding (Figure 2-3b) shows a different pattern. While it also describes the moving features of larger or denser particles, it concludes that larger or denser particles might be tracked on the top area inside a sandpile. As this embedding behavior is basically triggered by particles inertia nature and difference in density, it is also named “density segregation”. The last special case of trajectory segregation is push-away segregation, different from all other mechanisms, other than describing the moving pattern when heaps are formed,

push-away interprets the particles behavior when they were poured onto the free surface with initial velocities. It shows that when falling down to the free surface, heavier or larger particles can push away lighter particles which further cause lighter particles to segregate to the heap sides. This contacting feature is mainly decided by the density of particles, as shown in Figure 2-3d.

Figure 2-2 Trajectory Segregation (Silva et al. 2000)

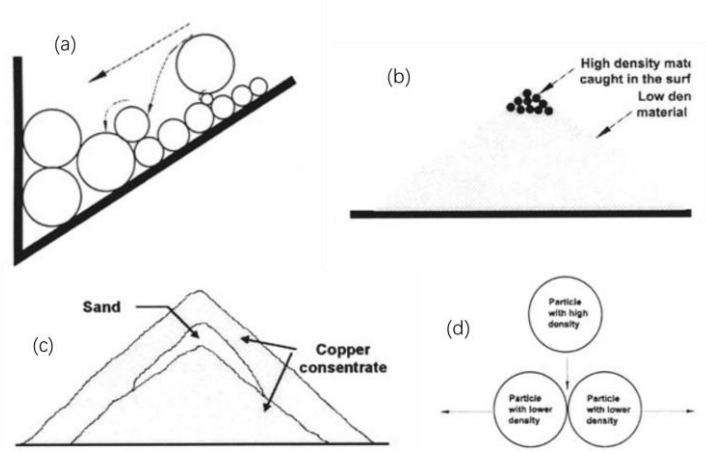

Figure 2-3 Rolling (a), Embedding (b), Angle of repose (c) and Push-away (d) (Silva et al. 2000)

Another well observed type of segregation is the top-to-bottom segregation. Tang and Puri (2004) further divided this type of segregation into two branches: sieving

segregation and fluidization segregation. Based on the segregation pattern and triggering factors, sieving mechanism is mainly focusing on the behavior of small particles while fluidization mechanism interprets the motion of fine particles.

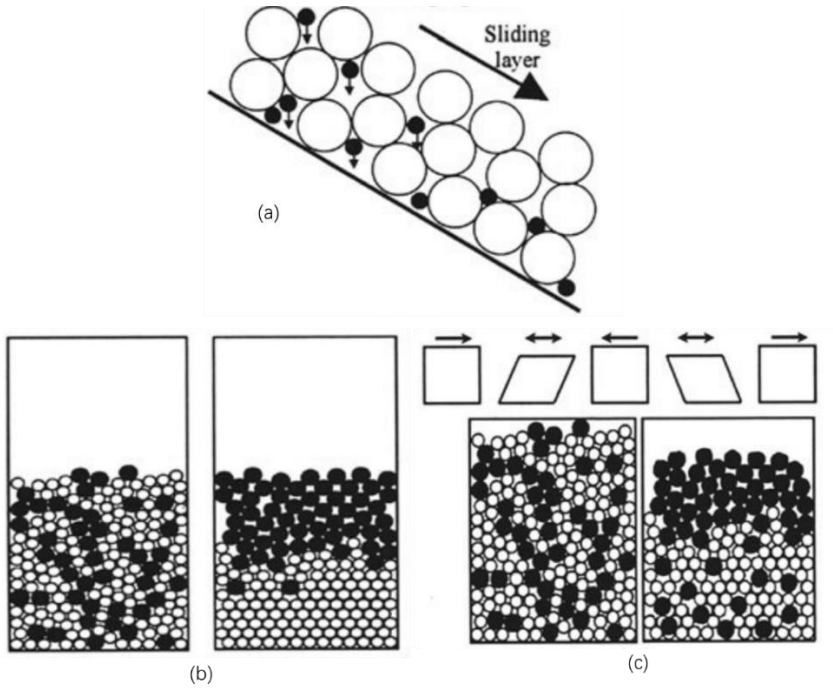

Figure 2-4 Sieving mechanism: Sieving (a), Displacement (b), Percolation (c) (Silva et al. 2000)

Sieving mechanism, as shown in Figure 2-4a, is widely used in free surface flows and vibration cases. This mechanism was first detailed described by Drahun and Bridgwater (1983). As it mainly focuses on the penetrating behavior of small particles, the displacement (shown in Figure 2-4b) and percolation (shown in Figure 2-4c) mechanism can also be regarded as its special cases. Sieving mechanism shows that when granular mixture is poured onto sliding chutes, small

particles tend to fill in the voids inside the flows during the sliding and rolling motion, which will further result in the pattern that small particles segregate at the bottom while larger particles float on top. As a special case of the sieving mechanism, displacement extend this pattern to vibration conditions. Due to size and density difference, vibration gives the granular mixture chance to reconstruct the inside pattern that small particles are able to sink inside the voids and accumulate at the bottom part. Percolation is rather similar to displacement as it also describes small particles sinking motion. The only difference is that percolation can happen without the help of input vibration that it can be motivated by localized shear. Therefore, the general idea about all three type of sieving segregation can be the void-filling nature of small particles when output energy is introduced, no matter it is vibration, chute flow, inertia, or local shear plane. And while another result of this segregation is that large particles will float on top, this type of mechanisms is also called “floating migration” (Salter et al.2000).

Different from the sieving pattern of top-to-bottom segregation, fluidization segregation shows an opposite result while small fine particles are observed to segregate on top. The fluidization mechanism, as shown in Figure 2-5a, is mostly observed pneumatic conveying and fluidized cases. While free falling particles are input, for example, when filling an industrial reactor or container, small fine particles which are fluidizable will largely segregate onto the surface area. This mechanism requires the fine particles to be a fluidizable component which differs

them from the "small particles" which were previously discussed. Another mechanism air current (shown in Figure 2-5b) is similar to this fluidization mechanism. Same to the requirement on the size and density of the fine particles, this air current segregation needs the small particles below 50μm in size to be input within the particle streams. While the air current shows a circulating pattern inside the silo, the fine particles will be carried away from the center zone to the wall area. Both of fluidization and air current segregation are mainly observed in silos and containers where fine particles and air flows are both introduced, which makes the pattern different from the sieving segregation.

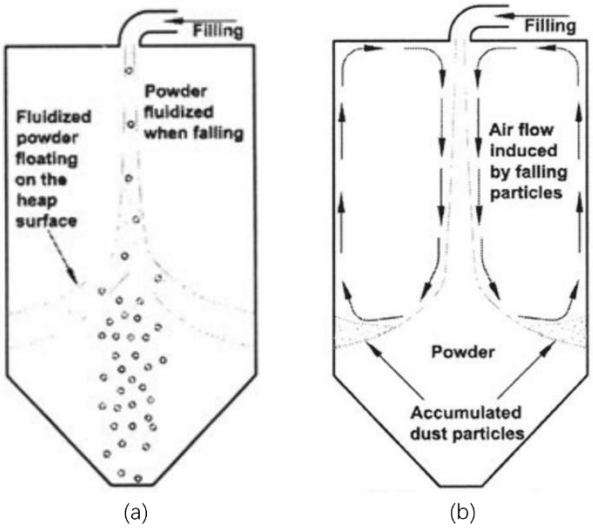

Figure 2-5 Fluidization segregation (a) and Air current segregation (b) (Silva et al. 2000)

The last type of segregation is called agglomeration (shown in Figure 2-6). Different from all other mechanisms, it describes the feature that fine particles may be able to form into large aggregates under certain circumstances.

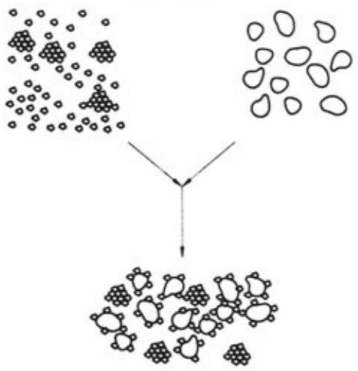

Figure 2-6 Agglomeration segregation (Silva et al. 2000)

2.2.2 Quantification of segregation

The segregation of granular materials is majorly a practical concern of many industry issues. The main purpose of studying this phenomenon is to minimize it and achieve better mixing properties. In order to well illustrate the inside mixing or segregation states, researchers have developed various ways to quantify the segregation phenomenon. In this section, several techniques are reviewed based on their physics fundamentals.

2.2.2.1 Porosity

Porosity ε is one of the most widely used parameter in segregation studies. It is well connected to another parameter packing density ρ, as shown in the following equation:

$$\varepsilon = 1 - \rho \tag{2.1}$$

In the past decades, porosity and packing density have both been largely used in

the characterization in granular mixing problems (Yu et al. 1992, Knight et al. 1993, Zou and Yu 2003, An et al. 2005, An et al.2008). The common understanding of the calculation of packing density ρ is based on the volume of particles and the volume of total packing space, as shown in the following equation:

$$\rho = \frac{v_p}{v_t} \tag{2.2}$$

where v_p is the volume of particles, v_t is the volume of the total packing space. This method gives a general way to directly calculate the packing density, and the porosity can be further calculated based on the relationship between porosity and packing density.

2.2.2.2 Lacey's mixing index

The basic understanding about a perfectly random mixing mixture is the mixture in which the probability to find a particle in a certain position is the same for all positions within the mixture. But the real mixing state of any practical mixture is always between perfect mixing and complete segregation, then it is of great significance to obtain quantification criteria to obtain the degree of mixing segregation.

In the last several decades, over 30 different methods to quantify the mixing states have been proposed, and they have been well summarized by Fan et al. (1970). Among all the methods, Lacey's mixing index (Lacey 1954, Lacey 1997) is one of the most widely used indexes.

Lacey's mixing index, M, describes the degree of mixing and its value is ranged from 0 (completely segregated) to 1 (perfect mixing). This method is based on the general understanding of measuring the statistical variation of target particle's volume fraction ($\frac{the\ volume\ of\ target\ particles}{the\ volume\ of\ the\ sample\ square}$) among its samples, where S stands for the standard deviation of the drawn samples, and S^2 can be referred as the variance. Then the mixing index, M is calculated based on the following equation:

$$M = \frac{{S_0}^2 - S^2}{{S_0}^2 - {S_r}^2} \tag{2.3}$$

where ${S_0}^2$ is the variance considering a completely segregated mixture, and ${S_r}^2$ is the variance for a perfect random mixture. Furthermore, ${S_0}^2$ and ${S_r}^2$ are also given, respectively,

$${S_0}^2 = P(1-P) \tag{2.4}$$

$${S_r}^2 = \frac{P(1-P)}{n} \tag{2.5}$$

where P is the overall target particles fraction for the granular mixture, and n is the number of samples that the whole mixture is divided into.

Lacey's mixing index can be well used for various granular mixtures ranging from mono-size mixtures to multi-size mixtures. But this method can be largely affected by the sampling method, so it may not be practically convenient when considering cases of granular mixture with abnormal shapes.

2.2.2.3 Coordination number based mixing index

Coordination number was first introduced by Smith et al. (1931). This method accurately defines the number of particles that are contacting with the target particle, and it is also regarded as one of the most significant parameters characterizing the mixing of granular materials. In detail, the contact of two particles is tested based on the shortest distance between the surfaces of the two particles. The critical value for the gap distance is sometimes varied due to different purposes, but the general understanding is 5% of the target particle's diameter. The use of coordination number can overcome several troubles that bothers the volume fraction based mixing index. One of the most important advantage is that different from the calculation of volume fraction, coordination number doesn't need the sampling step which makes it better for particles with abnormal shapes.

With the help of coordination number and Lacey's mixing index (Lacey 1954), a coordination number based mixing index was introduced by Chandratillede et al. (2012), and it is also known as particle-scale mixing index (PSMI). The coordination number based mixing index, M_c, is calculated from the following equation, which has the same form as Lacey's mixing index:

$$M_c = \frac{{\sigma_0}^2 - \sigma^2}{{\sigma_0}^2 - {\sigma_r}^2} \tag{2.6}$$

where σ^2 is the variance of particle fraction p_i, whose calculation will be talked

in detail in the following paragraph; $\sigma_0{}^2$ is the variance considering a completely segregated mixture, and $\sigma_r{}^2$ is the variance for a perfect random mixture.

For a binary granular mixture containing type-A particles and type-B particles, when type-A particles are the studied target particles. The particle fraction p_i is defined as the ratio of the number of contacts with type-A particles for target particle i against the total contacts for particle i. The calculation is shown as follows:

$$p_i = \frac{C_{A(A)} + 1}{C_i + 1} \tag{2.7}$$

Where $C_{A(A)}$ is the number of contacts with type-A particles for target particle i, and C_i is the total number of contacts for particle i.

Similar to Lacey's mixing index, the calculation of $\sigma_0{}^2$ and $\sigma_r{}^2$ is based on the following equations:

$$\sigma_0{}^2 = P(1-P) \tag{2.8}$$

$$\sigma_r{}^2 = \frac{P(1-P)}{n} \tag{2.9}$$

where P is the number ratio of the target particles among all particles, and n is equivalent to: 1 + the average coordination number. For spherical particles, n is chosen as 7.

2.2.3 Influencing factors

The segregation process is affected by various factors. To categorize all the factors, there are basically three aspects: particle properties, operation process and environmental conditions. The trigger for segregation is the difference in particle properties, but all the other factors will also significantly influence the extent of the segregation phenomenon.

2.2.3.1 Particle properties

There are a great amount of material properties influencing segregation including particle size, size ratio, particle shape, particle density, morphology, surface texture, cohesivity, elasticity, brittleness, adhesion, chemical affinities, and ability to absorb moisture. Among all these parameters, particle size, particle size ratio, particle shape, particle density and other physical properties which will affect the flowablity are the most important ones.

Particle size

Particle size will decide the types of force that dominate the segregation process. Perschin demonstrated that the segregation decreases while the particle size is smaller than 500μm (Perschin 1990). Detailed explanation for the decrease of segregation is given by Harnby and Norman, they mentioned that particles with small sizes will be influenced by forces such as van der Waals and capillary forces (Harnby 2000). Still, there is no quantification evidence proving the relation

between particle sizes with segregation.

Particle size ratio

Size ratio is a triggering factor leading to segregation. According to Johanson, the size ratio must be larger than 2:1 to let segregation happen (Johanson 1996). Other researchers also observed the segregation phenomenon with size ratio of 1.5:1 (Drahun and Bridgwater 1983, Benito et al. 2013, Benito et al. 2014, Rodriguez et al.2015). Therefore, instead of a strict value to start the segregation, the critical value always needs to operate with other parameters jointly. And what has been accepted is that for free surface flows, the segregation tend to increase with the increase of size ratio (Sommier et al. 2001).

Particle density

Density segregation is weaker compared to size segregation (Lawrence and Beddow 1969, Harris and Hildon 1970, Vallance and Savage 2000). It was studied and found that segregation rate is higher for particles with higher density (Tang et al. 2003, Tang and Puri 2004), and with increase in components number, this segregation rate will reach a maximum value (Shinohara and Golman 2002).

Particle shape

Particle shape is the crucial factor affecting angle of repose. As mentioned before, angle of repose is also an individual mechanism that might lead to particle segregation. Particles with different shapes have dissimilar abilities to flow, for

example, the potential energy needed to drive spherical particles to flow is much less than cubic particles. Yi et al. (2001) studied the shape effects on segregation and stated two possible reasons: 1) the irregularly shaped particles can lodge in interstitial void spaces; and 2) the void spaces formed by irregularly shaped particles (coarse) are larger compared to regularly shape particles (fine). Similar to the density segregation, researchers have agreed that the effects of shape are weaker than the effect of size ratio (Lawrence and Beddow 1969, Vallance and Savage 2000).

2.2.3.2 Operation process

Operation process is another factor that needs to be paid attention to. As studied before, the segregation process varies from different handling processes, which includes packing, mixing, and conveying. Associated with these processes, some operation parameters are also affecting the segregation. Parameters such as falling height, feeding rate, heap size, hopper size, friction coefficient have been extensively studied and were proved to be significantly related to the segregation mechanisms (Drahun and Bridgwater 1983, Mosby 1996, Sleppy and Puri 1996, Zhu et al. 2007).

2.2.3.3 Environmental conditions

Environmental conditions such as residence time, relative humidity, vibration and temperature have effects on segregation. For example, vibrations drive the larger

particles to move upwards through a granular mixture, and with the increase of vibration frequency, the segregation reduces (Williams and Shields 1967, Ahmad and Smalley 1973).

2.3 DEM (Discrete element method)

Particle technology has been rapidly developed due to its wide use in both nature and industry. However, the understanding of granular matters is still poor and limited. Behind the macroscopic features shown by particulate system, further knowledge should be obtained in a rather microscopic view. The macroscopic behavior is basically decided by the force interactions between individual particles. Therefore, it is of great significance to better understand the inside force structure to obtain comprehensive knowledge of a granular system. An efficient way to achieve this goal is to conduct particle scale research with the help of numerical methods. There are several techniques available for discrete modelling, including Monte Carlo method, cellular automata, and DEM (discrete element method). Different from the other options, DEM can offer detailed information of the forces acting on each individual particle, which will be perfect for the study of microscopic dynamics. Furthermore, as the high cost and limitation of physical experiments, the use of DEM has largely increased the research efficiency and was therefore well developed in the past decades. As shown in Figure 2-7, in the past decades, the studies based on DEM simulations have rapidly increased.

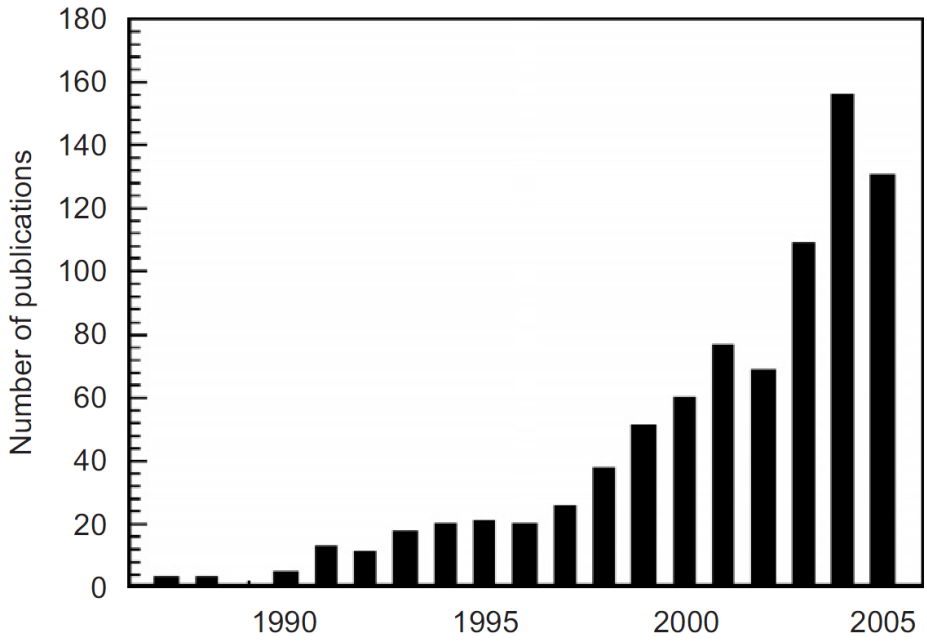

Figure 2-7 Number of publications related to discrete particle simulation in the recent decades, obtained from the Web of Science with the following keywords: discrete element method/ model, distinct element method/model, discrete particle simulation/ method/ model, and granular dynamic simulation.(Zhu et al.2007)

There are generally two force models for DEM: soft-particle model and hard-particle model. Soft-particle model is firstly introduced by Cundall and Strack in 1979 (Cundall and Strack 1979), and it was also the first attempt of DEM. In this model, interactions between particles will cause the deformation of particles, which will further be used to calculate the interaction forces, including elastic force, plastic force and frictional force. Newton's law is respected as the main principle deciding particles' further motion. The primary feature of this soft-particle model is that it can well handle quasi-static systems while multiple particle contacts should be dealt with. In contrast, hard-particle model consider

particle contact as an instaneous process and only one collision can be processed at one time. These two models have both been applied to study multiple industrial cases including mixing, packing, piling, and hopper flows. For stockpiling process, as it is associated with the contacts of multiple particles, it can be better simulated based on a soft-particle model.

For an individual particle inside a granular system, its motion can be divided into two types: translational and rotational. The governing equations for these two types of motion are based on Newton's second law of motion:

$$m_i \frac{dv_i}{dt} = \sum_j F_{ij}^c + \sum_k F_{ik}^{nc} + F_i^f + F_i^g \tag{2.10}$$

$$I_i \frac{d\omega_i}{dt} = \sum_j M_{ij} \tag{2.11}$$

where m_i and I_i represents the mass and moment of inertia of particle *i,* respectively, v_i and ω_i are the translational and angular velocities of particle *i,* respectively, F_{ij}^c and M_{ij} are the contact force and torque acting on particle *i* by particle j or walls, F_{ik}^{nc} is the non-contact force acting on particle i by particle k or other sources, F_i^f and F_i^g are the particle-fluid interaction force and gravitational force, respectively.(Zhu et al. 2007) The force and torque used in DEM is schematically showed in Figure 2-8.

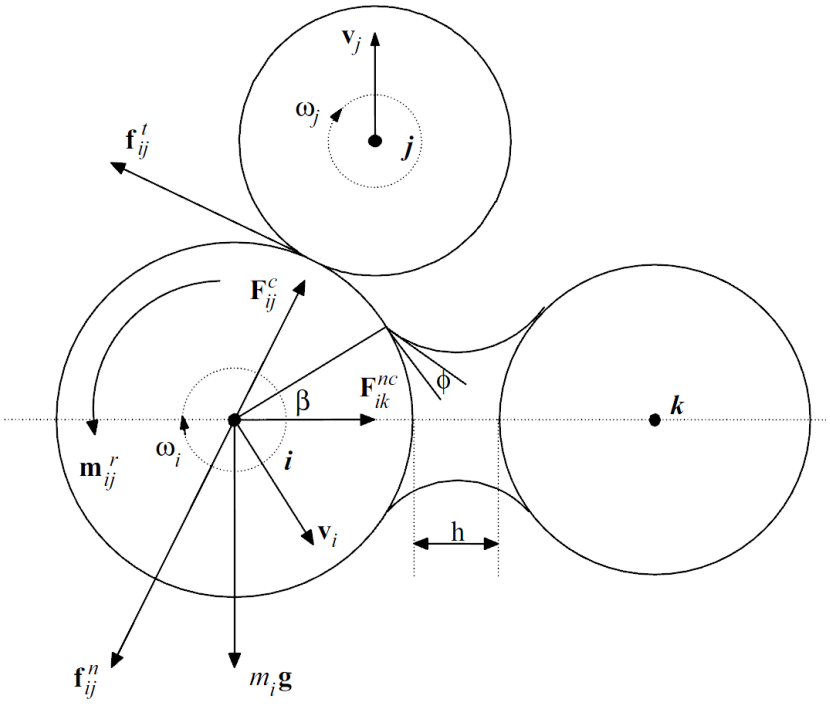

Figure 2-8 Scheme of force and torque acting on particle I in DEM simulation (Zhu et al. 2007)

With these equations, the motion of every individual particles can be calculated based on Cundall and Strack's hypothesis on timestep (Cundall and Strack 1979). In order to simplify the force structure, it is assumed that during a very short time step, particles will stay still so their further movement will not disturb the calculation of forces or torques acted by neighbor particles.

In order obtain the motion of every particle, the further problem appears to be the calculation of the exact forces and torques acting on particles. There are two types of forces acting on particles: contact force and non-contact force. The models developed for them are separate.

For contact forces, there has been many attempts to obtain the factual force models.

The attempts can simply be divided into two types: linear and non-linear.

Cundall and Strack (1979) use a linear spring-dashpot model to conduct the simulation. The spring is responsible for the elastic deformations while the dashpot is placed for the dissipation caused by plastic interaction. The latter dissipation was modelled with a damping depending on velocity. Walton and Braun (1986) further developed this model by changing the spring with a different elastic constant. Di Renzo and Di Maio (2004) tried similar model but without using dashpot.

Different from the linear models, the non-linear models tend to be more complicated but can better present the real cases. The most well-known model is the Hertz-Mindlin and Deresiewicz model. This model uses the Hertz's elastic theory (Hertz 1882) for the calculation of normal contact forces and Mindlin and Deresiewicz's theory (2013) for the tangential contacts. This model can offer more accurate mathematical representation of the force structure, but it also largely increases the computational difficulty as it is much more time-consuming than the linear models. Therefore, the further attempts of optimization have been focused on simplifying this model. (Thornton and Yin 1991, Tsuji et al. 1992, Walton 1993, Langston et al. 1994, Thornton 1997, Vu-Quoc and Zhang 1999)

Non-contact forces generally include capillary force, Van der Waals force, and electrostatic force, but for the granular materials studied in this thesis, the particle

size is large enough to ignore the influence of these forces.

2.4 Stockpile/ Sandpile stratification and segregation

Figure 2-9 Formation of a sandpile as grains flow from a funnel onto the flat surface (Liu et al. 2011)

As shown in Figure 2-9, granular stockpiles form when particles are poured onto a surface. While granular stockpiles are widely observed in both nature and daily lives, the better standing of these patterns will directly benefit many industries. The formation of granular stockpiles is simple but the inside mechanisms and microscopic motions are complex, these features will in turn make the studies of stockpiles important and significant for fundamental research. One of the most troubleshooting topics is stress distribution within the stockpile, especially the stress dip at the bottom of the sandpiles. Lots of researchers such as Zuriguel and

Mullin (2008), Zhu et al. (2013), Zhou et al. (2014), Liu et al. (2011) and Liffman et al. (2001) have put much efforts on studying the affecting factors and causes of this phenomenon. Another topic is the mixing of the granular sandpiles, as one of the most significant study about the sandpiles features, it has drawn attention from lots of research groups in the last several decades. In this part, the sandpile's mixing problem will be reviewed. Based on Fan et al.'s categorization (2012), this review will be divided into the study of stratification phenomenon and segregation phenomenon.

2.4.1 Stockpile stratification

Normal size segregation demonstrates the phenomenon that large grains spontaneously segregate near the base while small grains are more likely to be found near the top when forming a granular pile. However, there is another size-separation effect known as stratification. As compared in Figure 2-10, when granular mixture was pouring inside the two-dimensional silo, the pile shows layered features rather than the segregation pattern. This part will basically introduce the previous researches about sandpile stratification from the views of physical experiments and numerical simulations.

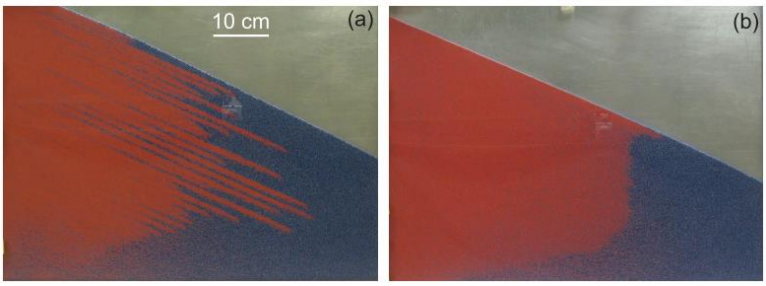

Figure 2-10 Comparison of Stratification(a) and Normal segregation(b) (Fan et al. 2012)

2.4.1.1 Physical Experiments

The stratification phenomenon was first reported by Makse et al. (Makse, Havlin et al. 1994). In their experiments, they used a vertical 'quasi-two-dimensional' cell to construct half stockpiles instead of full stockpiles. The granular mixtures were chosen to contain particles with different sizes and different shapes on basis of the equal-volume criteria. When the mixtures were poured near the left edge of the silo at a constant rate, half stockpiles were formed as shown in Figure 2-11a and Figure 2-11b. Instead of normal segregation, the stockpile showed a stratification pattern that the mixture spontaneously stratified into separate layers with constant wavelength. Through their experiments, they also tested the cohesive effects of density, size and particle shape. They firstly confirmed that the density of grains did not largely affect the stratification phenomenon. Furthermore, considering size and shape, they noticed that the stratification was only obtained when larger cubic grains and smaller spherical grains were used. In contrast, if mixtures contained large particles with smaller angle of repose and small particles with larger angle of repose, the stratification phenomenon disappeared and only

segregation was observed. Based on the physical experiments, a physical mechanism was constructed. Due to fact that a pair of layers were formed during every avalanche, they defined ‘kink’ (Figure 2-11b) which can stop particles movements. In detail, the small particles were first stopped which make them form a layer underneath the large particles (Figure 2-11d). On the other hand, the stopped particles will continuously form the new ‘kink’ which literally can be illustrated as the kink’s moving-up behavior. Through this mechanism, the cause of stratification was well interpreted. And by using several parameters introduced in the mechanism, the ‘wavelength’ of the layers was also successfully predicted, which had already been confirmed experimentally.

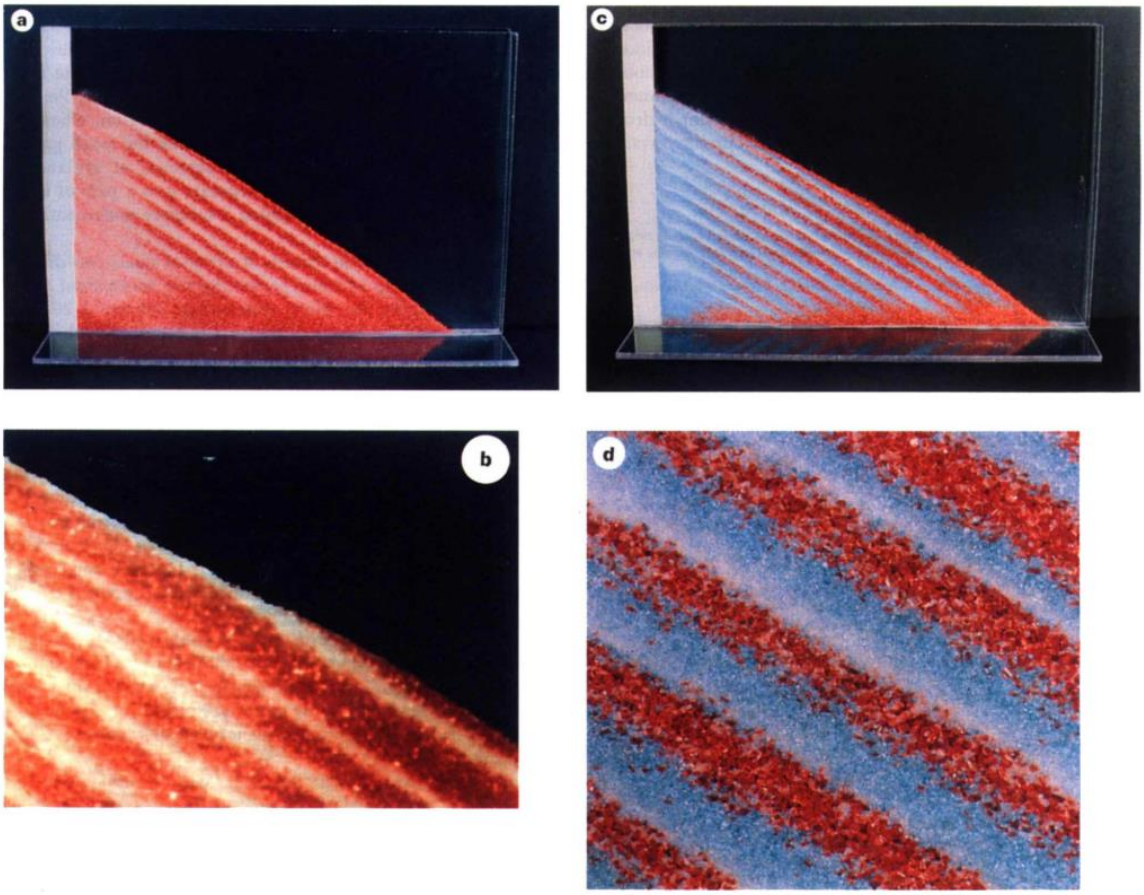

Figure 2-11 Experimental results of Makse et al.'s study (1994). (a) Stratification obtained with a mixture of glass beads (average diameter 0.27mm, white) and sugar crystals (size 0.8mm, red); (b) the formation of 'kink' that small grains go underneath while larger grains segregate on top; (c) Stratification obtained with a mixture of nearly spherical white glass beads (0.15mm, angle of repose 26°), blue sand (0.4mm, angle of repose 35°) and red sugar crystals (0.8mm, angle of repose 39°); (d) Details of the stratified layers.

Based on Makse et al.'s experiments (1994), lots of researchers started putting efforts on further interpreting the stratification phenomenon from different aspects. Koeppe et al. (1998) studied the wall effects on this phenomenon and

found that the wavelength of the stratified layers significantly decrease when the gap of the silo gets larger. Grasselli and Herrmann (1998) did further physical experiments studying this geometry effects, and they also investigated the effects of particle size and mass flux. In their experiments, binary mixtures containing rough particles (sand) and smooth particles (glass sphere) were input into the two-dimensional silo at steady rate. They firstly studied the effects of size ratio Φ (*size of rough particles*/*size of smooth particles*) on mixing patterns, and they successfully constructed the phase diagram as shown in Figure 2-12. It was concluded that: for value of Φ greater than 1.5, stratification was observed; for value of Φ lower than 0.8, segregation was observed and the two components of the segregation pattern show different angles of repose; for value of Φ within the range of 0.8 to 1.5, normal segregation with continuous angle of repose was observed. Considering the effects of silo gap d and mass flux W, it was found that they cohesively decided the wavelength of stratified layers in stratification. More specifically, as shown in Figure 2-13, the wavelength of the stratified layer λ depends on W/d that λ proportionally increases when W/d increases.

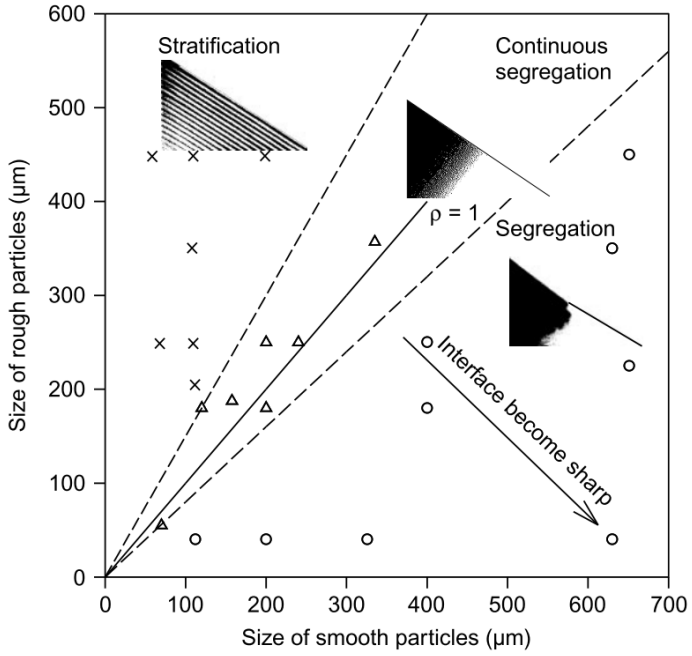

Figure 2-12 Phase diagram of the effects of size ratio Φ on stockpile mixing. (mass flux W =2.5g/s and silo gap d =3mm) The mixing patterns are classified by: × stratification, ▵ continuous segregation, ○ segregation.(Grasselli and Herrmann 1998)

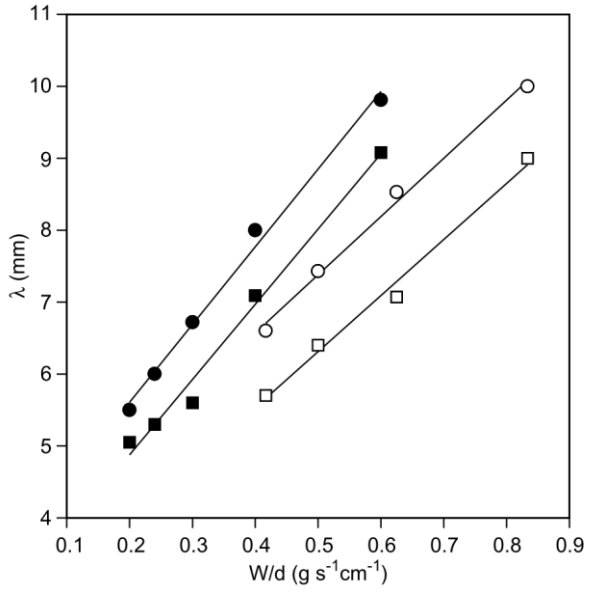

Figure 2-13 The relationship between λ and W/d with different sets of size ratio Φ and mass flux W. (Grasselli and Herrmann 1998)

Similar to Grasseli and Hermann's efforts on investigating the phase transaction between mixing patterns, Fan et al. (2012) also studied this phenomenon focusing on identifying the boundary between the three final states: stratified, segregated and mixed. From their work, it was concluded that the boundary between stratified pattern and segregated pattern is controlled by flow rate, and the exact critical flow rate depends on particle size ratio and flowing layer length; about the transition from segregated states to mixed states, it is basically decided by the rise velocity of the heap, and the critical velocity also depends on the particle size ratio.

As the experimental studies above all suggested that stratification only happens when there is marked difference in particle shape (angle of repose), Baxter et al. (1998) performed experiments to prove that stratification can also happen in absence of the particle shape factor. From Baxter et al.'s work, stratification of granular matters is an issue cohesively resulted by multi factors including fill rate, size ratio and particle shape. While testing the effects of fill rate, they conducted experiments using mixtures with same angle of repose. Remarkably, as shown in Figure 2-14, heap flow well stratified when slow feeding process was approached while well-mixed heap formed in fast feeding process. This work updated the understanding of stratification as it emphasized the importance of filling rate in absence of particle shape.

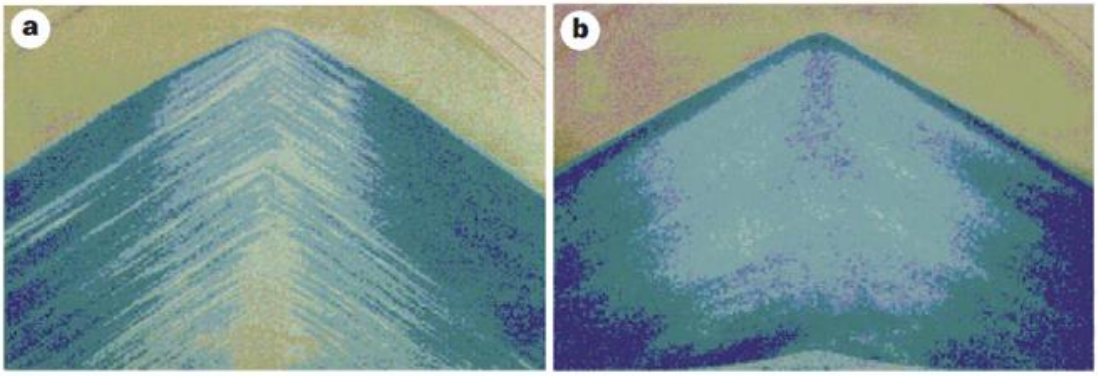

Figure 2-14 (a) Stratified heap formed in slow feeding process; (b) well-mixed heap formed in fast feeding process.(Baxter et al. 1998)

Another group of researchers used only spherical particles in their physical experiments (Benito et al. 2013, Benito et al. 2015). As shown in Figure 2-15, they also observed noticeable stratification when adopting large size ratio and small injection height. Their work is consistent with Baxter et al.'s work considering feeding rate and injection height. But Benito et al.'s work has well indicated that spherical particles can also perform obvious stratification.

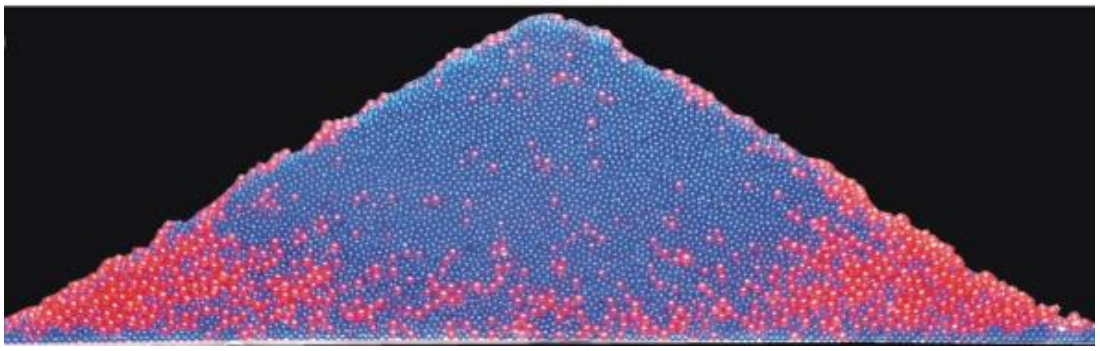

Figure 2-15 Built-up stockpile for an injection height equal to 10mm and size ratio of 3:2. Large particles are red and small particles are blue. (Benito et al. 2013)

2.4.1.2 Simulation methods

Different from physical experiments, numerical simulations can easily offer detailed velocity, force, location profiles within the stockpile, and theoretical models can also be applied to verify the physical mechanisms, so a lot of researches have been done through numerical methods.

As the pioneer of stratification researches, Makse's group also put much efforts on numerical simulations (Makse et al. 1994, Makse 1997, Makse et al. 1997, Makse 1998, Makse et al.1998, Makse and Herrmann 1998, Cizeau et al. 1999). They first developed a 'mean field' type model (Makse et al. 1994) in which the spin orientations of particles were decided by the net magnetization. In order to investigate this problem from a microscopic view, the particles inside the model follow the microscopic rules instead of macroscopic features. For example, the motion of particles will be influenced by local angles of repose rather than the angles of the whole stockpile. By using this theoretical model, they successfully reproduced the mentioned 'kink' mechanism and stratification phenomenon, as shown in Figure 2-16.

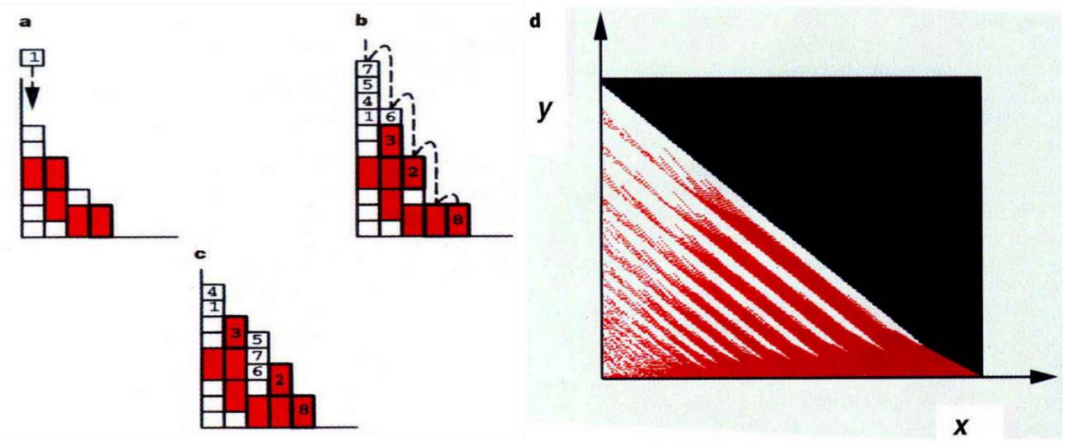

Figure 2-16 'Kink' mechanism (a, b, c) and flow patterns obtained through 'mean field' model (d) (Makse et al. 1994)

In order to obtain more microscopic profiles, two more fundamental models were introduced to study the stratification phenomenon (Makse et al. 1997, Makse et al. 1998, Cizeau et al. 1999). They developed a discrete model with granular mixture of different sizes and shapes. From the results, they configured four types of local piling patterns with different local angles of repose as shown in Figure 2-17a. They found that when a group of large particles were on top of a layer of small particles, the angle would be like θ_{22} which was lower than θ_{12}, this would result in a layer of small particles being trapped on top and the formation of stratified layers. This method further interprets the key feature of 'kink' mechanism that the small particles are stopped first. Through this model, the stratification scheme was also successfully represented as shown in Figure 2-17b.

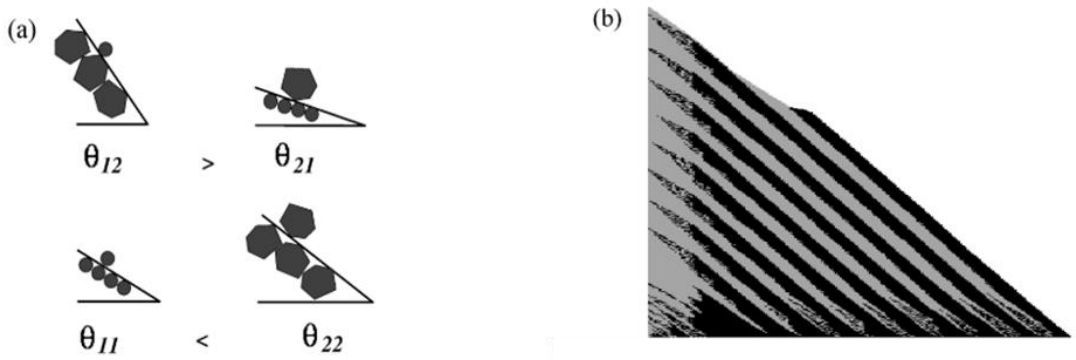

Figure 2-17 Scheme of the four local piling patterns (a) and the obtained stratified stockpile (b). (Makse et al.1997)

Another model is based on the continuum theory proposed in Boutreux and De Gennes.'s work (Boutreux and De Gennes 1996). The continuous model is governed by the motion equations as follows:

$$\frac{\partial R_\alpha}{\partial t} = -v_\alpha \frac{\partial R_\alpha}{\partial x} + \Gamma_\alpha \tag{2.12}$$

$$\frac{\partial h}{\partial \mathrm{t}} = -\sum_\alpha \Gamma_\alpha \tag{2.13}$$

where $R_\alpha(x,t)$ describes the two thickness of the particles with $\alpha = 1, 2$, respectively, for small and large particles, $h(x,t)$ is the height of the sandpile, v_α is the downhill convection velocity of specified particle type α, and Γ_α represents the interaction between particles and surface. Through this continuous model, the stratification was reproduced and it was concluded that difference in particle size dominates the segregation while difference in angles of repose triggers the stratification (Makse et al. 1997). With the help of these two models, Makse et al.

also studied the determining factors of wavelength λ (Makse et al. 1998), and they found the following relation:

$$\lambda \propto \frac{v}{\gamma} + R^0 \tag{2.14}$$

where v represents the downhill velocity of particles, γ represents the effectiveness of interaction, and R^0 is the thickness of the particles.

After further optimization, Cizeau et al. (1999) summarized the previous two models and included Makse's new opinion about thick-flow regime and percolation effect (Makse1998). And they further concluded that stratification will only occur when granular mixture contains large particles with larger angle of repose and small particles with smaller angle of repose, while complete segregation can be triggered when large particles have smaller angle of repose. These findings through theoretical simulations are also consistent with the previous physical experiments studies (Makse et al.1994).

Benito et al. (2015) used a simple pseudo-dynamic model to verify their findings for stratification experiments with only spherical particles (Benito et al. 2013). This method is based on the influence of gravity and local geometric constraints, which on the one hand accelerates the calculation and simplifies the model from various classical motion equations. While on the other hand, this method cannot offer as much motion profiles as discrete models and continuous models do. Through this model, they approached the flow patterns as shown in Figure 2-18

which presented the general features of stratification phenomenon. It was concluded that geometric effects are relevant to stratification and when the value of *RS* increases, segregation phenomenon appeared.

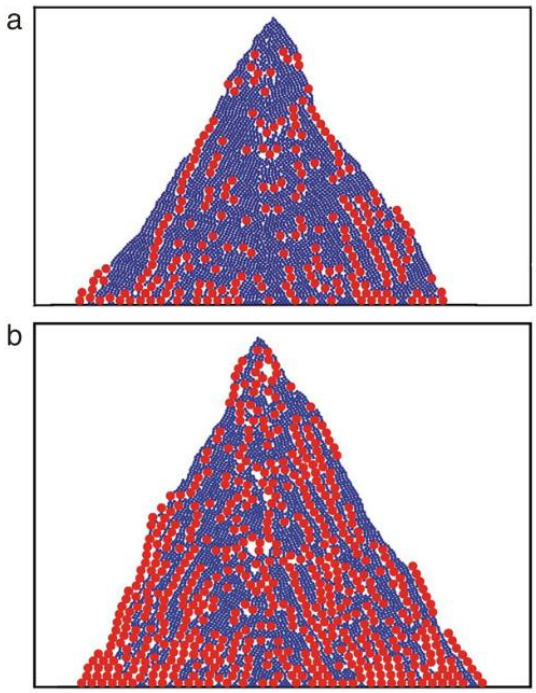

Figure 2-18 Piles obtained using pseudo-dynamic model. Size ratio 3:1; Surface ratio (a) *RS*=0.5, (b)*RS*=1.5 (Benito et al. 2014)

2.4.2 Stockpile segregation

Similar as the researches of stockpile stratification, the normal segregation phenomenon has also been extensively studied by both physical experiments and numerical simulations.

2.4.2.1 Physical Experiments

Drahun and Bridgwater (1983) studied the segregation phenomenon in two-

dimensional heap formation through physical experiments. By pouring batches of particles onto the inclined plane, the locations of the tracer particles were recorded considering different sets of parameters. Several significant conclusions have been made through this experimental study: (i) the free surface segregation was cohesively triggered by three mechanisms (avalanching, inter-particle percolation and particle migration) together; (ii) the segregation phenomenon was largely influenced by particles' size ratio that small particles tended to sink by percolation near dropping location while large particles could float on the surface and segregate to the far end through particle migration; (iii) the segregation can also be triggered by particles' density ratio that dense particles tend to stay around dropping location while less dense particles will migrate to the far end.

Fan et al. (2012) also did sets of physical experiments, and they investigated the pattern formation of stockpiles and influences of several parameters on segregation. In order to define the boundaries among stratification, segregation and mixing, they first introduced the parameters I and σ_I, which represented the local intensity of the chosen sample and the standard deviation of I data, respectively. They further found that while larger $\sigma_I/\bar{I}$ indicated the transition from segregation to stratification, $\sigma_I/\bar{I}$ significantly decreased when the flow rate q increased, as shown in Figure 2-19. Then it was concluded that segregation can be approached by increasing the flow rate. Also, considering the phase diagram of the three piling patterns, they included particle size ratio R and heap rise velocity

v_r along with the flow rate q, as shown in Figure 2-20. Other than the investigation of the transition among different patterns, they also found that the value of size ratio will decide the triggering mechanism of segregation. The degree of segregation was found to be decided by competition between advection and percolation, which can be interpreted by the rise velocity v_r and percolation velocity $\overline{v_p}$, which are dominated by the particle size ratio.

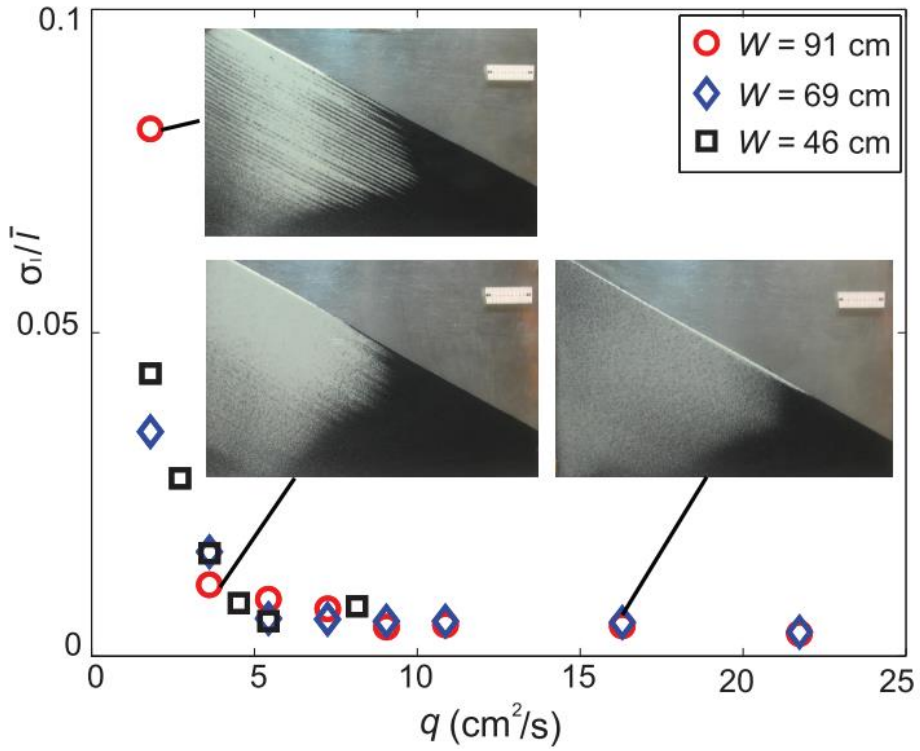

Figure 2-19 The relation between $\sigma_I/\bar{I}$ and q when size ratio is set to be 2.2. W indicates the value of the silo's gap distance. (Fan et al.2012)

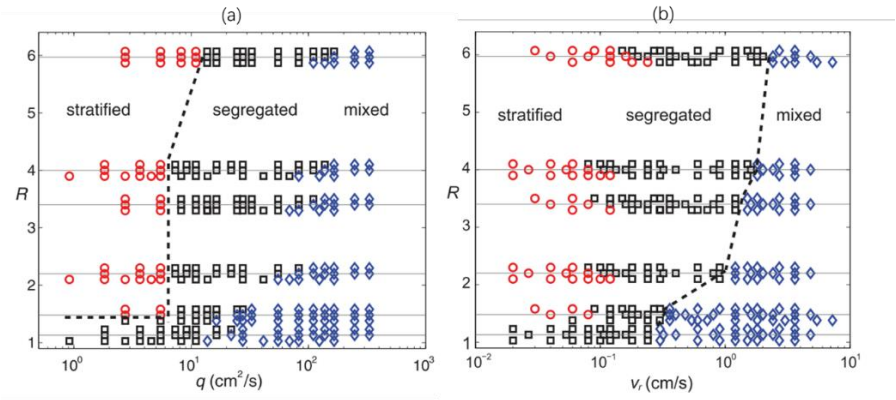

Figure 2-20 Phase diagram of three piling patterns considering the effects of rising velocity v_r, size ratio R and q. (Fan et al. 2012)

Quantified experiments were also conducted to study the segregation phenomenon (Benito et al. 2013, Benito et al. 2014, Rodriguez et al. 2015). With the help of the experimental system shown in Figure 2-21, they were able to transfer physical piling pattern into digitalized data to further quantify the study.

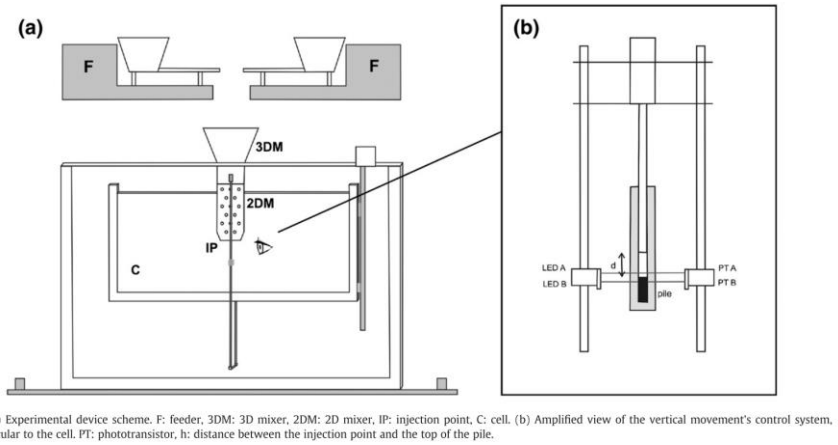

Fig. 1. (a) Experimental device scheme. F: feeder, 3DM: 3D mixer, 2DM: 2D mixer, IP: injection point, C: cell. (b) Amplified view of the vertical movement's control system, perpendicular to the cell. PT: phototransistor, h: distance between the injection point and the top of the pile.

Figure 2-21 (a) The scheme of Benito et al.'s experimental device. (b) The details of the vertical movements system. F: feeder; 3DM: 3D mixer; IP: injection point; 2DM: 2D mixer; PT: phototransistor. (Benito et al. 2013)

In the experiments, they used binary mixture of spherical glass beads with controlling particle size ratio, dropping height and mass ratio m_{LS} (the whole mass of large grains versus small grains). It was found that the segregation patterns were decided by the three parameters together. For the situation of size ratio equals to 3:1, when m_{LS} is greater than 1, segregation occurs for dropping height around 25mm; and when m_{LS} is smaller than 1, segregation only occurs for large dropping height around 50mm. On the other hand, for size ratio 3:2, segregation is observed with any dropping heights when m_{LS} is smaller than 1. Other than the parameter study, they also developed a method to experimentally quantify the stockpile segregation. Based on the sampling technique shown in Figure 2-22, they introduced two indices I_H and $I_\perp$ as:

$$I_{H,\perp} = \frac{2n_L}{\frac{an_s}{27} + n_L} \quad \begin{cases} a = 1 \text{ for size ratio } 3{:}\,1 \\ a = 8 \text{ for size ratio } 3{:}\,2 \end{cases} \tag{2.15}$$

where n_L and n_s represents the number of large particles and small particles within the chosen sample, respectively. Through this method, they first made characterization for the two indices under extreme circumstances (complete segregation, complete stratification), and they then compared the obtained patterns with the ideal curves. In summary, this new quantified method has enabled a better characterization of the piling patterns, especially for differentializing segregation and stratification.

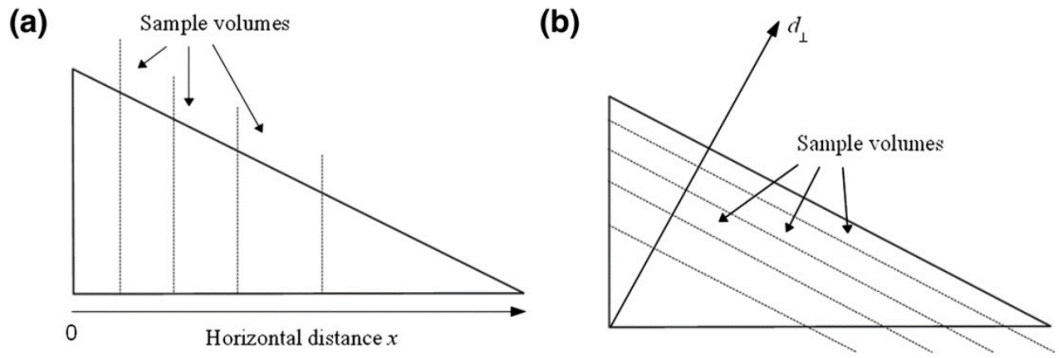

Figure 2-22 Scheme of the sample volumes for (a) I_H and (b) $I_\perp$. (Benito et al. 2013)

Instead of using two-dimensional silo set-ups, Yu et al. (2018) did three-dimensional physical experiments to study the size segregation in a pile of binary pellets. Through their experiments, they conclude that the small particles tend to percolate into the space between large particles while large particles can flow down to the bottom of the file, which results in the segregation pattern that small particles concentrate in center area while large particles segregate at bottom. Also, the three-dimensional results are also consistent with previous two-dimensional studies.

Shimokawa et al. (2015) advanced the segregation study from binary mixtures to ternary mixtures. In their experiments, by using particles with different sizes and different repose angles, they observed four types of piling patterns: (1) stratification; (2) segregation; (3) upper stratification-lower segregation (4) upper segregation-lower stratification. It was then concluded from the experimental results that the ratios of the repose angles between particles can largely decide the pattern form, and a phase diagram (shown in Figure 2-23) was

constructed with respect to θ_{11}, θ_{22}, and θ_{33} which are the repose angles of the smallest specie, middle specie and largest specie, respectively.

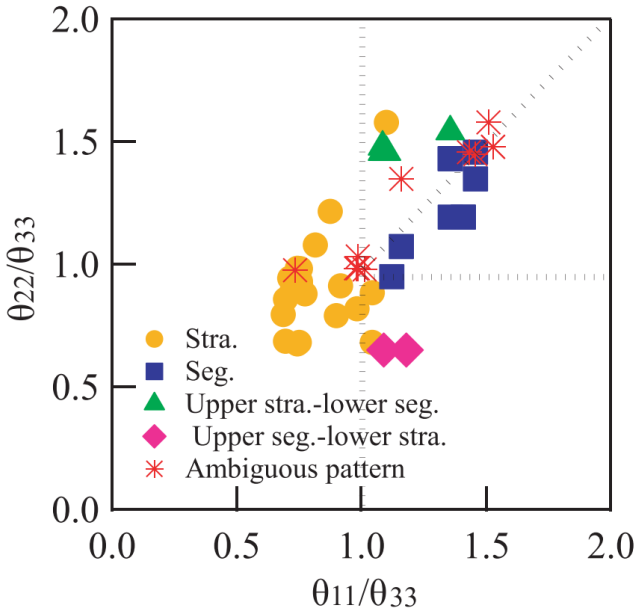

Figure 2-23 Phase diagram of four different patterns for ternary mixtures (Shimokawa et al. 2015)

2.4.2.2 Simulation methods

Different from physical experiments, numerical simulations can accurately control studied factors and simplify the quantification procedures. Therefore, lots of researchers have put more efforts on the modelling studies of the segregation phenomenon.

The segregation mechanisms were first investigated based on both two-dimensional and three-dimensional models (Jullien and Meakin 1990, Meakin 1990, Meakin and Jullien 1992). They developed and compared two two-

dimensional deposition models with circular particles to illustrate the basic segregation phenomenon (as shown in Figure 2-24) and mechanisms (Meakin 1990). They then advanced to three-dimensional simulation with binary mixture of spherical particles of different sizes (Jullien and Meakin 1990, Meakin and Jullien 1992), and the mechanism shown in Figure 2-25 was obtained. It was concluded that particles size segregation was resulted by the fact that large particles roll over bulk solids of small particles, and the degree of the segregation was influenced by both size ratio and number ratio.

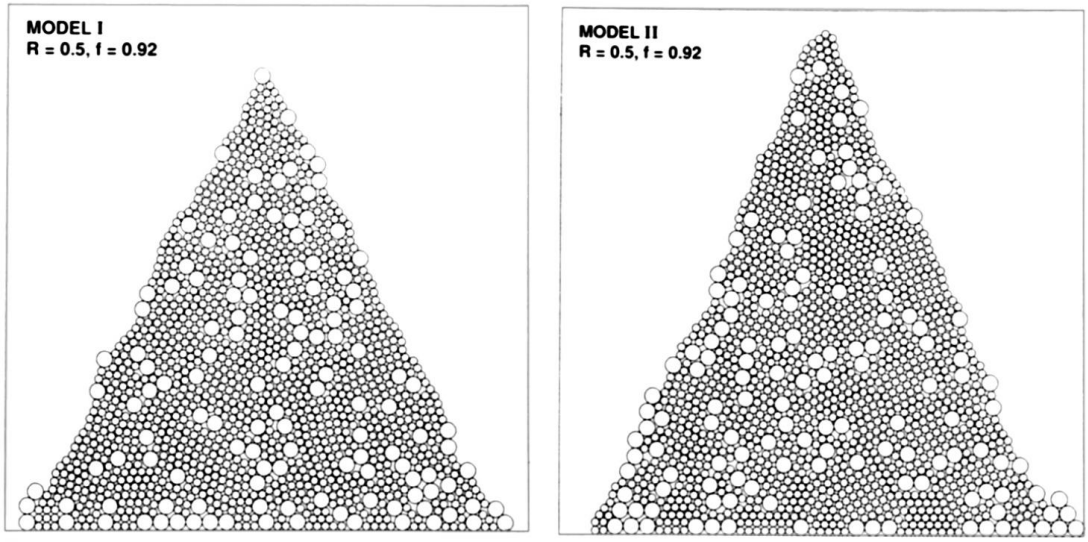

Figure 2-24 Results generated from two models. The size ratio $R = 0.5$; the fraction of small particles $f = 0.92$. (Meakin 1990)

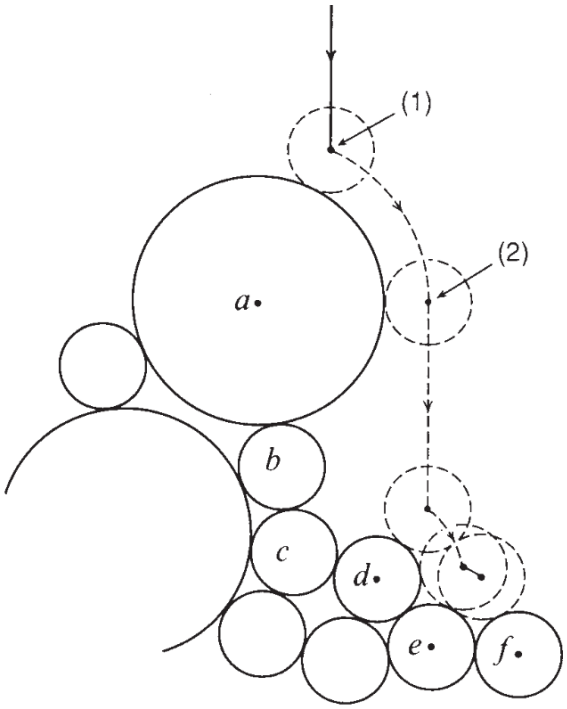

Figure 2-25 The two-dimensional scheme of the adopted three-dimensional model.

(Jullien and Meakin 1990)

Baxter et al. (1997) offered a granular dynamics simulation solution for heap formation but only for monodisperse particles, and this method was further adopted in Smith et al.'s (2001) researches on heap segregations. Different from other researches, they applied Fourier methods to conduct time series analysis on the obtained data. It was then concluded that the feed rate can influence the degree of segregation that sufficiently high feed rates could largely minimize the segregation.

Urbanc et al. (1997) aimed to study the segregation phenomenon through the view of phase space which was determined by size dispersion and creep difference.

They developed two one-dimensional models with binary particle mixture of different sizes. They obtained two complete segregated patterns as shown in Figure 2-26, which enabled them to define an order parameter to further investigate the effects of size dispersion and creep difference. The order parameter η was set 0 for a complete mixing system and ranged from -1 (Figure 2-26b) to 1 (Figure 2-26a) for different piling patterns. It was concluded that when small dispersion was small enough, the piling could transform from complete segregation to oppositely complete segregation.

Makse (1998) conducted simulations to study the segregation in two-dimensional silo on the basis of BdG equations (Boutreux and De Gennes 1996) for surface flows. Through this method he investigated the thick flow regime where particles' rolling motion dominated the segregation. After included kinematic sieving and percolation into the model, he configured a steading filling state for the piling process, and the patterns obtained were shown consistent with the previous experimental work.

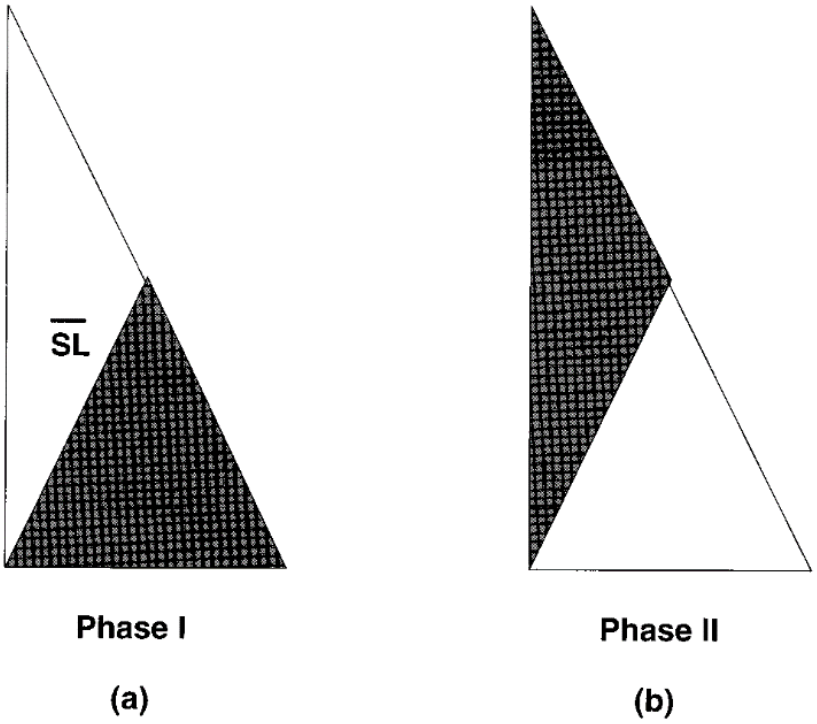

Figure 2-26 Scheme of the two complete segregation patterns. (a) $\eta = 1$; (b) $\eta = -1$.

(Urbanc and Cruz 1997)

Recently, Yu et al. (2018) used discrete element method (DEM) to conduct three-dimensional simulations on stockpile segregation with binary pellets. Their simulations well represented the results obtained from physical experiments, as shown in. Figure 2-27. The percolation effects were also illustrated by their numerical model.

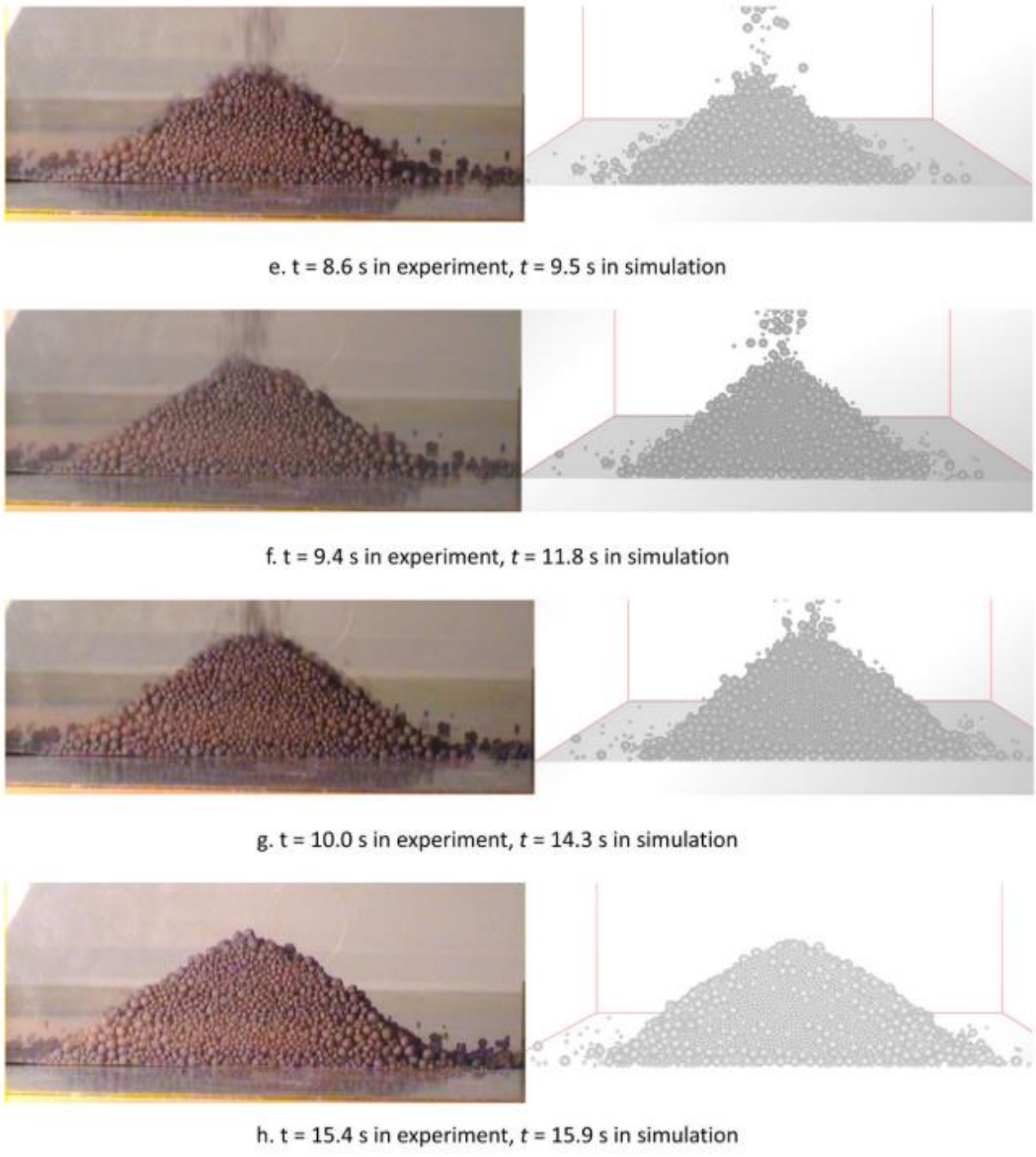

Figure 2-27 Comparison of physical experiments and DEM simulations. (Yu et al. 2018)

Gray' s group have done great amounts of work studying the theory of granular avalanche and free surface flows (Gray and Hutter 1997, Gray and Chugunov 2006, Gray and Ancey 2009, Gray and Kokelaar 2010, Gray and Ancey 2011). Considering particle segregation, they have developed a continuum model to predict the segregation phenomenon (Gray and Kokelaar 2010, Gray and Ancey 2011).

Vandewalle (1999) developed a stochastic model to study segregation especially the avalanching behavior. He found that the mixing of different particles could induce the formation of broad avalanche size distribution. he also mentioned that with this method, multi-mixture beyond binary mixture would be hard to study.

Other researchers tried numerically investigating the sandpile segregation with more than two species. Shimokawa et al. (2015) used a simple phenomenological model to simulate this phenomenon with ternary mixtures. The simulation results qualitatively confirmed the phase diagram obtained from physical experiments, and it was also suggested that the difference of repose angles among the three species could largely influence the pattern formation.

2.5 Vibration-induced segregation

Vibration-induced segregation is another type of granular segregation that has been extensively studied for decades. Different from stockpile segregation's self-motivation features, the vibration-induced segregation was motivated by the vibrated containers. As this segregation often shows a vertically segregated pattern, it is also called Brazil-nut effect (BNE) as large particles can accumulate on top while small particles tend to segregate at the bottom. There are lots of factors that can affect this phenomenon, of which the most important ones are particle size ratio, particle density ratio and vibration parameters (vibration frequency and vibration amplitude). Recently the reverse Brazil-nut effect which describes the phenomenon that large particles accumulate at the bottom was also observed and investigated by several researchers (Brone and Muzzio 1997, Akiyama et al. 2001, Yan et al. 2003, Schroter et al. 2006). But the normal BNE is still the major topic due to its inevitable significance in industries.

In this part, the vibration-induced segregation will be basically reviewed considering its mechanism, affecting factors and research methods. Specifically, the previous researches will be divided into physical experiments and numerical simulations based on the methods used.

2.5.1 Experimental studies

Williams and Shields (1967) first studied the vibration-induced segregation with

binary mixtures based on physical experiments, but as he used only vibrated screening which ignore the effects of side walls, so a basic vertical segregation pattern hasn't been observed. Ahmad and Smalley (1973) observed the BNE phenomenon and several significant conclusions have been made through their experiments with only one large particle (the mixture of one large particle and bulk solids of fine particles): (1) acceleration is the most critical factor influencing the segregation phenomenon; (2) the larger the coarse particle is, the stronger the segregation is; (3) the segregation can be weakened by increase the density of the large particle. While recording the particles movement had always been difficult for physical experiments, Harwood (1977) adopted a radioactive tracer technique to present the particles' movements in vibration-induced powder segregation. But as the cohesive forces cannot be neglected for powder materials, this study cannot support the basic studies of BNE.

Cooke et al. (1996) experimentally studied the size segregation in vibration conditions with one intruder out of bulk solids of small particles. In this experiment, the digital high-speed photography was used to obtain the trajectory maps, based on which it was found that the rising speed of the intruder particle was the same as its surrounding particles. This feature on the other hand indicated the importance of convection mechanism in motivating the vertical segregation. Based on the experiment, they also obtained the effects of size ratio and acceleration on the vertical motion of intruder particle, as shown in Figure 2-28

and Figure 2-29. It was then concluded that the segregation rate increases with the increase of size ratio and peak acceleration. In addition, it was found that, with small size ratio and low peak accelerations, the motion of the intruder showed an intermittent pattern, while with large size ratio and high accelerations, the motion of intruder showed a linear and continuous pattern.

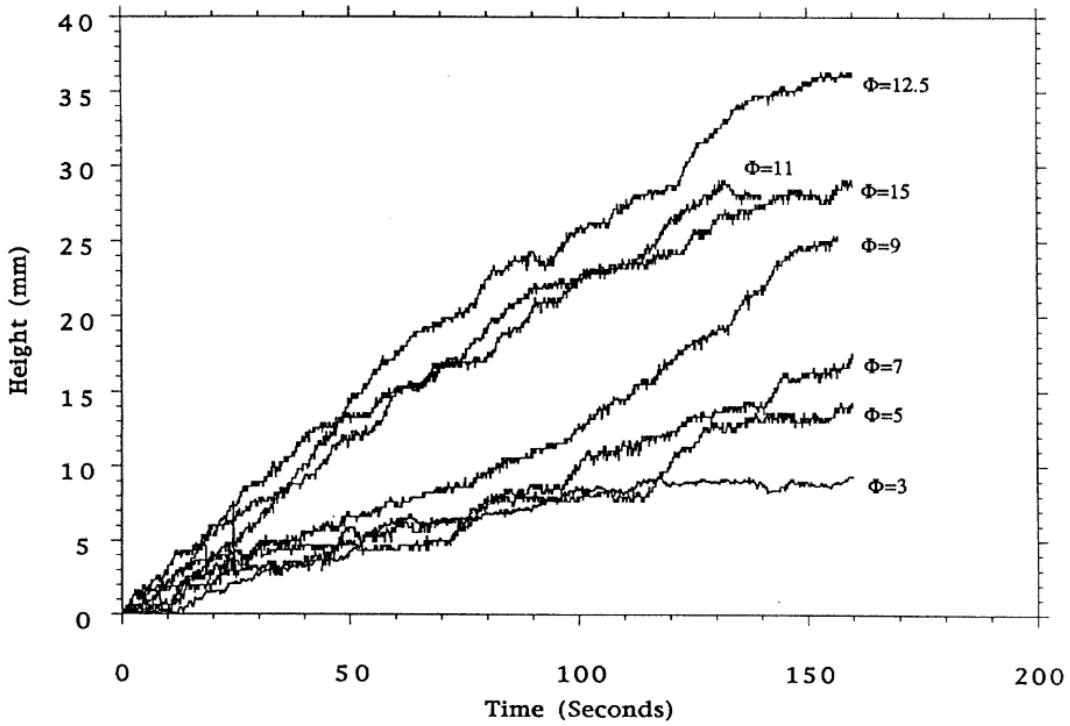

Figure 2-28 Intruder height against time for different size ratios Φ=3, 5, 7, 9,11 ,12.5, and 15. (Cooke et al. 1996)

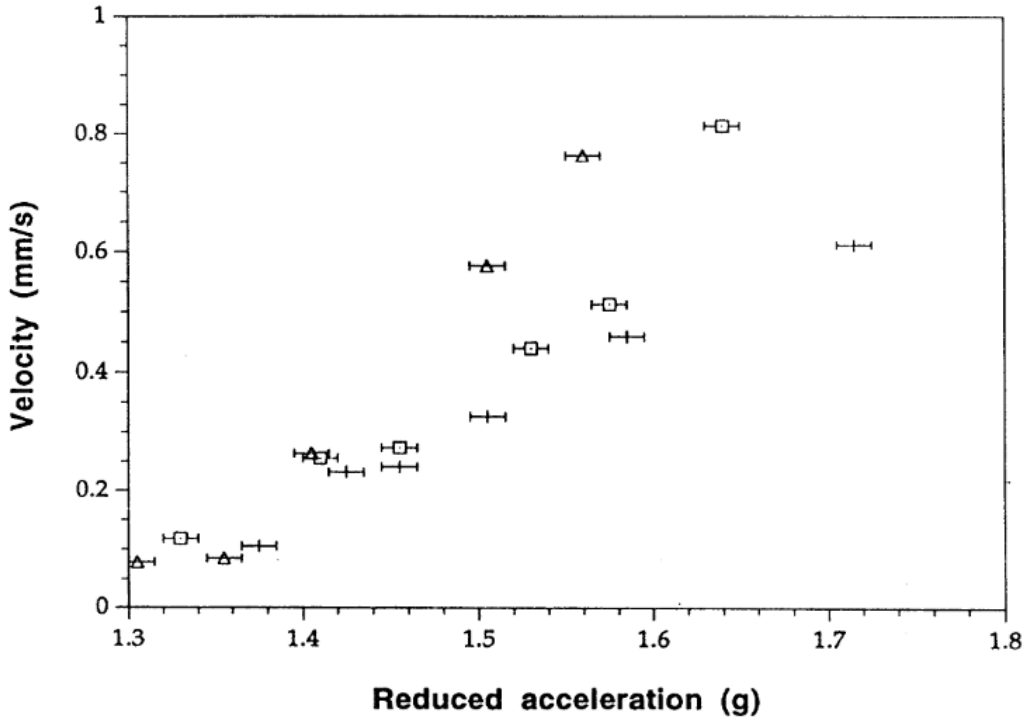

Figure 2-29 Average rise velocity of intruder particle against dimensionless acceleration considering different size ratios. Crosses, squares, and triangles represent the profiles of Φ=3, 7, and 12.5 respectively. (Cooke et al. 1996)

Liffman et al. (2001) studied the behavior of a single metal disk in a bed of monodisperse granular material with vertical vibration. The obtained flow patterns are shown in Figure 2-30. It was found that when the vibrational acceleration was set to be around 1.2, the bulk convection of the particulate bed showed nearly no influence on the motion of the large metal disk. In addition, the rising behavior of the intruder disk presented a buoyancy feature that the drag force of the granular material was proportional to the weight of the material displaced by the disk. Based on these findings, they also developed a numerical

model which further confirmed their theory. The numerical model will be further introduced in next section.

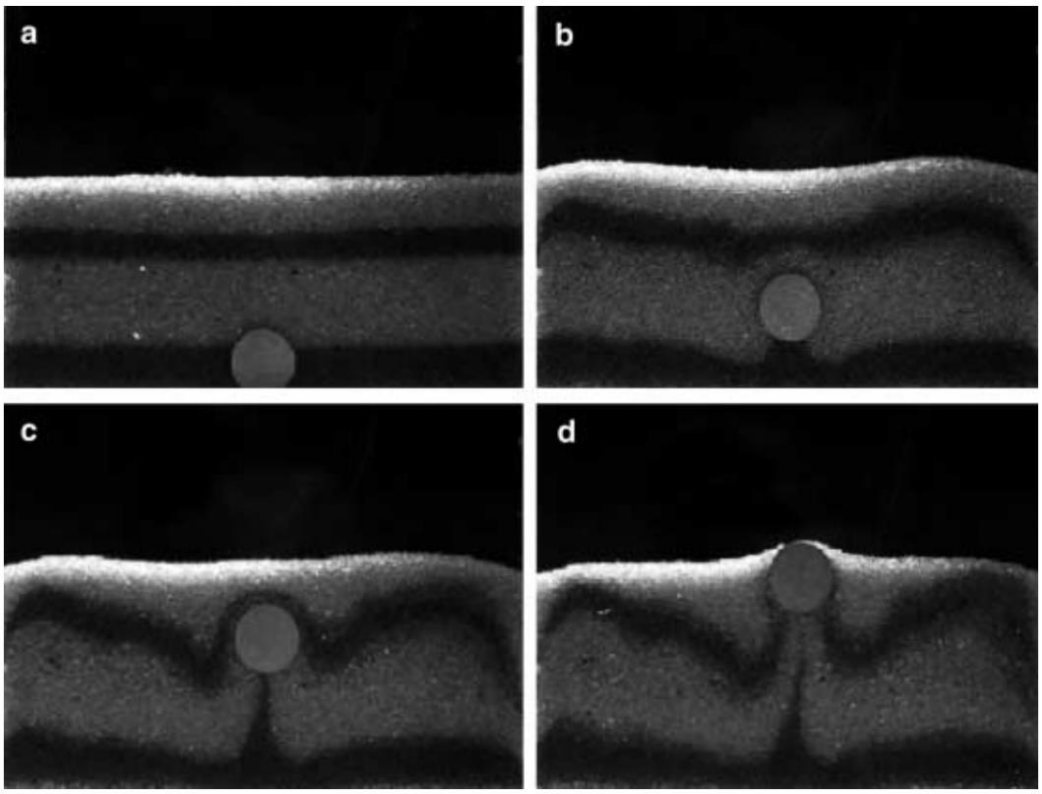

Figure 2-30 The flow patterns of the vibrated bed. (Liffman et al. 2001)

Fernando and Wassgren (2003) explored the motion of the large intruder when convection can be neglected. In order to largely minimize the side-wall convection, walls with low frictions were adopted in the physical experiments. It was concluded that at this situation, the method of vibration dominated the motion of the large intruder. To illustrate the motion of large intruder, they also introduced a rise rate defined as:

$$\text{rise rate of intruder} = \frac{vertical\ distance\ traveled\ by\ the\ intruder}{number\ of\ vibration\ cycles} \qquad (2.16)$$

It was then found that continuous vibrations could result in a maximum rise rate while discrete vibrations enabled the rise rate to increase with increasing vibration velocity amplitude.

Schroter et al. (2006) systematically studied the mechanisms influencing the vibration-induced size segregation. In addition, they also included the reverse Brazil-nut effect in their experimental studies. They stated that the vertical size segregation is basically triggered by the void-filling mechanism, side-wall driven convection mechanism, and the thermal diffusion mechanism. Based on the physical experiments and molecular dynamic simulations, they have generated three conclusions in respect to the three mechanisms: (1) the void filling mechanism induces strong Brazil-nut effect when the vibration frequency is around 80Hz, and this effect can be weakened by increasing the number of large particles; (2) the convection mechanism dominates when the frequency is around 15 Hz and amplitude is up to 1.5 large particle diameters, and the Brazil-nut effect in this situation can be strengthened by increasing the size ratio and decreasing the number of large particles; (3) the thermal diffusion mechanism works when the amplitude is over 1.5 large particle diameters, in which situation the large particles tend to segregate at bottom to maintain the minimum system energy, and this will lead to the reverse Brazil-nut effect.

The density segregation also plays an important role in the vibration-induced segregation. Hsiau et al. (2002) studied the convection feature of the vibration-

induced density segregation and obtained the velocity field shown in Figure 2-31. In addition, they also found that for binary granular mixtures, the vertical segregation could be amplified by increasing density ratio and vibration intensity (Hsiau and Chen 2002). Recently, they adopted different parking ratios and filling layers in the study of density segregation (Tai et al. 2010). It was found in their experiments that the convection mechanism dominated the vertical segregation when filling layers of the mixtures were higher, and heavier particles tended to migrate to the convection center when packing ratios increased. Based on the previous studies of the convection features, they also investigated the influence of base roughness and vibration parameters on the intruder's rise time (Liao et al. 2014), as shown in Figure 2-32. It was then concluded that with greater base roughness factor, the vertical segregation was weakened with longer rise times, which was contrary to the general knowledge that roughness of a wall surface can strengthen the vertical segregation.

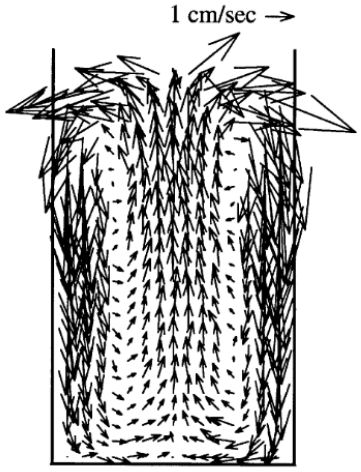

Figure 2-31 Velocity fields of the particles near the container wall. (Hsiau et al. 2002)

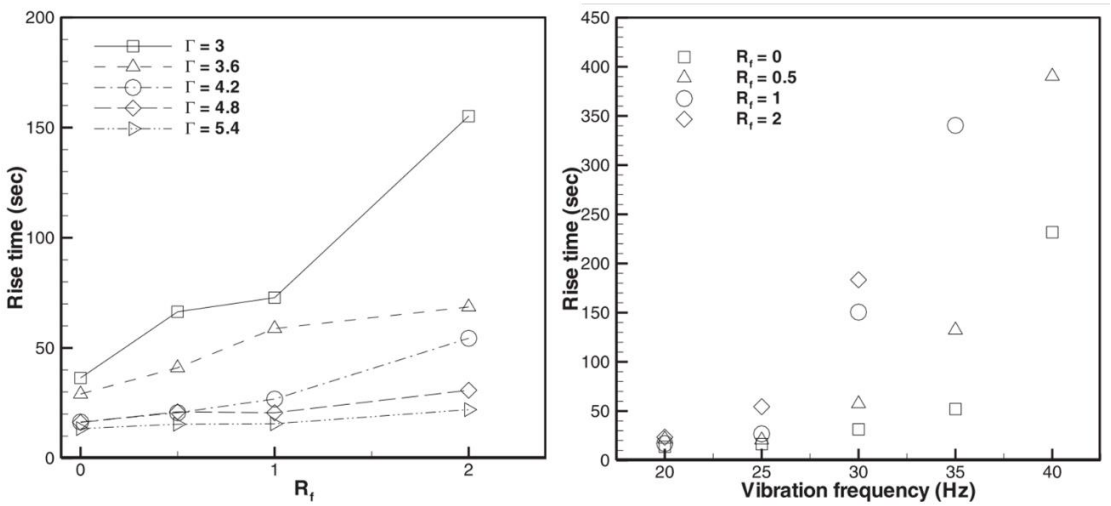

Figure 2-32 Rise time as functions of base roughness coefficient R_f, vibration acceleration Γ and vibration frequency. (Liao et al. 2014)

Huerta and Suarez (2004) systematically studied the factors influencing the motion of intruders cohesively with the triggering mechanism. Based on the density segregation experiments, they summarized that there were only three physical mechanisms dominating the vertical segregation. In detail, for cases with acceleration larger than 1, the inertia mechanism acts when the density of bed particles is lower than the density of the intruder particles, while the convection mechanism works when the density of bed particles is larger. The buoyancy mechanism only dominates when the granular bed is fluidized which requires small amplitudes and high frequency.

Shi et al. (2007) also investigated the density segregation with vertical vibrations. In their experiments, they used granular mixture of different densities and same sizes. The obtained segregated patternsare shown in Figure 2-33, which clearly

shows that the segregation gets stronger with larger density ratio. To better illustrate the experimental results, they also defined four typical patterns named as lighter-and-mixed state (LMS), purely segregated state (PSS), completely mixed state (CMS) and the throwing state. They generated a phase diagram (shown in Figure 2-34) for these patterns with respect to the vibration acceleration Γ, vibration frequency f and the material type of particles with larger density. This research confirms the findings that for situations with moderate density difference, the granular mixture will present a partially segregated state under vertical vibrations. This state demonstrates the pattern that lighter particles can form pure layers on the surface while heavier particles tend to segregate at the bottom.

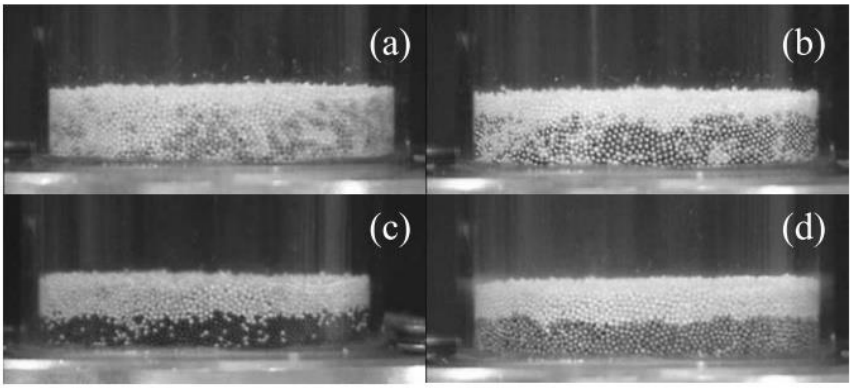

Figure 2-33 obtained segregation patterns with different granular mixtures. The particles with lower density are made of aluminum oxide (density=1.31g/cm^3) while the particles with larger density are made of (a) zirconium oxide (density=2.87g/cm^3), (b) titanium alloy (density=4.45g/cm^3), (c) cobalt-chromium-molybdenum alloy (density=8.37g/cm^3), and (d) tungsten alloy (density=18.0g/cm^3). (Shi et al. 2007)

Yang (2006) also experimentally studied the density segregation with vertical vibration, but the initial states of the granular mixtures were set to be horizontally segregated, and the time evolutions of the flow patterns are shown in Figure 2-35. The results show that the steel particles first move toward the center and then accumulate at the two convection central areas. In order to further investigate the particles' behavior, they also constructed numerical models to obtain the spatial distributions with different vibration acceleration. It was further concluded that the vibration intensity and the mixture's packing height can largely influence the segregation patterns. In detail, the segregation gets stronger with greater vibration intensity, while the mixing rate gets larger with greater initial packing height.

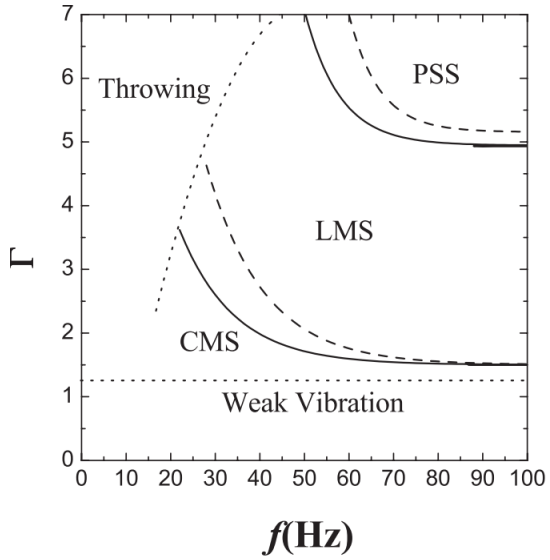

Figure 2-34 Phase diagram of the defined patterns in Γ versus f space. The results for mixture of aluminum oxide and cobalt-chromium-molybdenum ally, aluminum oxide and titanium alloy are shown as solid lines and dashed lines. (Shi et al. 2007)

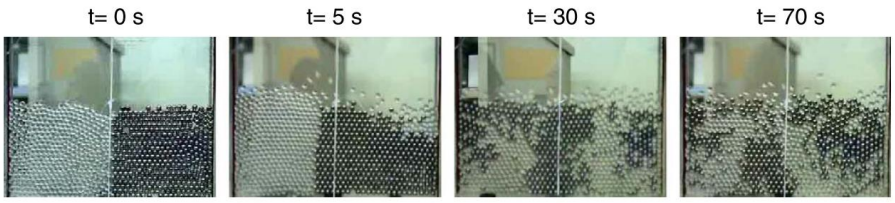

Figure 2-35 time evolution of the flow patterns for the binary mixture of steel-glass beads. (Yang 2006)

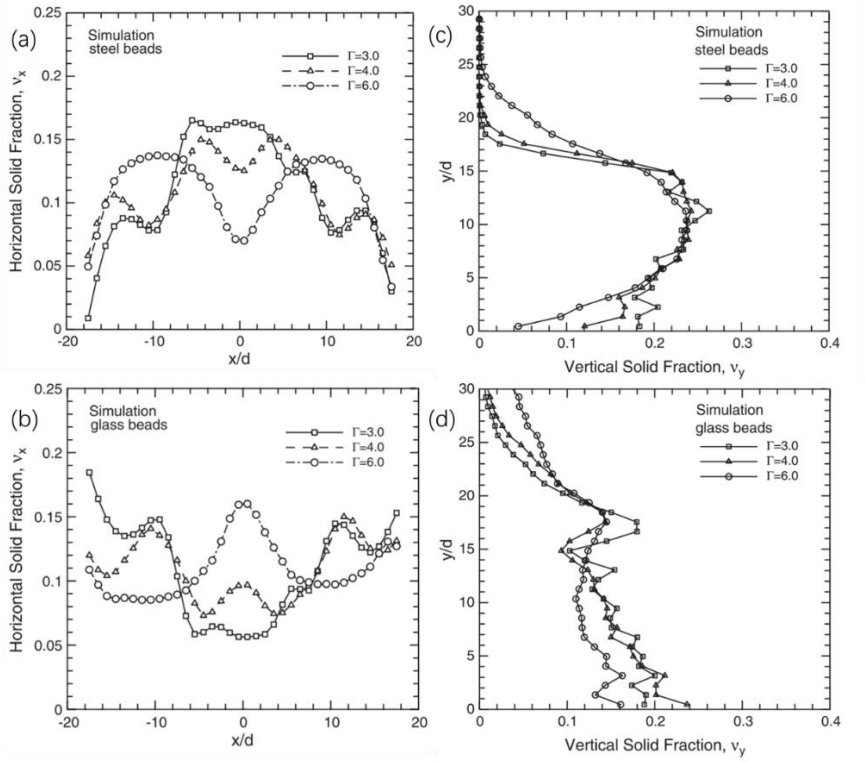

Figure 2-36 Effect of vibration intensity Γ on the solid fraction of the granular bed. (a) steel beads in horizontal direction; (b) glass beads in horizontal direction; (a) steel beads in vertical direction; (a) glass beads in vertical direction. (Yang 2006)

2.5.2 Simulation methods

Even researchers have developed various techniques to record and demonstrate the motion of particles within a vibrated bed, it is still impossible to capture the

comprehensive profiles of particles through physical experiments. Therefore it is both essential and sufficient to conduct numerical simulations to investigate the vibration-induced segregation.

Rosato et al. (1987) adopted the Monte Carlo method in the investigation of vertical segregation. In order to simulate the vibration process, they treated the shaking procedure as particles being lifted and then dropped to the bottom, therefore the continuous vibration process was modeled as separated numbers of shakes. Through simulations they successfully represented the Brazil-nut effect for cases with both one intruder and batches of intruders, the process configurations are shown in Figure 2-37 and Figure 2-38, respectively. It was concluded in this study that, the lateral shaking was not important in promoting segregation, while the shaking distance largely affect the segregation.

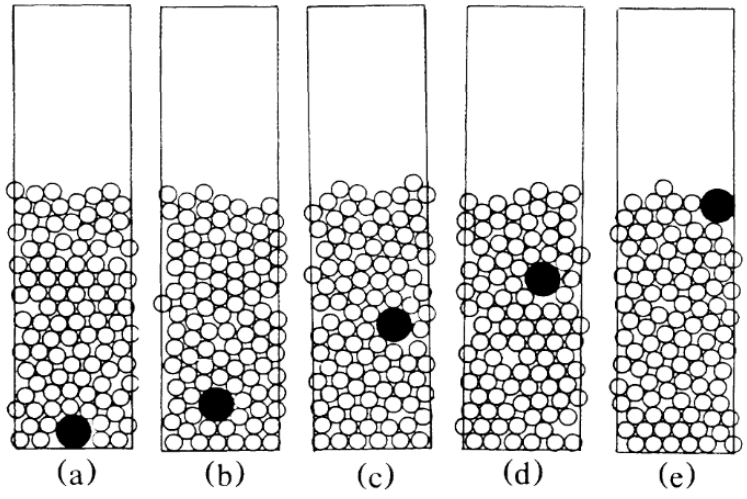

Figure 2-37 The configuration of the process for granular mixture with only one large particle. (Rosato et al. 1987)

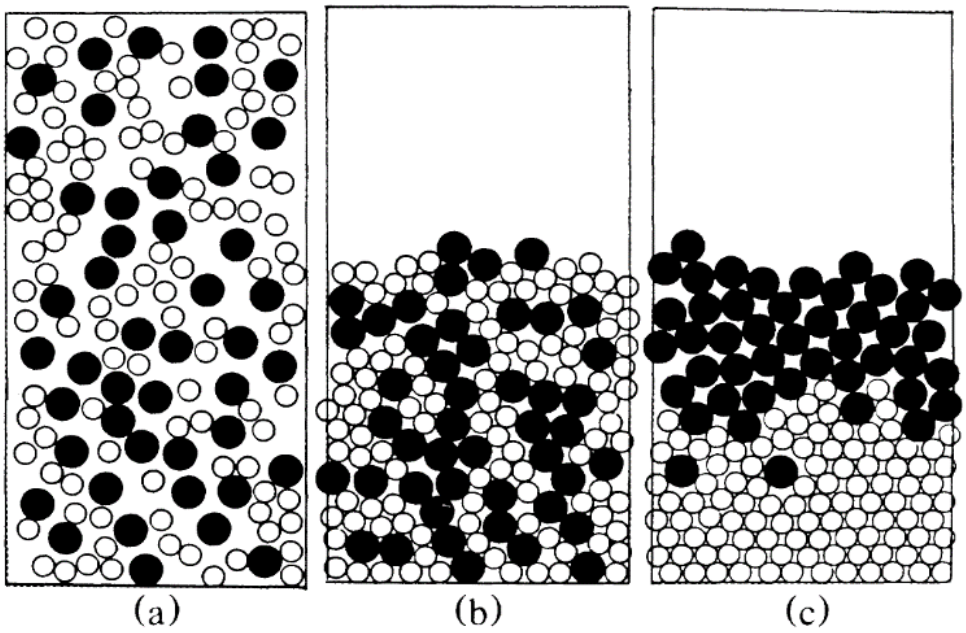

Figure 2-38 The configuration of the process for granular mixture with half small particles and half large particles. (Rosato et al. 1987)

Abreu et al. (2003) also applied the Monte Carlo method to simulate this segregation issue. In their simulations, they constructed the model in three dimensions and adopted binary granular mixtures of spherocylinders with identical density to investigate the effects of particle shape and particle size, and the patterns observed are shown in Figure 2-39. It was concluded from their work that when granular mixture contained particles with same volume but different shapes, the granular bed tended to maintain at the level with lowest potential energy which made the particles with lower mixing porosity to segregate at the bottom. And for cases with granular mixture of different volumes, the segregation pattern was decided by particle size rather than particle shape, which enabled the Brazil-nut effect that larger particles tended to accumulate at the top. In addition,

even the Brazil-nut effect may result in a higher level of system potential energy, it still dominates the segregation pattern for granular mixtures with different volumes.

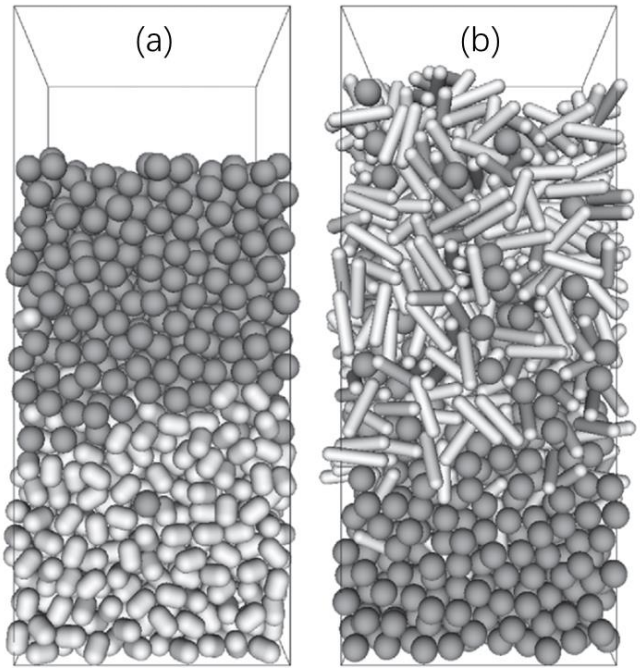

Figure 2-39 Three-dimensional flow patterns of two granular mixtures with same densities and volumes. (Abreu et al. 2003)

Poschel and Herrmann (1995) applied Molecular Dynamics in their simulations, and their finding further confirmed the importance of convection for vibration-induced segregation. They stated that the convection cells were even observable for cases with very low frequencies, and the convection could be triggered by the single intruder itself.

As the methods previously discussed may not be able to offer detailed force and velocity profiles, Lan and Rosato (1997) adopted the discrete element method for

further simulation studies. Through the simulations, they obtained the configurations of the velocity fields (shown in Figure 2-40) for the whole particulate bed and the motion trajectory of the large intruders (shown in Figure 2-41). These results first confirmed the convection mechanism as the velocity field showed a vortex-like feature throughout the bed, and it was then found that the convection phenomenon was relevant to the product term of vibration amplitudes and acceleration rather than the acceleration alone. Based on these findings, they further investigated the mechanisms triggering the segregation, and they concluded that the vibration-induced segregation was still triggered by the void-filling mechanism while convection sufficiently enhanced this phenomenon (Rosato et al. 2002).

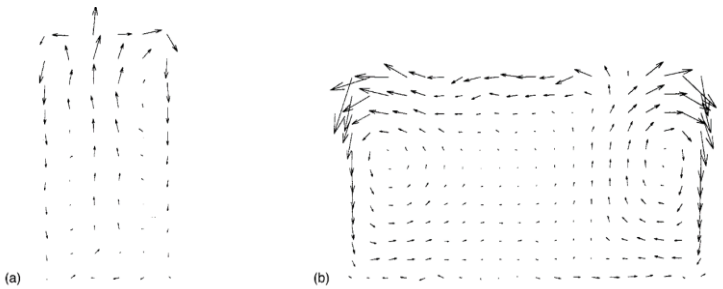

Figure 2-40 Long term velocity field of the granular bed. (a) bed width=6 small particle diameters; (b) bed width=20 small particle diameters. (Lan and Rosato 1997)

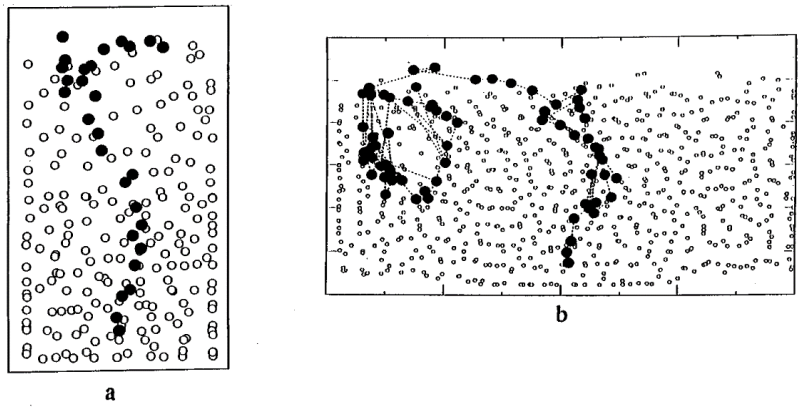

Figure 2-41 The trajectory of the large intruder throughout the vibration process. (a) bed width=6 small particle diameters; (b) bed width=20 small particle diameters. (Lan and Rosato 1997)

Fernando and Wassgren (2003) also used the discrete element method to interpret their observations from physical experimetns. The dimensionless rise rate was applied to demonstrate the motion of the large intruder, and the effects of vibration acceleration and amplitude were illustrated in Figure 2-42. It was concluded that at discrete vibration conditions, the rise rate significantly increased with increasing vibration velocity amplitude while the continuous vibration condition can result in a maximum value for rise rate.

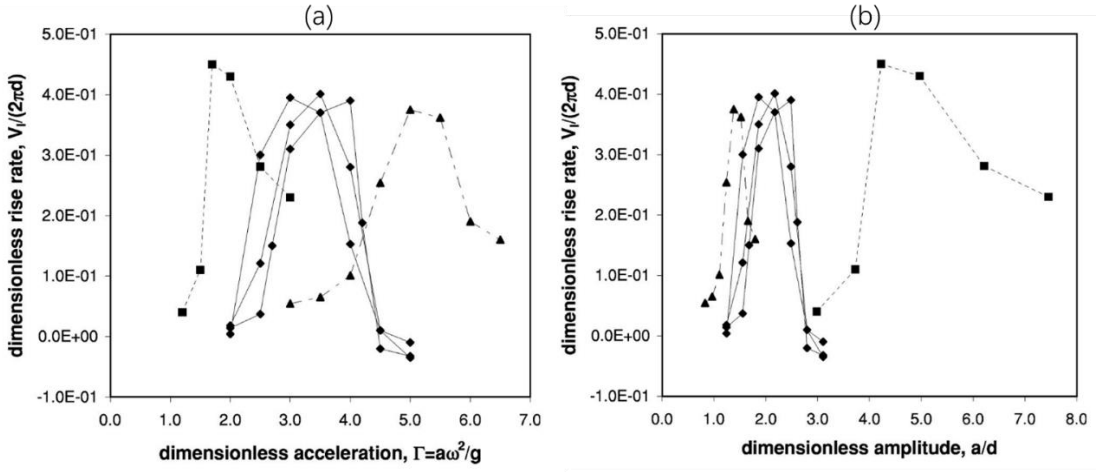

Figure 2-42 The average dimensionless rise rate of the intruder against (a) dimensionless vibration acceleration and (b) dimensionless vibration amplitude. The dimensionless frequencies are set as 0.6 (■), 1.3(◆), and 1.9 (▲). (Fernando and Wassgren 2003)

With the help of the discrete element method, Yang (2006) explored the density effects on the vibration-induced segregation. Their simulation results showed that convection mechanism was also significant for density segregation.

Fang and Tang (2007) did a comprehensive study on the vibration-induced segregation with the help of discrete element method. Considering the influencing factors, they studied various factors including size ratio, density ratio, initial depth of the intruder, and the vibration coefficients (acceleration, frequency, amplitude. The results of the parameter studies are shown in Figure 2-43, Figure 2-44 and Figure 2-45. In addition, they also investigated the triggering mechanisms under different circumstances. For weak vibration, the vertical segregation is decided by

the competition between percolation mechanism and gravity induced inertia; for moderate vibration, the convection motion within the granular bed dominates the occurrence of segregation phenomenon; for strong vibration, the granular bed may get fluidized which may weaken the segregation phenomenon.

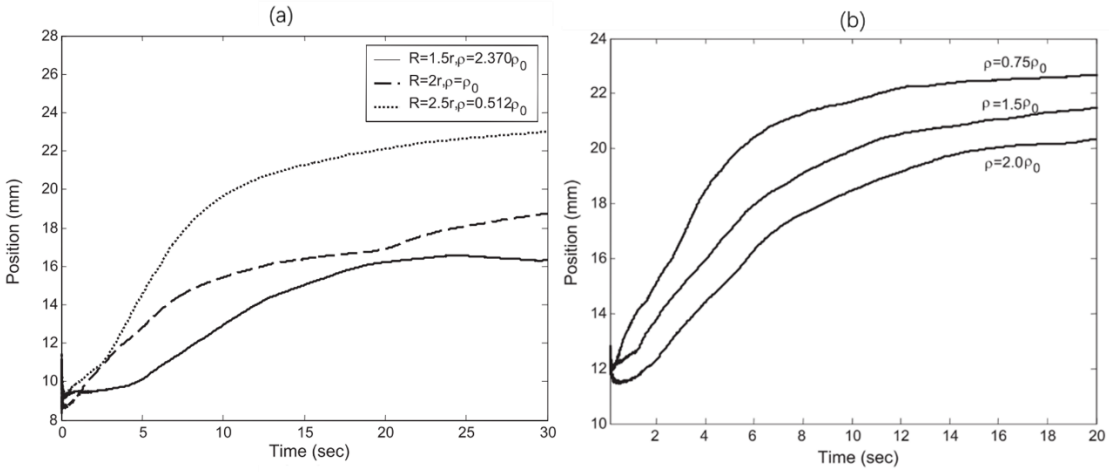

Figure 2-43 Time evolution of the vertical coordinates of the intruder when vibration amplitude A=2mm and frequency f=20Hz. (a) Granular mixture with different size ratio and density ratio; (b) Granular mixture with different density ratio but same size ratio. (Fang and Tang 2007)

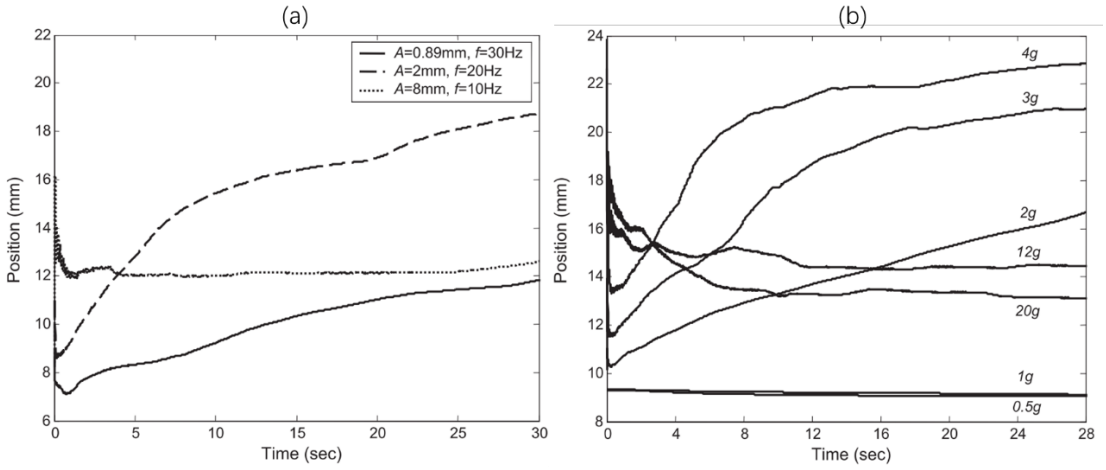

Figure 2-44 Average vertical coordinate of the intruder over the simulation time when size ratio equals 2 and no density difference. (a) Granular mixture with different vibration amplitudes and frequencies; (b) Granular mixture with different vibration acceleration when vibration frequency f=20Hz. (Fang and Tang 2007)

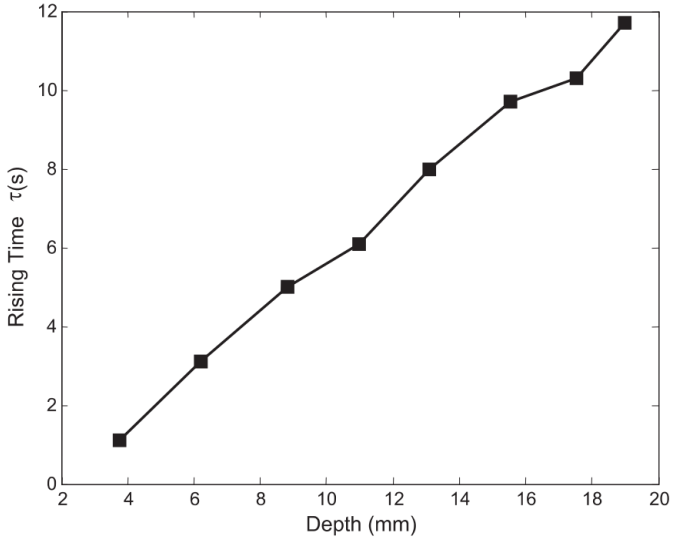

Figure 2-45 Rising time of the intruder with different initial depth when size ratio equals to 2 and no density difference. The vibration coefficients are set as, f=20Hz and A=2mm. (Fang and Tang 2007)

2.6 Summary

This Chapter fully reviewed the experimental work and numerical simulations about two typical granular segregation phenomena, stockpile segregation and vibration-induced segregation. For the cases of stockpile segregation and stratification, the previous researches have mainly focused on the studies of the influencing mechanisms for specific phenomena and the associated parameter studies, while there is still lack of researches in interpreting a physical mechanism in respect to illustrate the segregation and stratification together. In addition, as physical experiments have pointed out the possible effects of particle shape in segregation issues, it is of great significance to conduct numerical simulations on investigations of the shape effects due to the convenience in accurately controlling the shape coefficient. For the cases of vibration-induced segregation, although various parameters have been studied through experiments and simulations, it is still essential to further explore the effects of vibration conditions in rather extreme situations, and as the effects of particle shape haven't been fully understood, the use of discrete element method may help to further illustrate the shape effects on vertical segregation.

Considering the several research gaps, this project applies both physical experiments and discrete element method to systematically study the stockpile segregation and vibration-induced segregation. The specific objectives and research overviews are as followed:

1) Investigate the fundamental mechanism triggering the stockpile stratification and segregation with binary spherical mixtures, and conduct associated parameter studies on specific segregation processes. This part of work will be presented in Chapter 3.

2) Study the shape effect on stockpile segregation with a DEM based ellipsoidal model and related physical experiments, and further interpret the physical mechanism considering the non-spherical mixtures cases. This part of work will be presented in Chapter 4.

3) Study the vibration-induced segregation with only one large intruder using the discrete element method. Explore the fundamental mechanism and further study the influencing parameters including high frequency and high amplitude cases. This part of work will be presented in Chapter 5.

4) Study the vibration-induced segregation with more than one intruders using the discrete element method. Explore the effects of particle shape on vertical vibration and study other influencing parameters including high frequency and high amplitude cases. This part of work will be presented in Chapter 6.

Chapter 3 Stockpile segregation and stratification of spherical particles

3.1 Introduction

The mixing states of granular stockpiles are generally classified as segregation and well mixing. Fan et al. gave a new understanding and introduce stratification into the classification, as shown in Figure 3-1.

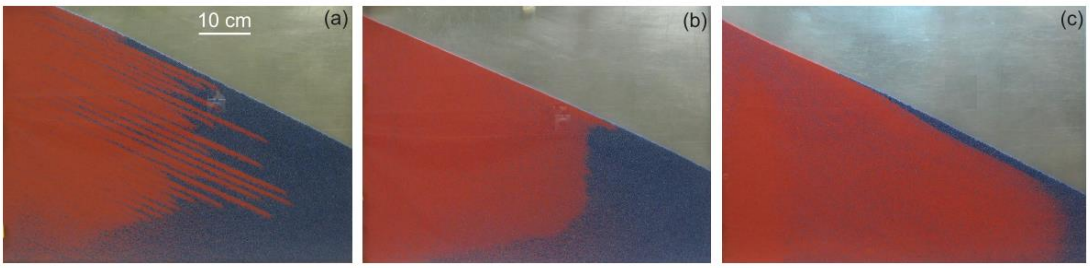

Figure 3-1 Three final particle configurations of bidisperse granular mixtures in quasi-2D heap flow. (a) stratification; (b) segregation; (c) near complete mixing

Stratification was also regarded as a special case of segregation. Different from the normal segregation that particles simply segregate to the stockpile bottom or top, stratification describes a situation when particles of different properties form several different layers inside the stockpile. A comprehensive study has been made about this phenomenon using particle of different shapes, and it was found that the difference in repose angles triggers the stratification behavior (Makse et al. 1997, Makse 1998, Makse et al. 1998, Cizeau et al. 1999). Recently, Benito et al. (Benito et al. 2014) conducted physical experiments to study the pile segregation, and it was claimed that stratification could also be observed with spherical particles. However, further numerical study considering the stratification with spherical particles still needs to be put efforts on. Here we use a DEM model to

simulate this situation. Except for a validation of Benito et al's results, the profiles approached from the DEM calculation can also help to investigate the inside mechanism triggering the stratification and segregation. Furthermore, a detailed parameter study will also be conducted considering size ratio, injection height and mass ratio. And in order to give a quantified conclusion about these factors' influence, a segregation index is used to define the mixing state and segregation extent of the stockpile.

The primary aim for this part is to build an eligible and trustable model for future studies of particle shapes. With the spherical model, mechanism of segregation and stratification is also investigated considering several influencing factors. Furthermore, if the mechanism introduced is correct, it can help to understand the segregation of ellipsoids, which will further contribute to the development of practical techniques.

3.2 Research Methods

3.2.1 Discrete element method (DEM)

The simulations were conducted based a spherical DEM model built by Zhou et al. (1999). The granular materials in this model are semi-rigid particles and the interaction is dominated by contact forced. The translational and rotational motion is described by Newton's law of motion. The governing equations describing the interaction between particle *i* and *j* are as follows:

$$m_i \frac{d\mathbf{v}i}{dt} = \sum_{j=1}^{k} \left(\mathbf{f}_{c,ij} + \mathbf{f}_{d,ij}\right) + m_i \mathbf{g} \tag{3.1}$$

$$I_i \frac{dwi}{dt} = \sum_{j=1}^{k} T_i \tag{3.2}$$

where $\mathbf{v}_i$ and $\boldsymbol{\omega}_i$ are the translational and angular velocities of particle i, respectively. k is the number of particles contacting with particle i, while m_i and I_i are the mass and moment of inertia of the particle, respectively. The acting forces and torques are schematically shown in Figure 3-2, which includes gravitational force $m_i\mathbf{g}$, elastic force $\mathbf{f}_{c,ij}$, viscous damping force $\mathbf{f}_{d,ij}$, torque T_i generated by inter-particle forces. The equations used to calculate these forces and torques are summarized in Table 3-1, and detailed descriptions can be referred in Zhou et al. (1999).

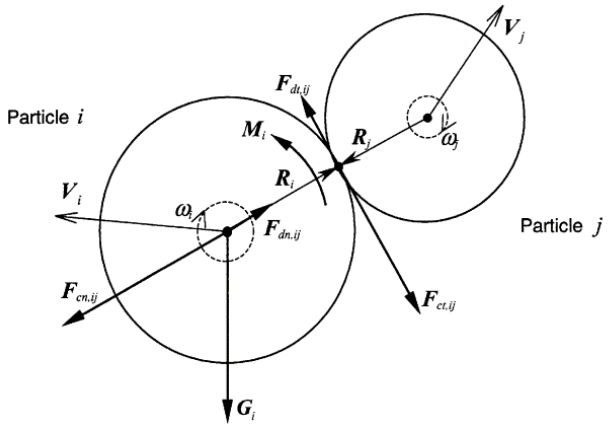

Figure 3-2 Illustration of the forces acting on particle i in contact with particle j. (Zhou et al. 1999)

Table 3-1 Equations used in numerical simulations

Forces and torques		Symbols	Equations
Normal elastic force		$\mathbf{f}_{cn,ij}$	$-4/3E^{*}\sqrt{R^{*}}\delta_n^{3/2}\mathbf{n}$
Normal damping force		$\mathbf{f}_{dn,ij}$	$-c_n(V_{ij}\cdot n)n$
Tangential elastic force		$\mathbf{f}_{ct,ij}$	$-\mu_s\lvert\mathbf{f}_{cn,ij}\rvert(1-(1-\delta_t/\delta_{t,\max}{}^{3/2})\hat{\delta}_t$, $(\delta_t<\delta_{t,\max})$
Rolling	Damping	$\mathbf{f}_{dt,ij}$	$-c_t(V_{ij}\times n)\times n$
	Torque	T_i	$R_i\times(\mathbf{f}_{ct,ij}+\mathbf{f}_{dt,ij})$
	Friction torque	M_i	$-\boldsymbol{\mu_r}\mathbf{f}_{dn,ij}\widehat{\boldsymbol{\omega}}_{\boldsymbol{i}}$

where $\frac{1}{R^*}=\frac{1}{R_i}+\frac{1}{R_j}$, $\mathbf{E}=\frac{E}{2(1-\nu^2)}$, $\boldsymbol{V_{ij}}=\boldsymbol{V_j}-\boldsymbol{V_i}+\boldsymbol{\omega_j}\times\boldsymbol{R_j}-\boldsymbol{\omega_i}\times\boldsymbol{R_i}$

$\widehat{\boldsymbol{\omega}}_{\boldsymbol{i}}=\frac{\boldsymbol{\omega_i}}{\boldsymbol{\omega_i}}$, $\mathbf{n}=\frac{R_i}{R_i}$, $\boldsymbol{\delta_{t,max}}=\boldsymbol{\mu_s}\frac{2-\nu}{2(1-\nu)}\boldsymbol{\delta_n}$, $\boldsymbol{M_i}$ describes the rolling resistance.

3.2.2 Simulation Conditions

The simulated problem is shown schematically in Fig. 1. The device includes two parts: a particle injection device and a receiving box ($200mm\times100mm\times5mm$). During the growth of the stockpile, the distance between injection surface and top of stockpile (injection height) was set constant by moving the injection surface vertically during the stockpile formation. Specifically for this work, the injection height is set as either 10mm or 50mm to study its effects on pattern formation.

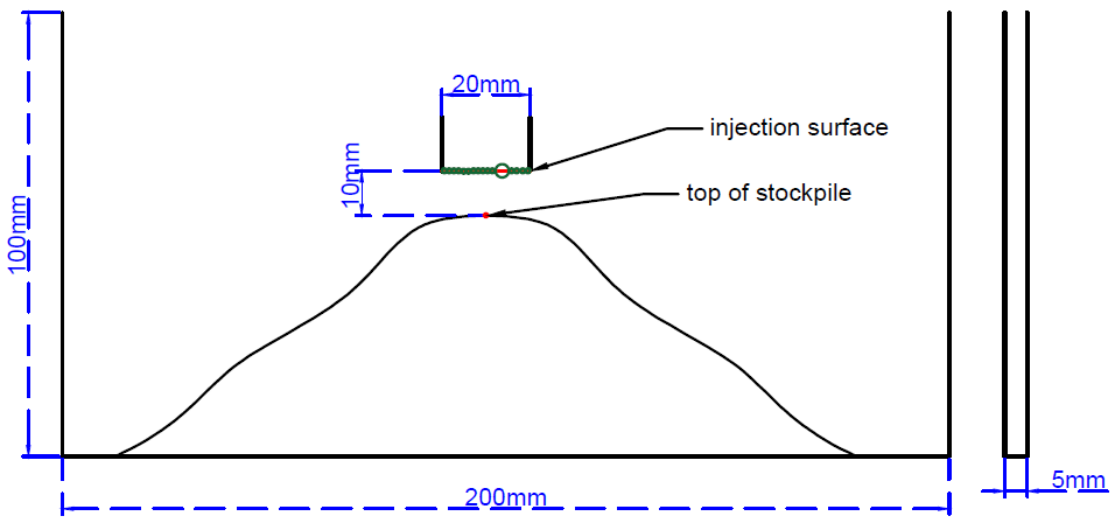

Figure 3-3 Schematic diagram of the simulation conditions. (Injection surface: the surface where particles are generated and released; top of stockpile: the highest point of the formed stockpile)

The binary granular mixtures used in the simulations are formed by spherical particles of two different size ratios (1mm and 3mm, 2mm and 3mm). The mass ratio R (the total mass ratio of the two species which also represents the flow rate ratio of large particles versus small particles) was set to be 0.5 or 1. Other physical properties of the particles were set to those of glass beads. The reason for choosing glass beads as the standard particle is due to their wide applications in real life, and as none of glass beads' physical properties is showing unreasonable anomalies, it is then well accepted to set them as standard particles. Details of the input variables and their values are shown in Table 3-2.

Table 3-2 Simulation conditions and related parameters

Input variables	Value
Size ratio	3:2.7, 3:2.3, 3:2, 3:1.5, 3:1
Injection height /mm	10, 20,30, 40, 50
Mass ratio	0.3, 0.5, 0.8, 1, 1.5
Simulation timestep	10^{-3}s
Young's module	1×10^8 N/m^2
Poisson's ratio	0.3
Sliding coefficient (P-P)	0.4 (standard), 0.1, 0.2, 0.3, 0.6, 0.9
Sliding coefficient (P-W)	0.4 (standard), 0.1, 0.2, 0.3, 0.6, 0.9
Rolling coefficient (P-P)	0.3 (standard), 0.01, 10
Rolling coefficient (P-W)	0.3 (standard), 0.01, 10
Particle density	2.7×10^3 kg/m^3
Particle number	20,000
Flow rate	0.1g/s

3.2.3 Physical experiments

The physical experiments were carried out using the transparent three-dimensional container shown in Figure 3-4 (a). The width of the slot is 20mm and which was around 7 times the diameter of large particles. The granular materials used in the experiments are spherical grains with density around 2.7×10^3 kg/ m^3, the surface properties of the particles are similar as the properties of glass beads. The granular materials were injected through a ball valve. These physical

experiments can only offer qualitative information to validate the DEM model. Further quantified studies will be conducted mostly based on the numerical simulations.

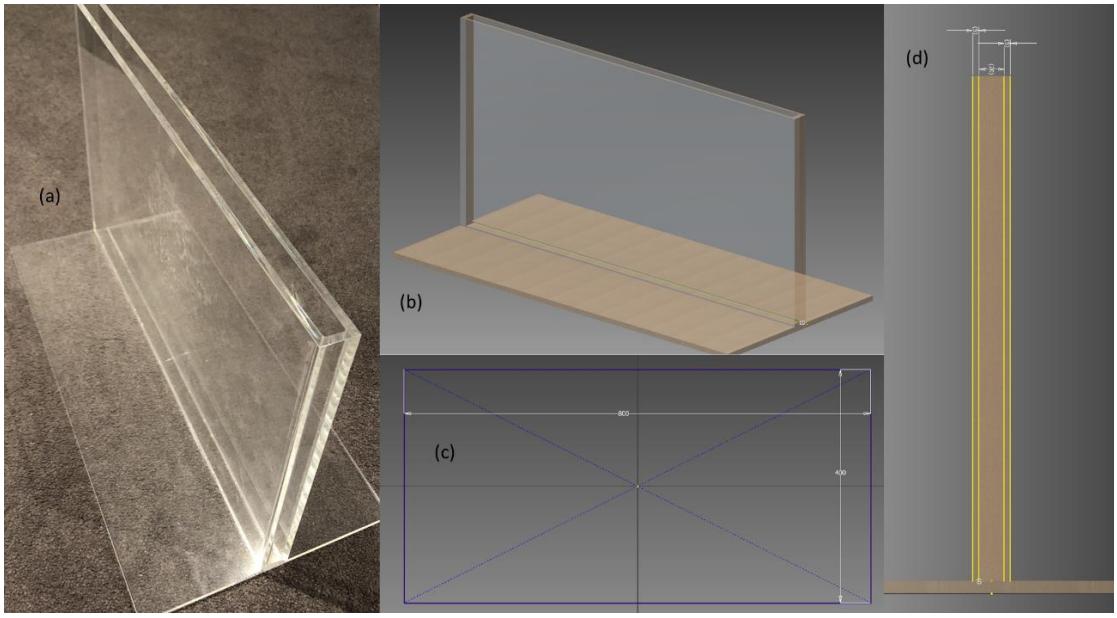

Figure 3-4 Container used for physical experiments (a) and its CAD designs (b) (c) (d).

3.3 Results and Discussions

3.3.1 Model validations

To verify the DEM model, physical experiments corresponding to several typical simulation conditions were conducted. In order to test the accuracy of the numerical model, binary grains of spherical particles with size ratio 3:1 were injected into the two-dimensional silo. The flow patterns were recorded by camera during the stockpile formation, and a comparison between simulation and experiment results is shown in Figure 3-5. It can be clearly observed from the

results that the simulated patterns successfully reproduce the stratification phenomenon as well as the normal segregation.

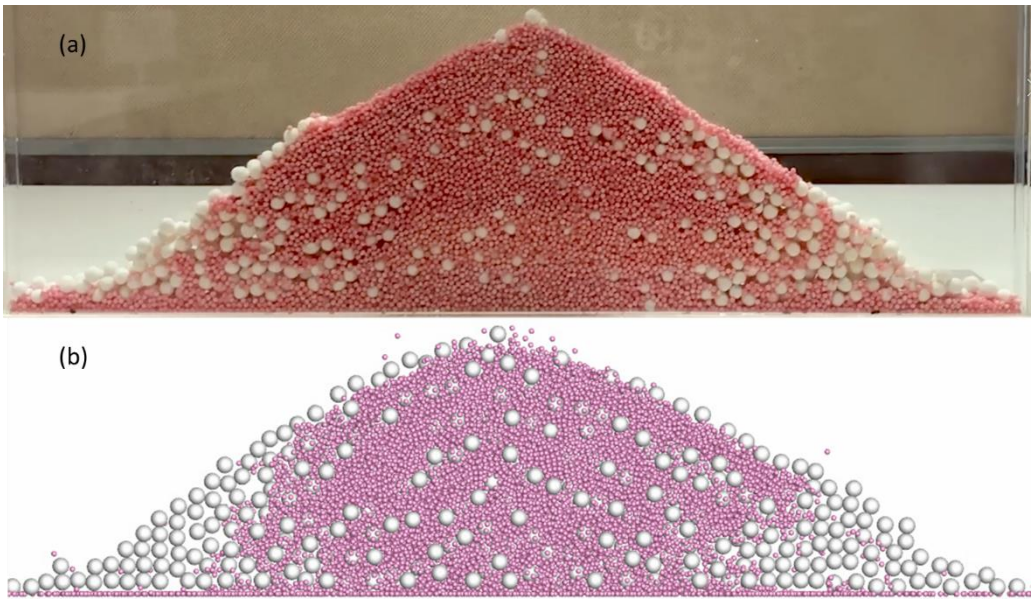

Figure 3-5 Schematic comparison between (a) physical experiments and (b) numerical simulations. The granular mixture contains spherical particles with 1mm and 3mm as particle diameter. The injection height is 10mm and mass ratio of the two species is 1:1. Pink grains: small particles; White grains: large particles.

3.3.2 Void-filling mechanism

3.3.2.1 Stratification

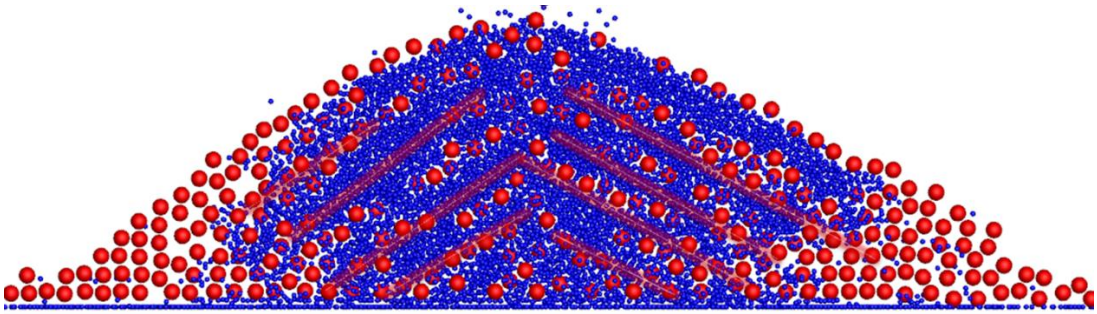

Figure 3-6 Obtained stockpile patterns with binary spherical mixture. (size ratio 3:1, mass ratio 1:1, injection height 10mm)

As shown in Figure 3-6, particle stratification can be easily observed. This stratification phenomenon can be explained by a void-filling mechanism which has been used to explain the situations in chute flow and vibrated granular beds (Savage and Lun 1988, Arshad 2004). When particles of different sizes are mixed together within an active system, this mechanism presents the process that gravity and inertia which drives small particles to sink or percolate into the voids between large particles instead of flowing on the particle surface. Figure 3-7 shows the specific situation for the stockpiling process. When pouring well mixed granular mixtures onto a flat surface to form a pile, the small particles percolate into the voids while large particles are able to flow on the top of the surface. This difference in motion will then cause the accumulation of small particles between large

particles, thus dividing the large particles into separate single layers. The lower layer remains motionless while the upper layer is free to slide until the particles reach a "block".

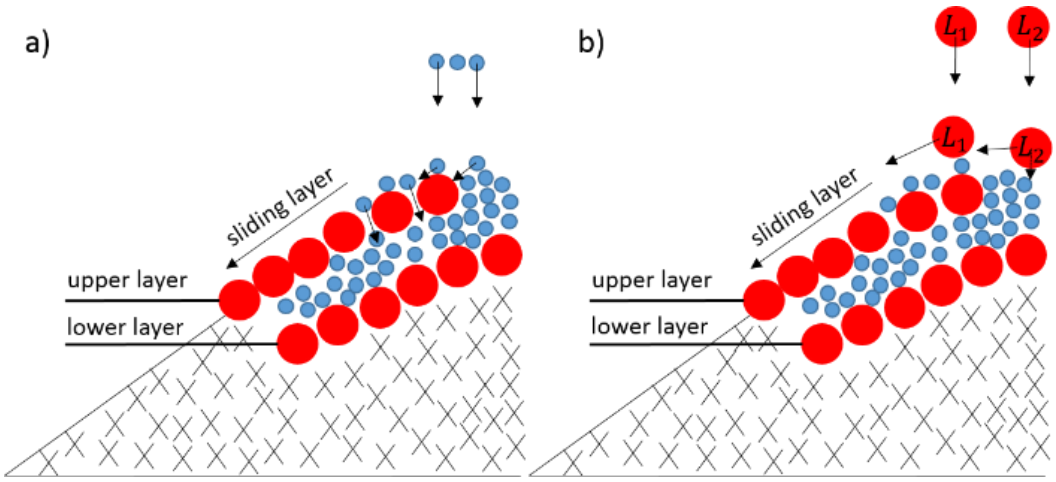

Figure 3-7 Comparison of the motion of different particles: (a) motion of small particles; (b) motion of large particles

The "block" is a special area within the region where the void-filling process occurs. With the growth of the stockpile, available voids for small particles to fill into become fewer and the porosity of the area decreases. When some critical points have extremely low porosity, the void-filling process will then stop. The area with extremely low porosity has a high resistance to flow and represents the "block". Figure 3-8 shows the "block" inside the stockpile identified from spatial distribution of porosity. The spatial porosity is defined as: $1 - \frac{total\ volume\ of\ particles}{total\ volume}$, and the porosity is calculated in each meshed part. The size of the mesh is $1.5d \times 1.5d \times w$ (d represents the diameter of the large spheres,

and *w* represents the thickness of the piles).

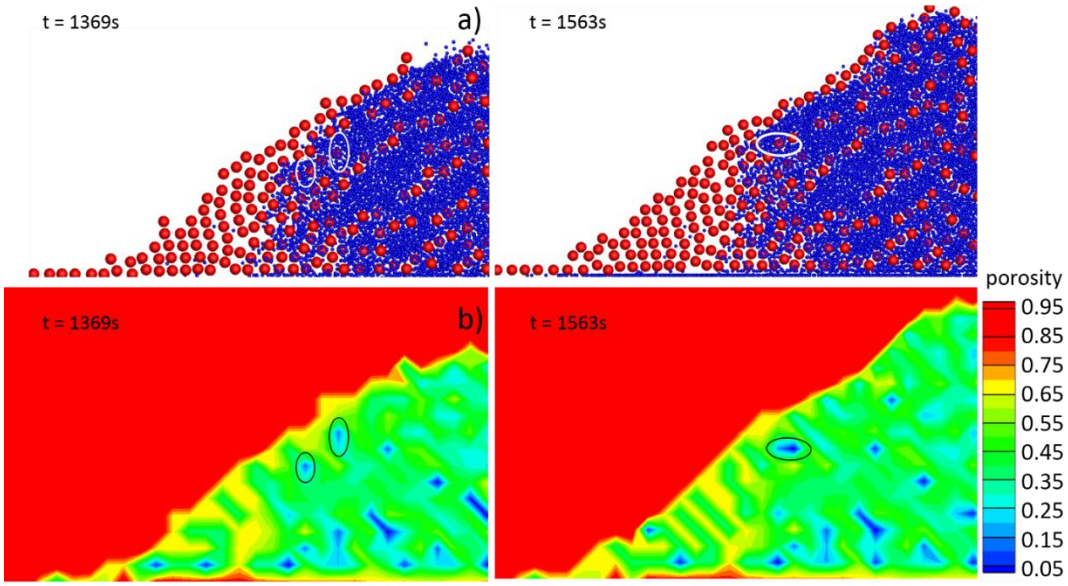

Figure 3-8 (a) Stockpile particle distribution patterns and (b) porosity spatial distribution when the void-filling process stops. The figures were captured at 2 different times (t = 1369s and t = 1563s); the circled area is where "block" is located; particle sizes have been scaled in the figure (scale factor = 0.7).

As the "block" stops the small particles' penetration motion, the outer layer of the stockpile becomes more instable as additional particles drop onto the pile. This instability then causes further avalanche of the outer particles, especially for large particles. This avalanche behaviour consequently reforms the distribution of outer particles and removes the "block", which will then reinitiate the void-filling process and successively regenerates the stratification phenomenon leading to the regular layered stratification pattern.

The regular motion of large particles is shown schematically by particle L1 in

Figure 3-7b. These large particles tend to flow onto the particle surface until reaching the pile bottom or forming the sliding layer until a “block” is formed. However, there is still another type of particle motion that should considered. Sometimes, for large particles like L2, their inertia drives them to sink into the pile and subsequent burial by the later particles. Such particles remain motionless within the pile and their presence can be used to explain the irregular distribution of some large particles at the centre area of the stockpile.

The mechanisms discussed above can be used to explain the effects of different parameters on stratification. It was also found that stratification cannot be observed for cases with large injection height and small size ratio. For large injection height, it will significantly influence the impact velocity when particles drop on the stockpile, as large particles with higher impact velocity will easily percolate into the pile instead of flowing on the particle surface. As mentioned above, this motion will then cause the irregular distribution of large particles within the stockpiles instead of the stratification. For size ratio, as stratification is mainly driven by the void-filling mechanism, available voids can be the most important factor for triggering this process. Lower size ratio will make the voids comparably smaller for small particles which increases the difficulty for them to enter the available voids. This decrease of available voids will then weaken the void-filling process, thus decreasing the stratification.

3.3.2.2 Segregation

Segregation specifically represents the phenomenon that large particles tend to segregate at the bottom of the stockpile. This phenomenon can be clearly observed from the patterns simulated in Figure 3-6.

As shown in Figure 3-7 the void-filling mechanism differentiates the motion of particles with different sizes. For large particles, gravity and inertia drive them to flow onto the particle surface, and consequently, large particles will segregate to the bottom of the pile. Similarly, when the particles avalanche following the formation of a "block", the outer particles also flow to the bottom. Such avalanches also result in the segregation of large particles as the outer particles are mostly large particles as the small particles are more likely to percolate inside. This finding is also consistent with Drahun and Bridgewater's experiments with free surface flow (Drahun and Bridgwater 1983).

3.3.3 Segregation index

A common method to quantify the mixing quality of a granular mixture is the mixing index. Different researchers have given different definition for this index. As mixed is the opposite state of segregated, here we introduce a segregation rate based on a mixing index previously introduced by Lacey (1997) and Feng et al. (2004). The segregation rate is given by

$$M = 1 - \frac{{S_0}^2 - S^2}{{S_0}^2 - {S_R}^2} \tag{3.17}$$

Where S^2 is the actual variance, while ${S_0}^2$ and ${S_R}^2$ are the variances of the completely segregated and completely mixed states, respectively. Therefore, a completely segregated mixture will have M as 1, and well mixed mixture will have M as 0. More details about the related mixing index can be found in Feng et al.'s work (Feng et al. 2004).

3.3.4 Parameter studies of segregation

The studied parameters include injection height, mass ratio, size ratio, and friction coefficients.

Injection height is the distance between particles injection point and the top of pile. The value of it is set constant for every case by adjusting the injection point when pile grows. By changing this parameter, the initial velocity of particles when they fall onto the pile will be changed. From Figure 3-9, it can be observed that injection height does not contribute to the segregation rate which means it will not affect the overall mixing state of the particulate system. But from Figure 3-10, it can be clearly observed that larger injection height does not associate with stratification phenomenon. The potential cause is related to the void-filling mechanism which is talked about in previous sections.

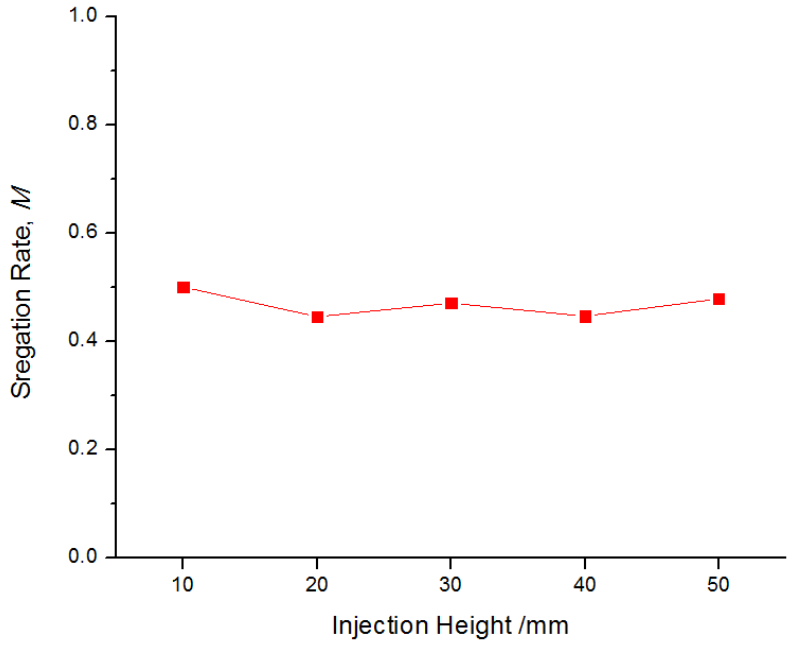

Figure 3-9 Effects of Injection Height on segregation rate

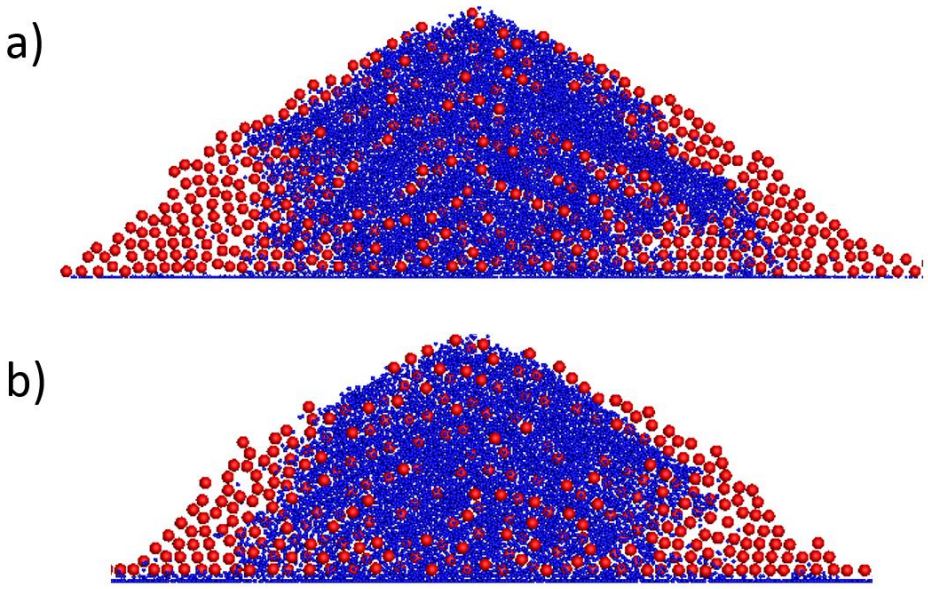

Figure 3-10 Obtained stockpile patterns (size ratio 3:1, mass ratio 1:1): (a) Injection height 10mm and (b) Injection height 50 mm

Mass ratio is another important factor affecting the stockpile formation. It represents the total mass of large particles versus the total mass of small particles.

More specifically, it represents the ratio of the different feeding rates of the two particles. As talked about in the void-filling mechanism, the cause of stratification and segregation is related to small particles' percolating behavior. Moreover, the motion of large particles can disturb the percolation of small particles. Therefore, with the increase of mass ratio, the disturbance of large particles will get stronger which will lead to the decrease of stratification and segregation.

As shown in Figure 3-11, segregation rate remarkably decreases when mass ratio increases, which is consistent with the above prediction. The stratification was also weakened and almost disappeared when mass ratio reaches 1.5 as presented in Figure 3-12.

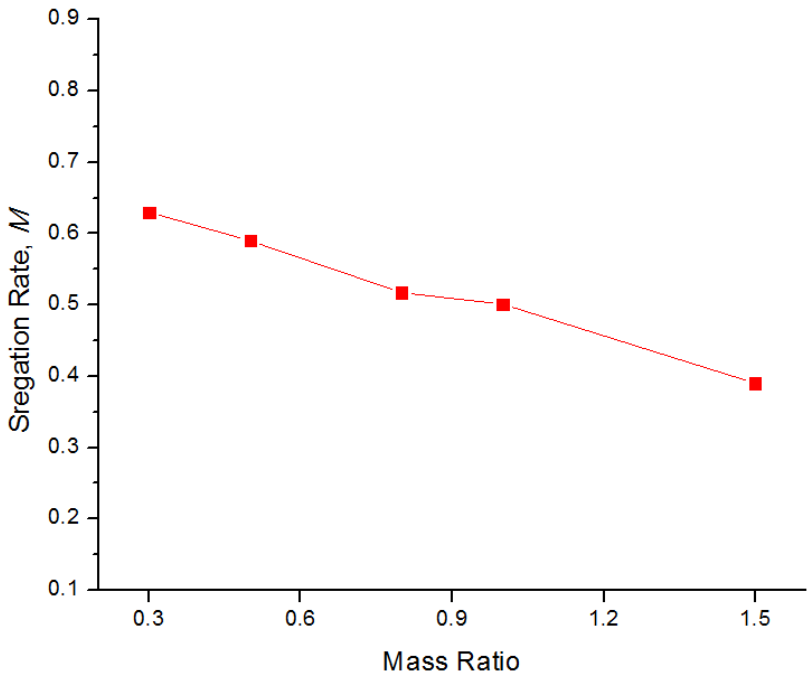

Figure 3-11 Effects of Mass Ratio on segregation rate

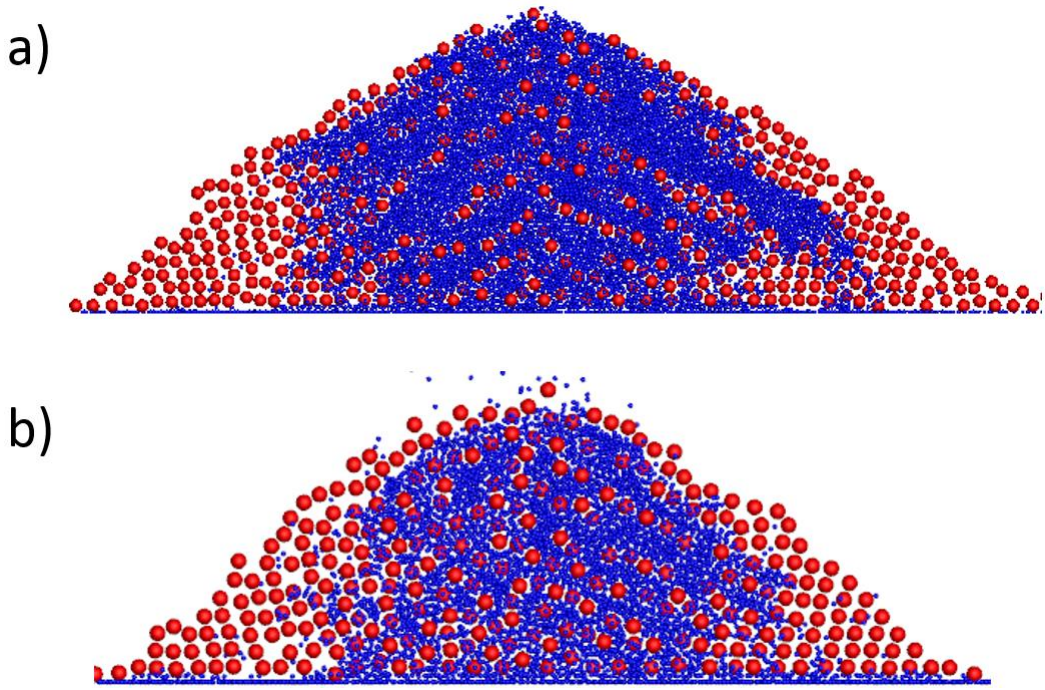

Figure 3-12 Obtained stockpile patterns (size ratio 3:1, injection height 10mm): a) mass ratio 1 and b) mass ratio 1.5

Size ratio has been regarded as the dominant factor influencing the segregation. In this work, several values of size ratio ranging from 3:2.7 to 3:1 were tested. We believe that the occurrence of segregation sensitively corresponds to the size difference. And it was confirmed from Figure 3-13 that segregation rate shows a continuous increase with the increase of size difference. Instead of trying to find a critical size ratio of segregation, we believe segregation happens gradually without an obvious trigger. Johanson (1996) reported a critical size ratio of 2:1, but as shown in Figure 3-14, even when size ratio is only 3:2.3, segregation can still be slightly observed.

But the stratification phenomenon presents a strict requirement on size ratio.

Among the values tested, only mixtures with size ratio 3:1 shows an obvious stratified pile. This finding is generally consistent with the finding of Benito et al. (2013), where they reported that stratification only happens with a large size ratio when it comes to spherical particles. Considering the possible reasons for this observation, we believe that although the void-filling mechanism might be satisfied even for smaller size ratios, stronger void-filling behavior is needed to form layered patterns. Another possible reason might come from the limitation of this model as the he simulations were conducted in a slot model where the thickness is comparably small.

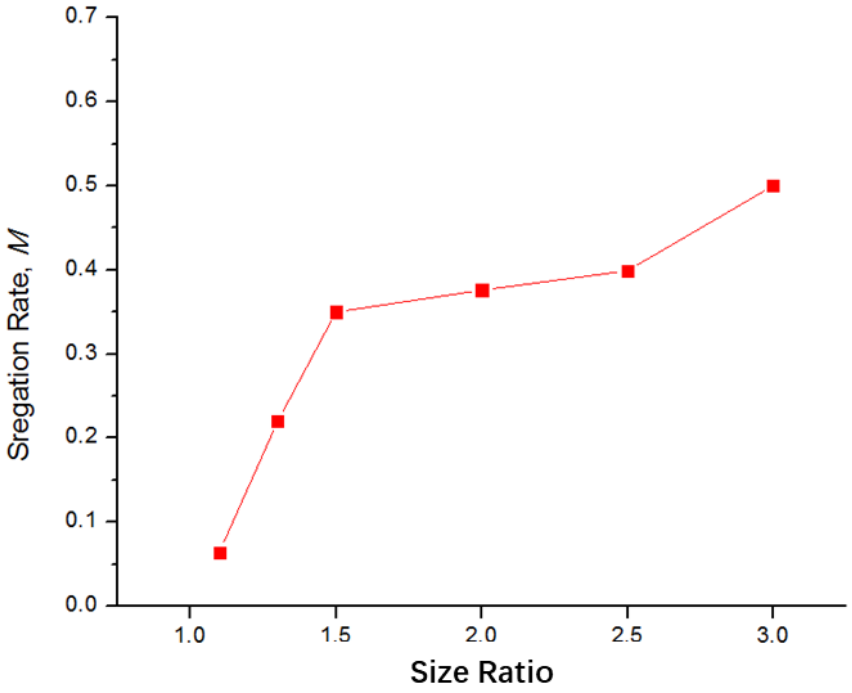

Figure 3-13 Effects of Size Ratio on segregation rate

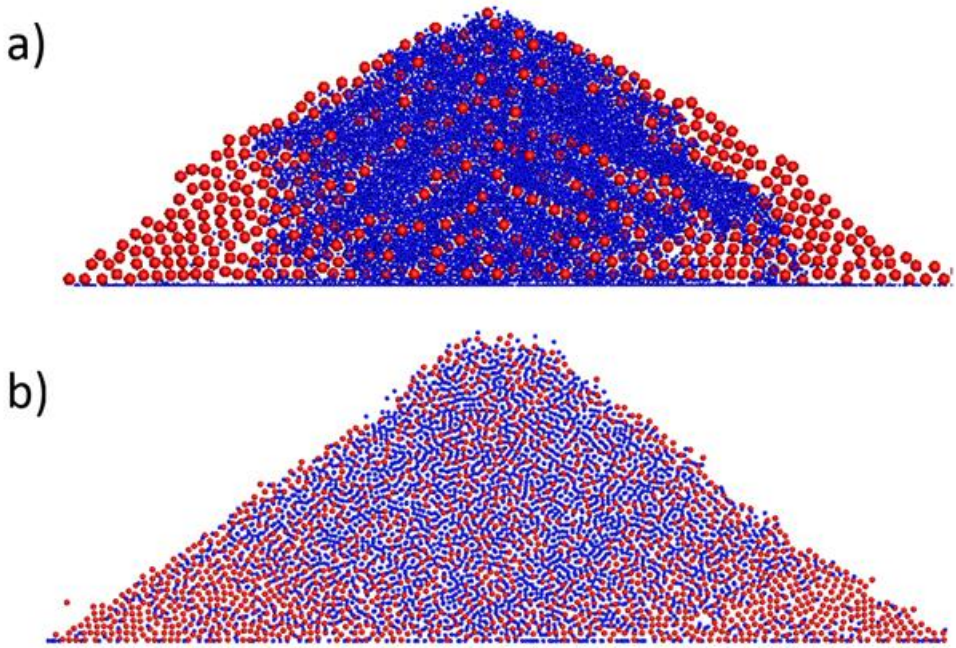

Figure 3-14 Obtained stockpile patterns (mass ratio 1:1, injection height 10mm): a) size ratio 3:1 and b) size ratio 3:2.3

Friction coefficients have been reported to be important for pile formation. But their effects on segregation haven't been studied yet. Here we tested both rolling coefficient and sliding coefficient.

From the obtained results, the rolling coefficient does not heavily affect the mixing state and the segregation rate almost stays the same when changing the rolling coefficient. However, the rolling coefficient can affect the building process and the void-filling process, and when large rolling friction was adopted, the stratification phenomenon disappeared.

As shown from Figure 3-15, sliding coefficients have significant effects on the

segregation rate. The sliding coefficients have two parts: particle to wall and particle to particle. The two coefficients were tested separately. Figure 3-16 shows that the effects of these two coefficients are similar, and 0.4 can be regarded as a critical value for both. When the coefficients are lower than 0.4, the segregation rate significantly increase with the increase of coefficients values. And after reaching the critical value, the segregation seems to reach a peak. To explain this phenomenon, we found that the angle of repose shows similar correspondences to these two coefficients as segregation rate does. Therefore, we believe that these two coefficients' effects on angle of repose will further affect the void-filling process. More specifically, the void-filling process is caused by the difference in motion of particles with different sizes, of which large particles tend to flow on the particle surface, but when angle of repose changes, the ability for large particle to flow on this particle surface will also change, then the void-filling process will be highly affected and give rise to the change in segregation rate and segregation patterns. Fig. 16 shows the patterns with different sliding coefficients.

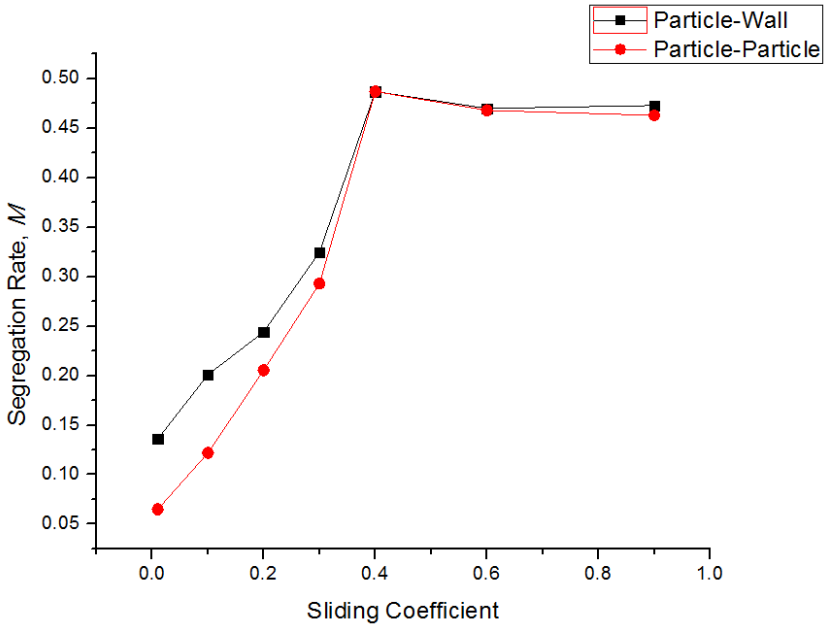

Figure 3-15 Effects of Sliding Coefficient

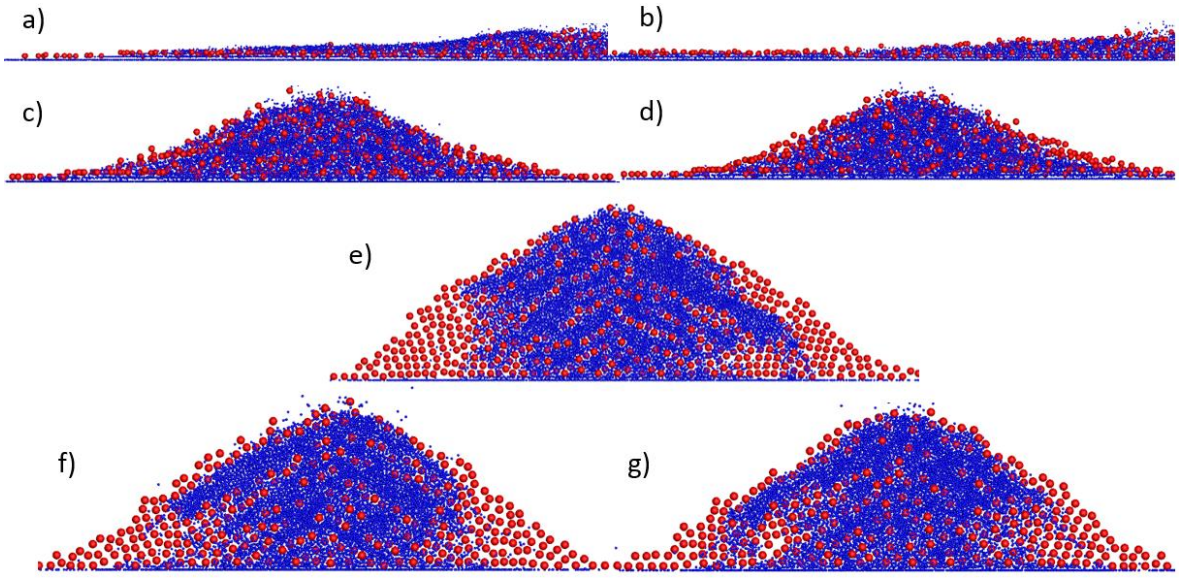

Figure 3-16 Obtained patterns with different sliding coefficients: a) Particle-Particle sliding coefficient (PPC)=0.01, Particle-Wall sliding coefficient (PWC)=0.4; b) PPC=0.4, PWC=0.01; c) PPC=0.2, PWC=0.4; d) PPC=0.4, PWC=0.2; e) PPC=0.4, PWC=0.4; f)

PPC= 0.9, PWC=0.4 g) PPC=0.4, PWC=0.9. a) and b) are with extreme conditions that normal piles can barely being built so half size patterns were taken to show the details of the angle of repose.

3.4 Conclusions

A numerical study based on DEM simulations was carried out to study the stockpile formation in terms of the segregation and stratification processes. The effects of factors including size ratio, injection height, and mass ratio, R were investigated, and a relationship between the mixing quality and these factors was found. Larger size ratio, comparably smaller R can induce stronger segregation, which also represents a lower mixing quality. Furthermore, the stratification phenomenon was successfully simulated with the use of spherical particles, and the simulation conditions and results are consistent with Benito et al.'s physical experiments [8].

In terms of the underlying mechanism causing stratification and segregation, the void-filling mechanism dominates the phenomenon and its effects can explain the occurrence of these two phenomena. This mechanism drives particles of unequal size to move differently, which will then induce the specific phenomena.

Chapter 4 Stockpile segregation of ellipsoidal particles

4.1 Introduction

Granular materials are widely observed in both nature and daily life. As the major raw materials for various industries, the studies of the granular matters are primarily triggered by practical concerns in numerous mixing processes happening in hoppers, rotating drums, stockpiles and all kinds of containers. Among all mixing issues, segregation is the most typical unmixed pattern and it plays a significant role in scientific researches. As one of the most fundamental phenomena, stockpile segregation has been extensively studied through physical experiments and numerical simulations.

Previous researches have proved that various factors are influencing the stockpile segregation jointly among which particle size, particle shape, particle density, and charging methods are the most crucial ones. Williams (1963, 1968, 1976), Drahun and Bridgewater (1983) conducted a great amount of experiments to study segregation in free surface flow. From their work, factors including size ratio, free fall height and density ratio were well studied. Another group of scientists proposed that the segregation phenomenon is induced by a “kink” mechanism and the key parameter controlling the process is the angle of repose, which is actually dominated by particle shapes (Makse et al. 1994, Makse et al. 1997, Makse et al. 1998, Makse and Herrmann 1998, Cizeau et al. 1999). But due to the limitations in quantitatively controlling the shape factor, there is still great need to better understand the shape effects on stockpile segregation with more advanced

techniques. In this work, with the help of a DEM model developed for ellipsoids, binary mixture of ellipsoidal particles will be applied to investigate the segregation phenomenon.

Firstly, ellipsoids mixture with same shape but different sizes were used. Under the ellipsoidal conditions, the particles' flowablities are highly limited, then the segregation phenomenon may differ from the results obtained in spherical cases. Parameter studies with particle size, density and charging methods related factors will also be carried out. Secondly, in order to further validate the real industrial situation, ellipsoidal mixtures of different shapes are used. Similar to the study of factors like size ratio, a factor defining the shape difference of granular mixtures will be introduced. And the effect of this factor will be studied based on the DEM model.

With the knowledge obtained from the basic cases interpreted above, the segregation mechanism can be further updated and evidence can be given for predictions of more complicated cases. Most significantly, with a better understanding of the segregation phenomenon considering all kinds of factors, practical techniques aiming to solve this industrial problem can be better developed.

4.2 Research methods

4.2.1 Discrete element method (DEM)

Simulations were conducted based on a DEM model previously developed by Zhou et al. (2014). This model can be used to conduct simulations for both spheres and well-defined ellipsoids. More specifically, an additional torque is introduced for ellipsoids as the direction of normal contact forces may not necessarily pass through the particle center. The granular materials in this model are semi-rigid particles and the interaction is dominated by contact forces. The translational and rotational motion is described by Newton's law of motion. The governing equations describing the interaction between particle *i* and *j* are as follows:

$$m_i \frac{d\mathbf{v}i}{dt} = \sum_{j=1}^{k} \left(\mathbf{f}_{c,ij} + \mathbf{f}_{d,ij}\right) + m_i\mathbf{g} \tag{4.3}$$

$$I_i \frac{dwi}{dt} = \sum_{j=1}^{k} \left(M_{t,ij} + M_{r,ij} + M_{n,ij}\right) \tag{4.4}$$

where $\mathbf{v}_i$ and $\boldsymbol{\omega}_i$ are the translational and angular velocities of particle *i*, respectively. *k* is the number of particles contacting with particle *i*, while m_i and I_i are the mass and moment of inertia of the particle, respectively. The acting forces and torques are schematically shown in Figure 4-1, which includes gravitational force $m_i\mathbf{g}$, elastic force $\mathbf{f}_{c,ij}$, viscous damping force $\mathbf{f}_{d,ij}$, torque $\mathbf{M}_{t,ij}$ generated by tangential force, $\mathbf{M}_{n,ij}$ generated by the normal force, and

$\mathbf{M}_{r,ij}$ generated by rolling friction. The equations used to calculate these forces and torques are summarized in Table 4-, and detailed descriptions can be referred in Zhou et al. (2014).

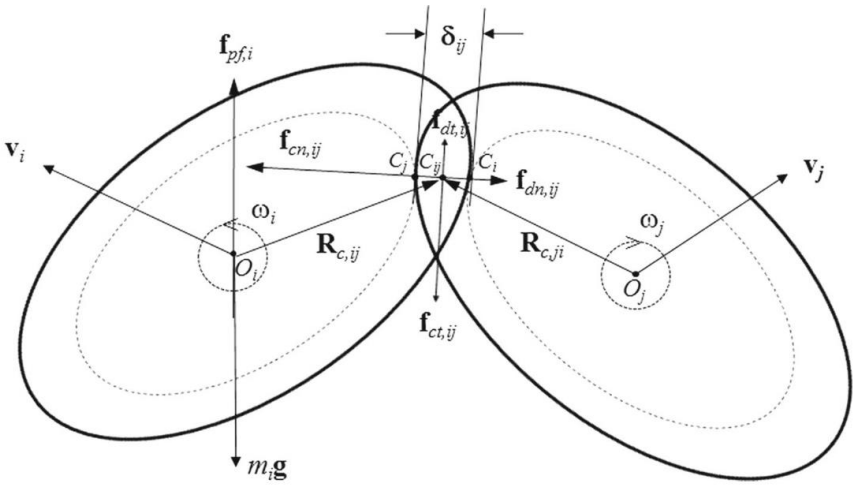

Figure 4-1 Scheme of the forces acting on particle i and particle j. (Zhou et al. 2014)

Table 4-1 Components of forces and torque acting on particle *i*

Forces and torques	Symbols	Equations
Normal elastic force	$\mathbf{f}_{cn,ij}$	$-4/3E^*\sqrt{R^*}\delta_n^{3/2}\mathbf{n}$
Normal damping force	$\mathbf{f}_{dn,ij}$	$-c_n\left(8m_{ij}E^*\sqrt{R^*\delta_n}\right)^{1/2}\mathbf{V}_{n,ij}$
Tangential elastic force	$\mathbf{f}_{ct,ij}$	$-\mu_s\lvert\mathbf{f}_{cn,ij}\rvert(1-(1-\delta_t/\delta_{t,\max}{}^{3/2})\hat{\delta}_t$, $(\delta_t<\delta_{t,\max})$
Tangential damping force	$\mathbf{f}_{dt,ij}$	$-c_t\left(6\mu_s m_{ij}\lvert\mathbf{f}_{cn,ij}\rvert\sqrt{1-\lvert\mathbf{v}_t\rvert/\delta_{t,\max}}/\delta_{t,\max}\right)^{1/2}\mathbf{V}_{t,ij}$, $(\delta_t<\delta_{t,\max})$
Coulumb friction force	$\mathbf{f}_{t,ij}$	$-\mu_s\lvert\mathbf{f}_{cn,ij}\rvert\hat{\delta}_t$, $(\delta_t\geq\delta_{t,\max})$

Torque by tangential forces	$\mathbf{M}_{t,ij}$	$\mathbf{R}_{ij} \times \left(\mathbf{f}_{cn,ij} + \mathbf{f}_{dt,ij}\right)$
Rolling friction torque	$\mathbf{M}_{r,ij}$	$\mu_{r,ij} \left\|\mathbf{f}_{n,ij}\right\| \widehat{\boldsymbol{\omega}}_{t,ij}^{n}$

where R* is the reduced radius of the particle *i* and *j* at the contact point. $1/m_{ij} = 1/m_i + 1/m_j$, $E^* = E/2(1-\nu^2)$, $\widehat{\boldsymbol{\omega}}_{t,ij} = \boldsymbol{\omega}_{t,ij} / \left|\boldsymbol{\omega}_{t,ij}\right|$, $\hat{\boldsymbol{\delta}}_t = \boldsymbol{\delta}_t / \left|\boldsymbol{\delta}_t\right|$, $\delta_{t,\max} = \mu_s(2-\nu)/2(1-\nu) \cdot \delta_n$, $\mathbf{V}_{ij} = \mathbf{V}_j - \mathbf{V}_i + \boldsymbol{\omega}_j \times \mathbf{R}_{c,ji} - \boldsymbol{\omega}_i \times \mathbf{R}_{c,ij}$, $\mathbf{V}_{n,ij} = (\mathbf{V}_{ij} \cdot \mathbf{n}) \cdot \mathbf{n}$, $\mathbf{V}_{t,ij} = (\mathbf{V}_{ij} \times \mathbf{n}) \times \mathbf{n}$. Note that tangential forces $(\mathbf{f}_{ct,ij} + \mathbf{f}_{dt,ij})$ should be replaced by $\mathbf{f}_{t,ij}$ when $\delta_t \geq \delta_{t,\max}$.

4.2.2 Simulation Conditions

The simulated problem is shown schematically in Fig. 1. The device includes two parts: a particle injection device and a receiving box ($200mm \times 100mm \times 5mm$). During the growth of the stockpile, the distance between injection surface and top of stockpile (injection height) was set constant by moving the injection surface vertically during the stockpile formation. Specifically for this work, the injection height is set to be ranging from 10mm to 50mm to study its effects on pattern formation.

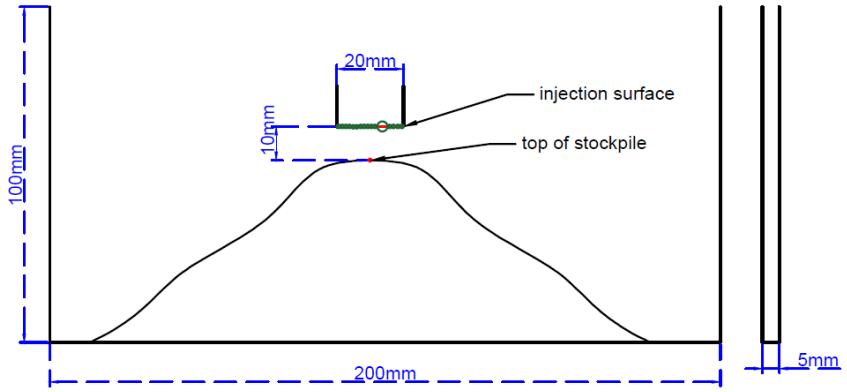

Figure 4-2 Schematic diagram of the simulation conditions. (Injection surface: the surface where particles are generated and released; top of stockpile: the highest point of the formed stockpile)

The binary granular mixtures used in the simulations are formed by spherical particles and ellipsoids. The mass ratio R (the total mass ratio of the two species which also represents the flow rate ratio of large particles versus small particles) was set to be 0.5 or 1. Other physical properties of the particles were set to those of glass beads. Details of the input variables and their values are shown in Table 4-2.

Table 4-2 Simulation conditions and related parameters

Input variables	**Value**
Size ratio	3:2, 3:1, 1:1
Injection height /mm	10, 20,30, 40, 50
Mass ratio	0.5, 1
Young's module	1×10^8 N/m^2
Poisson's ratio	0.3

Sliding coefficient (P-P)	0.4 (standard)
Sliding coefficient (P-W)	0.4 (standard)
Rolling coefficient (P-P)	0.3 (standard)
Rolling coefficient (P-W)	0.3 (standard)
Particle density	2.7×10^3 kg/m^3
Particle number	20,000
Flow rate	0.1g/s
Simulation Timestep	10^{-3}s

The shape of the ellipsoidal particles in this work is controlled by aspect ratio. For three-dimensional ellipsoids shown in Figure 4-3, the aspect ratio is defined as:

$$\text{Aspect Ratio} = \frac{a}{c} \tag{4.5}$$

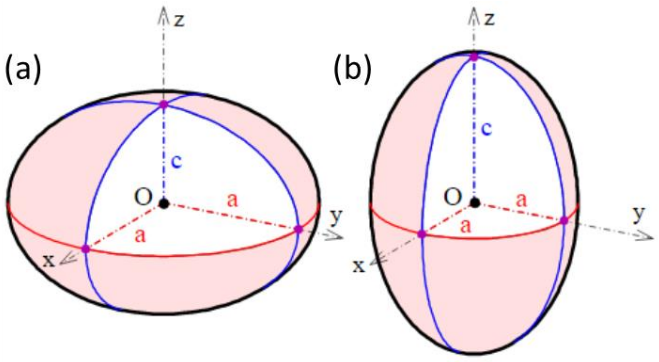

Figure 4-3 Scheme of three-dimensional ellipsoids.

There are basically two types of ellipsoids which are oblate particles and prolate particles. Oblate particles are tablet-like with aspect ratio greater than 1, and the scheme is shown in Figure 4-3 (a). Prolate particles are needle-like with aspect ratio lower than 1, and the scheme is shown in Figure 4-3 (a). If the aspect ratio

equals to 1, the ellipsoids will become normal spheres. The ellipsoidal particles used in this work have aspect ratios ranging from 0.2 to 3.5.

4.2.3 Physical experiments

The physical experiments were carried out using the transparent three-dimensional container shown in Figure 4-4 (a). The width of the slot is 20mm and which was around 7 times the diameter of large particles. The granular materials used in the experiments are spherical and ellipsoidal grains with density around 2.7×10^3 kg/m^3 , the surface properties of the particles are similar as the properties of glass beads. The granular materials were injected through a ball valve. These physical experiments can only offer qualitative information to validate the DEM model. Further quantified studies will be conducted mostly based on the numerical simulations.

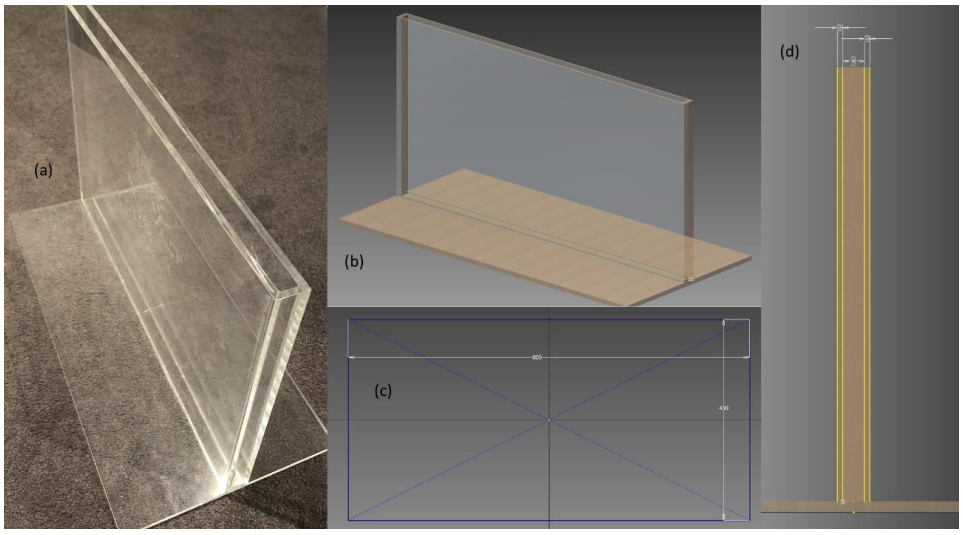

Figure 4-4 Container used for physical experiments (a) and its CAD designs (b) (c) (d).

4.3 Results and discussions

4.3.1 Model validations

To verify the ellipsoidal DEM model, physical experiments corresponding to several typical simulation conditions were conducted. The materials used in the experiments are food grains and glass beads with close density and friction coefficients. As the validations for binary mixtures with same shapes have already been demonstrated in Chapter 3, here the validations for mixtures with two different shapes were conducted. In order to test the accuracy of the numerical model, binary grains of spheres and ellipsoids with equivalent size around 1mm were injected into the two-dimensional silo. Firstly, prolate grains with aspect ratio around 0.5 were used as the ellipsoidal species. The flow patterns were recorded by camera during the stockpile formation, and a comparison between simulation and experiment results is shown in Figure 4-5. It can be clearly observed from the results that both patterns show a barely segregated pattern with same angle of repose.

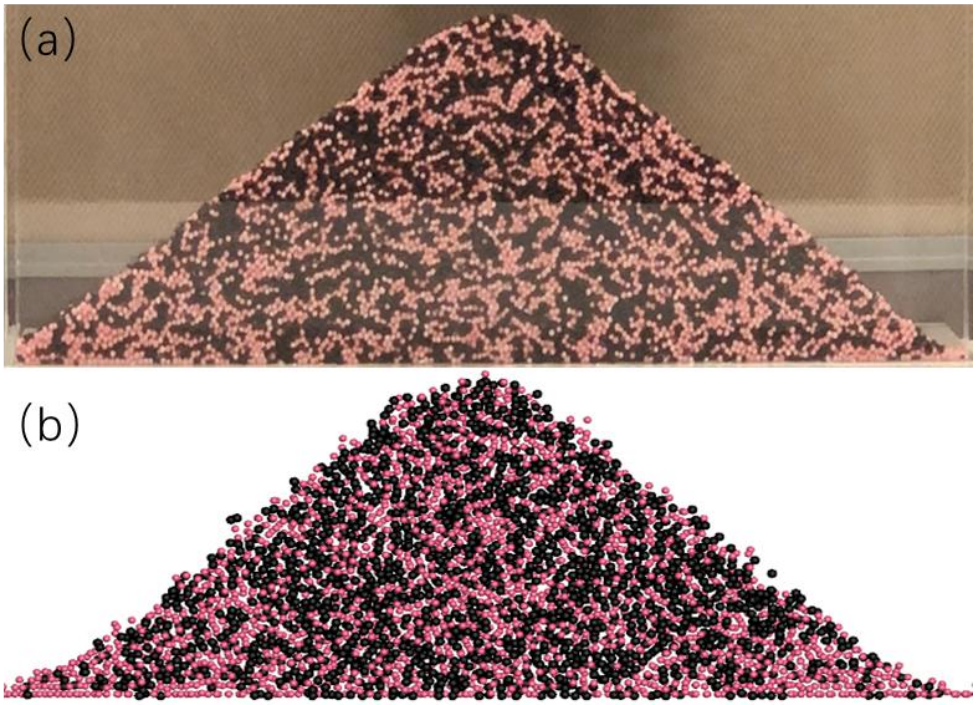

Figure 4-5 Schematic comparison between (a) physical experiments and (b) numerical simulations. The granular mixture contains ellipsoids and spheres with same equivalent size around 1mm, and the aspect ratio of the ellipsoids is around 0.5. The injection height is 10mm and mass ratio of the two species is 1:1. Pink grains: spheres; Black grains: ellipsoids.

In addition, the experiments with oblate particles were also conducted. For this set of experiments, granular mixture of spheres and oblate particles with equivalent size were used. In these experiments, as the densities of different particles are same, the equivalent size is defined considering both volume and mass. The binary mixture contains particles with equivalent size around 3mm, and the oblate species have aspect ratio around 1.5. A comparison between the simulation and experiment was shown in Figure 4-6, which further proves that the

DEM model can successfully demonstrate the real experiments.

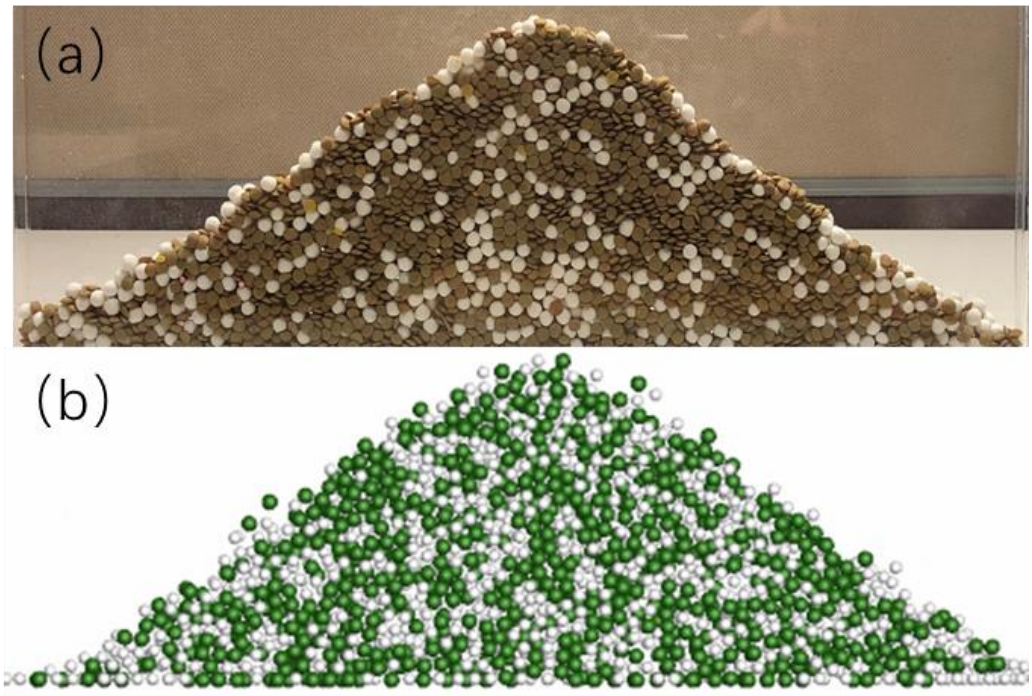

Figure 4-6 Schematic comparison between (a) physical experiments and (b) numerical simulations. The granular mixture contains ellipsoids and spheres with same equivalent size around 3mm, and the aspect ratio of the ellipsoids is around 1.5. The injection height is 10mm and mass ratio of the two species is 1:1. White grains: spheres; Green grains: ellipsoids.

4.3.2 Binary mixtures of particles with same shapes

In order to investigate the effects of particle shape on size segregation in piling processes. Simulations were conducted based on the DEM ellipsoidal model. The granular mixtures used are ellipsoids with different sizes but same shape. In addition, to eliminate the effects of mass ratio and injection height, they were set

constant as 1 and 10mm, respectively. Figure 4-7 shows several patterns obtained from the simulations.

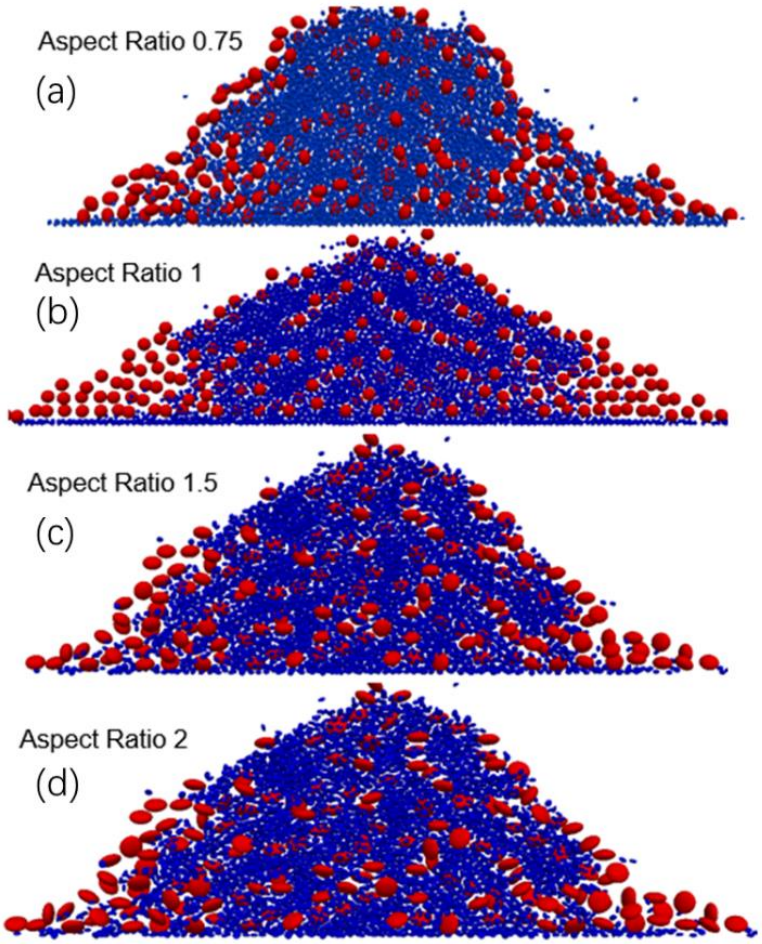

Figure 4-7 Scheme of the stockpile patterns obtained from the DEM simulations. The aspect ratios of the granular mixtures are (a) 0.75, (b) 1, (c)1.5, (d) 2. The injection height is 10mm, mass ratio of the two species is 1:1, and the equivalent sizes of the two species are 1mm and 3mm.

To demonstrate the exact segregation patterns for ellipsoidal mixtures, distributions of the volume fractions for large particles were constructed in

horizontal coordinates, as shown in Figure 4-8. It can be obviously concluded from the comparisons that for ellipsoidal mixtures, the large particles still tend to segregate at the sided bottom while small particles accumulate at the center area, which is the same as the results of spherical mixtures.

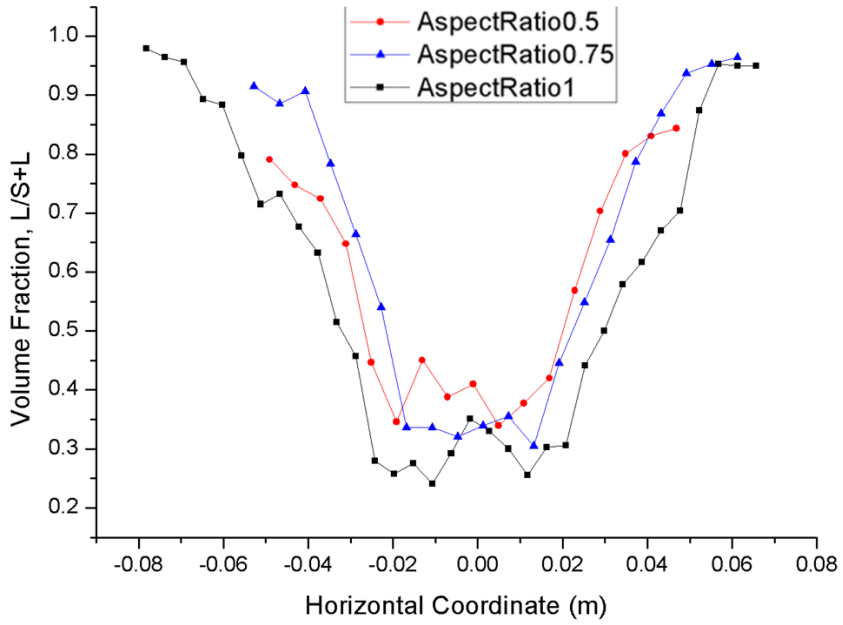

Figure 4-8 Horizontal distribution of volume fraction for large particles within the binary mixtures.

On the other hand, to investigate the shape effects on extent of segregation and stratification, it was found that decreasing the aspect ratio from 1 or increasing the aspect ratio from 1 can both weaken the segregation effects, which shows that decreasing the particles sphericity can directly restrain the granular segregation. To further interpret these effects on basis of void-filling mechanism, it was concluded that particle shape can firstly influence the void-filling processes and

then affect the stratification and segregation. As the void-filling features are based on the good flowabilities of granular materials, this process will be rather restrained when particles with less sphericity are adopted. But even though the segregation is largely weakened, there is still slight stratification observed from the flow patterns. To further illustrate the stratified layer shown in Figure 4-9 (a), it was found that these patterns were caused by the “static avalanche” instead of the void-filling mechanism. During the formation of the stockpile, the large ellipsoidal particles can form an abnormal layer of clusters due to bad flowability. These clusters, as shown in Figure 4-9 (b), have rather strong stability that it can afford a great amount of small particles to accumulate on their surface. But while the number of large particles on the surface increases, as shown in Figure 4-9 (c), this micro piling feature will reach a limit which results in the further avalanche in Figure 4-9 (d). However, this specific avalanche cannot affect the packing patterns of the abnormal clusters and these large particles can stay at the same position throughout the piling process. More specifically, as the exact group of large particles can stay as a layer during piling, this steady feature of the large particles during avalanches can be regarded as the main reason for stratification in ellipsoidal mixtures. This interpretation also explains the results that the stratification for ellipsoids is not as strong as for spherical mixtures as the layered clusters are small groups of large particles with abnormal packing patterns which cannot contain large numbers of particles as spherical cases do.

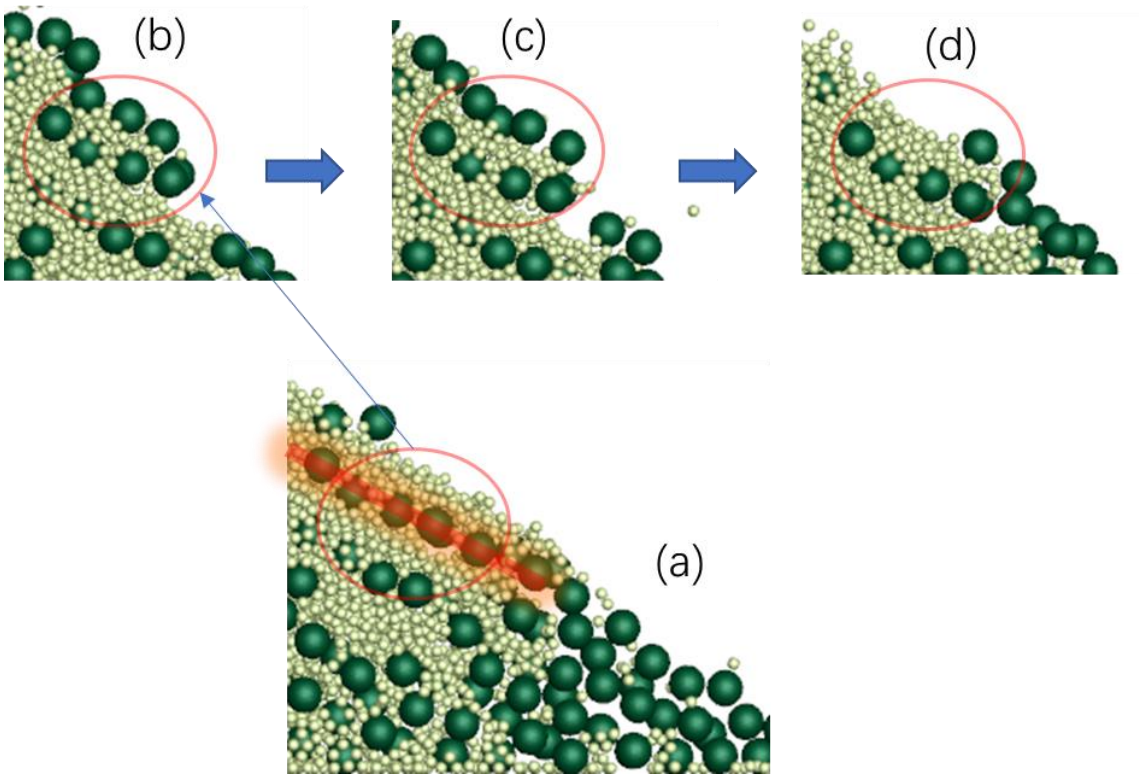

Figure 4-9 Scheme of "static avalanche" process. (a) Time=38s, the studied stratified layer of large particles; (b) Time=35s, the abnormal layered clusters; (c) Time=36s, small particles can accumulate on the surface of the layered clusters while large particles can float on top; (d) Time=36.5s, avalanche happens when the number of large particles reaches a limit, and this avalanche will not affect the positioning of the studied layered clusters. Ellipsoids are represented by spheres in this figure considering the convenience in visualization. The size ratio of the particles is 0.75, and the simulation is conducted under the following conditions: size ratio 3:1; injection height 10mm; mass ratio 1:1.

As for segregation behavior, previous conclusions in spherical cases show that segregation is triggered by the granular avalanches. But in ellipsoidal cases, as the flowability of the granular materials largely decrease, the behavior of particles will

start forming a much more randomized pattern which can reduce the difference between large particles and small particles. More importantly, there is a large difference between the avalanches happening in spherical mixtures and ellipsoidal mixtures. For spherical cases, granular avalanches can push the particles in sided area to the two sides which reconstructs the granular patterns around the avalanching area, which further induces the large particles to be pushed away to the bottom area. But for ellipsoidal cases, the avalanche will only cause the particles latterly injected to easily jump through the stuck layered clusters which will not affect the particles injected before avalanching. And the direct result of this "static avalanche" is that only large particles injected during the avalanching can segregate at the bottom while the already injected ones will maintain their positions which will later become the stockpiles' inner area. Based on this phenomenon, it can be then concluded that less sphericity will induce worse flowability which can further result in weakened segregation phenomenon.

In order to further study the shape effects under different simulation conditions, the effects of size ratio, mass ratio and injection height were jointly investigated along with different aspect ratios. As shown in Figure 4-10, the segregation index was calculated against different aspect ratio under different simulation conditions. It was concluded that the segregation index significantly decreased when the value of aspect ratio gets away from 1, which confirms the observations from the obtained flow patterns. In addition, greater injection height, larger size ratio and

smaller mass ratio can still enhance the extent of segregation for all aspect ratios, which is consistent with the findings concluded through spherical cases.

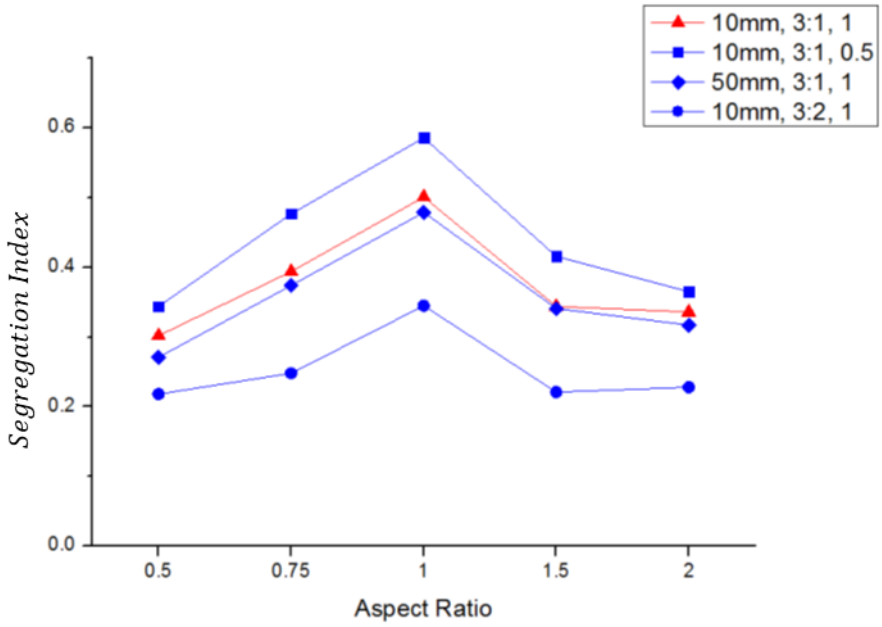

Figure 4-10 Segregation index against aspect ratio under different simulation conditions.

The segregation behavior of the ellipsoidal mixtures was also studied from a microscopic view. To compare the difference between spherical and ellipsoidal cases, the velocity evolutions of several typical particles were recorded under different circumstances, as shown in Figure 4-11. It can be concluded from the velocity profiles that for ellipsoidal mixtures, the velocity oscillations of the large particle nearly disappeared due to the bad flowability and “static avalanche”. Moreover, the early oscillations of small particles in spherical cases show that it is

easier for them to fill in the voids in early stages while small ellipsoids show more randomized oscillations, which further confirm the conclusion that the void-filling process is largely restrained for ellipsoidal mixtures.

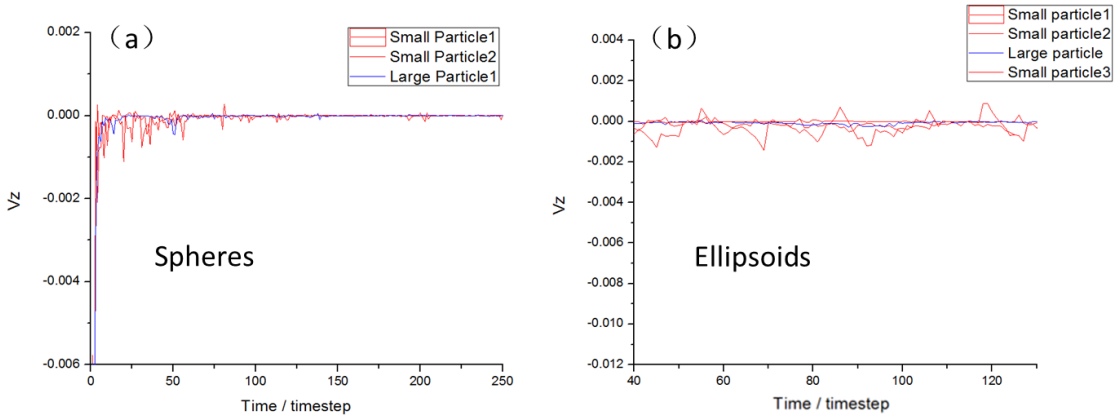

Figure 4-11 The time evolutions of vertical velocity profiles for several trace particles. The trace particles were chosen around the center of injection flow, and their final positions should be away from the pile center to ensure their active motion during the piling process. (a) mixture of spheres, size ratio 3:1, injection height 10mm, mass ratio 1:1; (b) mixture of ellipsoids, size ratio 3:1, injection height 10mm, mass ratio 1:1, aspect ratio 0.75.

4.3.3 Binary mixtures of particles with different shapes

To study the shape effects isolated from size effects, simulations were also conducted with binary mixtures of particles with different shapes but same equivalent size. More specifically, to highlight the difference of flowabilities between different species, the two species are set spheres and ellipsoids for all sets

of simulations.

During the investigation, it was found that the previously introduced segregation rate was no longer proper due to the difficulty in choosing sample size, therefore a particle-scale mixing index based on coordination numbers introduced by Chandratilleke et al. (2012) was adopted. This CN mixing index ranges from 0 to 1 while 0 represents the fully segregated pattern and 1 represents the complete mixing pattern.

Figure 4-12 shows several obtained flow patterns associated with their corresponding CN mixing index's time evolutions. A general conclusion can be made through the results that the segregation phenomenon can be barely observed with these granular mixtures. But it was found that there was still relation between particle shape and the stockpiles' mixing patterns based on the CN mixing index.

It was found that the particle shape may affect the segregation phenomenon by controlling the repose angle of the stockpile. Then the simulation results were recorded with respect to the repose angle of the specific stockpile. The constructed relations were shown in Figure 4-13. On the one hand, as the CN mixing index stays around 0.9 for all binary mixtures, it can be concluded that for binary mixtures with same equivalent size, the mixing properties of the stockpile cannot be significantly influenced by changing the particle shape. The weak effects of particle

shape on segregation extent can be found related to the piling repose angles. As mentioned by Zhou et al. (2014), for mono-typed granular stockpile packing, the angle of repose increases with smaller sphericity when aspect ratio ranges from 0.5 to 2. Here from our results for binary mixtures of ellipsoids, it was observed that the segregation gets weaker with smaller repose angle, and for aspect ratio ranging from 0.5 to 2, the angle of repose decreases when aspect ratio gets closer to 1. Therefor it can be concluded that, for contained ellipsoids with aspect ratio from 0.5 to 2, the repose angle of the stockpiles will get smaller with stronger sphericity, which will further result in weaker segregation.

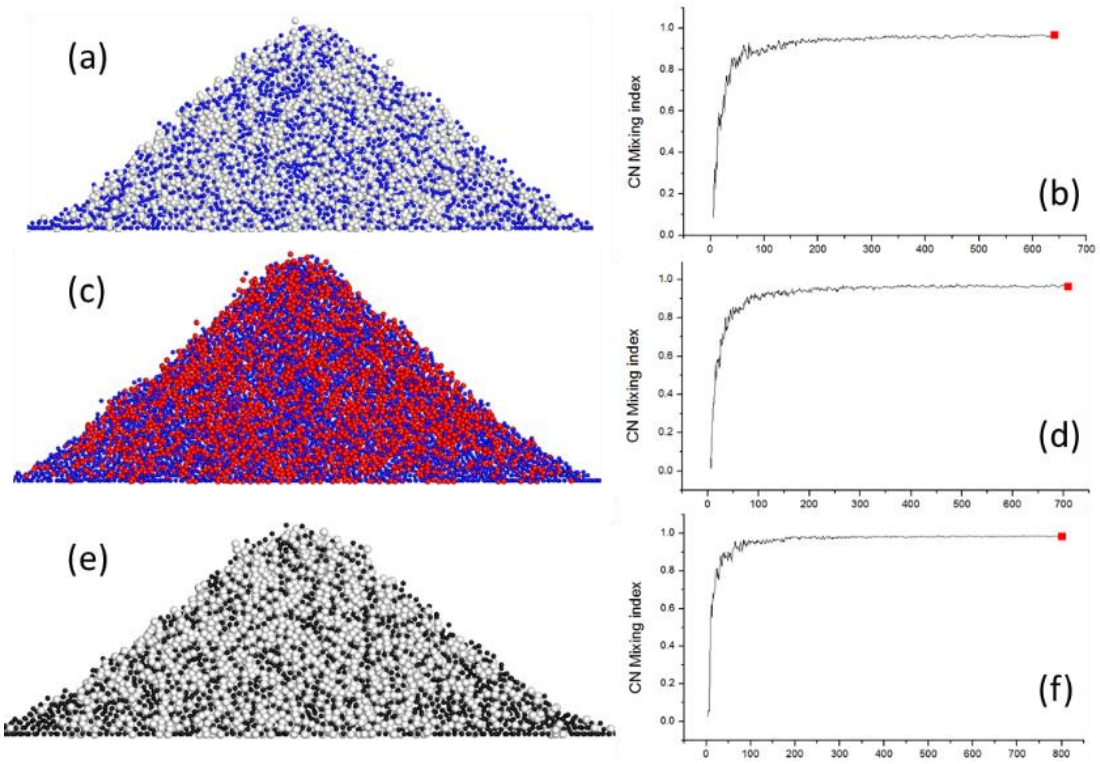

Figure 4-12 Obtained piling patterns with their corresponding time evolution of CN mixing index. The simulations were conducted with granular mixtures containing (a) (b)

blue spheres and white prolate particles (aspect ratio=0.3); (c) (d) blue spheres and red prolate particles (aspect ratio=0.5); (e) (f) black spheres and white oblate particles (aspect ratio=2,0). The equivalent size of the particles used is 1mm for all granular mixtures.

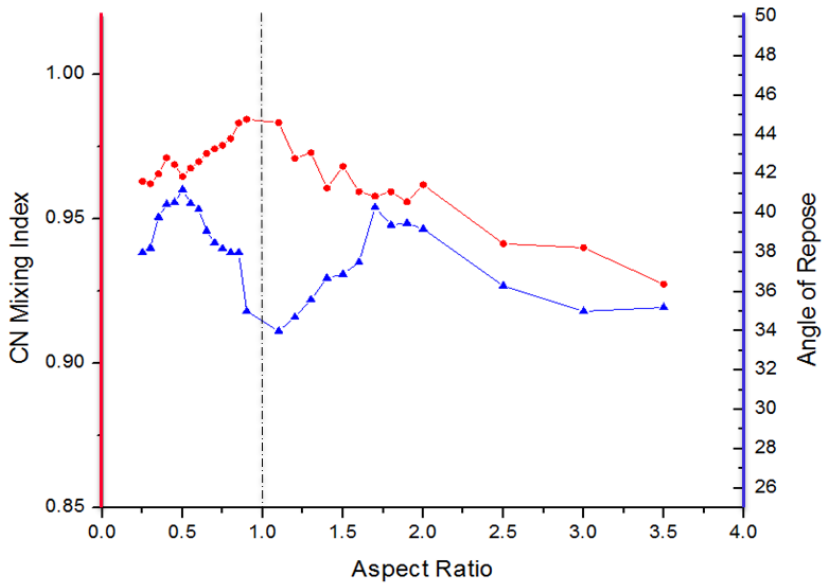

Figure 4-13 The relations among CN mixing index, ellipsoidal species' aspect ratio, and stockpiles' repose angle. The granular mixture contains spheres and ellipsoidal species with 1mm as the equivalent diameter. The mass ratio between the two species is 1.

In order to further study the shape effects on stockpile formation, the exponential fit was used to estimate the time needed to reach a mixing index steady point. The results were shown in Figure 4-14, where 95% of the final mixing index was respected as the cut-off point. It was found that the stockpiles could soon reach a steady point for granular mixtures with the same equivalent size. And when the shape of the contained ellipsoids gets less spherical, the time it takes to get to the

steady point gets longer. More specifically, for mixtures of spheres and prolate particles, it takes longer to get to the steady state when aspect ratio of the contained ellipsoidal species decreases, which is shown in Figure 4-14 (a). And for mixtures of spheres and oblate particles, it takes shorter time to get to the steady state when aspect ratio of the contained ellipsoidal species decreases, which is shown in Figure 4-14 (b).

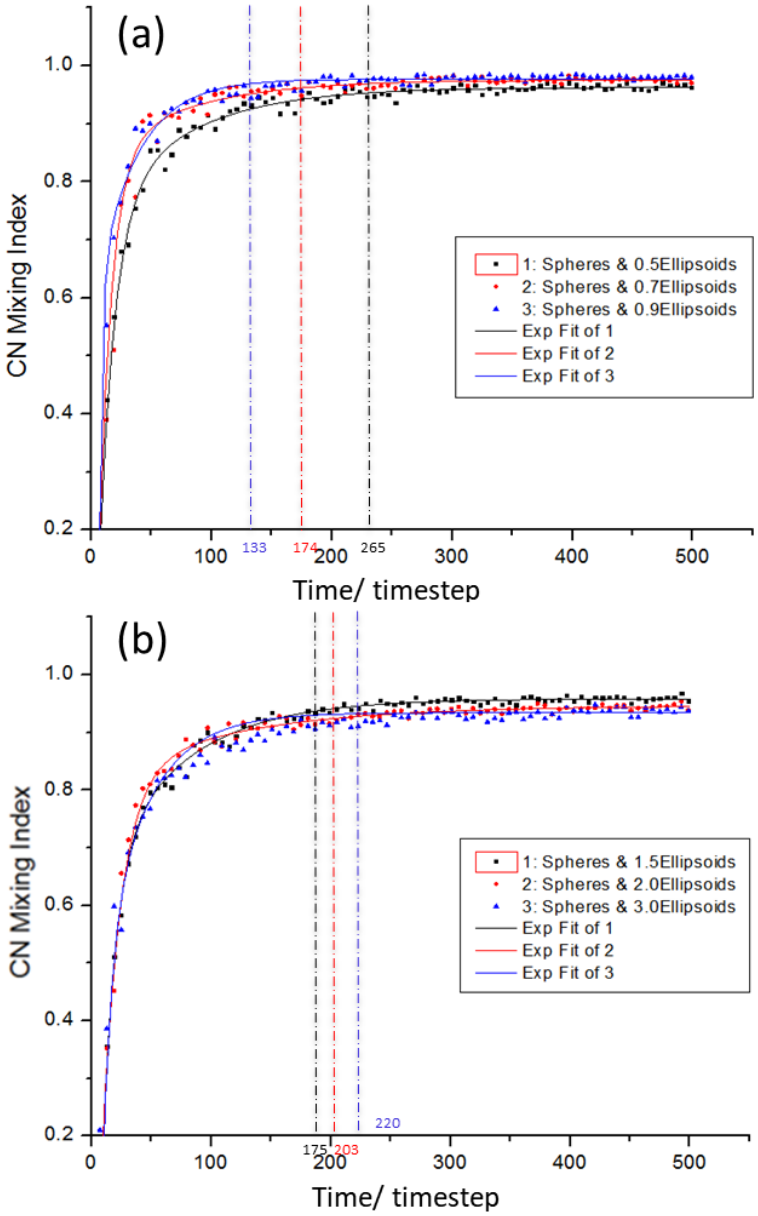

Figure 4-14 Time evolution of the CN mixing index during the formations of stockpiles. (a) Granular mixtures of spheres and prolate particles (aspect ratio lower than 1); (b) granular mixtures of spheres and oblate particles (aspect ratio greater than 1).

To investigate these mixture cases from a microscopic view, the time evolution of velocities for several tracer particles were recorded. The results are shown in

Figure 4-15. Compared to the cases with size difference, a general finding for the velocity profiles is that the oscillations of the velocities get rather weaker for binary mixtures with same equivalent size. These steady states of the particle velocities also show that particles soon settled down after falling on the granular surface and the further avalanches will not affect the positioning behavior of particles. As these static features are against the segregation nature that particles tend to reconstruct the local packing patterns during piling, it can further confirm the truth that shape difference alone cannot significantly result in stockpile segregation.

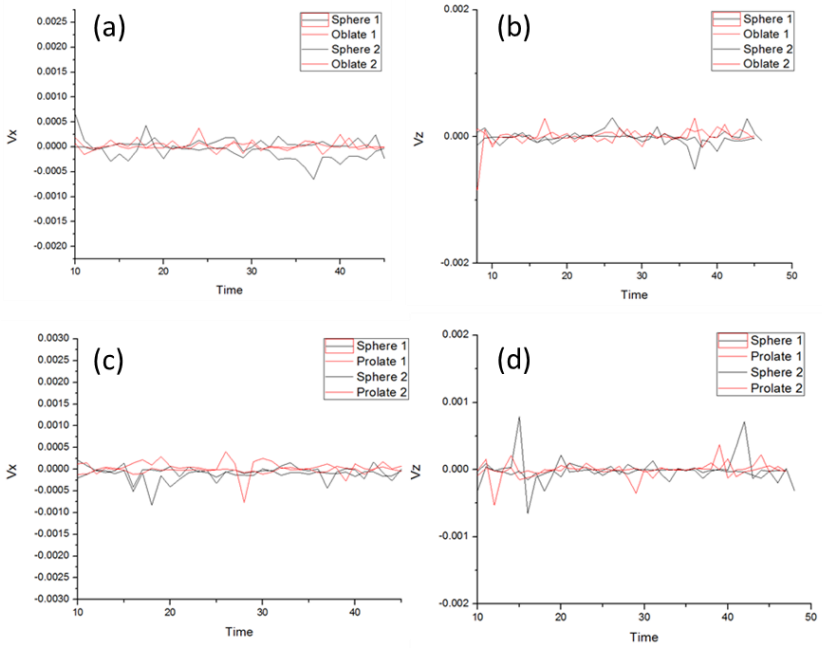

Figure 4-15 Time evolution of velocity profiles during stockpile formation. (a) Horizontal/ (b) Vertical velocities of tracer particles for granular mixture of spheres and oblate particles (aspect ratio 1.5); (c) Horizontal/ (d) Vertical velocities of tracer particles for granular mixture of spheres and prolate particles (aspect ratio 0.75)

4.4 Conclusion

In this part, DEM simulations have been conducted to study the shape effects on stockpile segregation. The ellipsoidal model has been qualitatively validated through physical experiments. By switching from spherical mixtures to ellipsoidal mixtures, the pattern formation during the piling processes significantly changed. More specifically, it was found that for granular mixtures containing ellipsoids, the "static avalanche" appear due to bad flowability. This phenomenon illustrates that pre-piled ellipsoids tend to maintain their positions instead of reconstructing the local pattern with upcoming particles. Based on this interpretation, it can be then demonstrated that worse flowability can induce weaker segregation. And the detailed parameter studies further confirm this theory.

For ellipsoidal mixtures with different sizes but same shape, it was concluded that segregation significantly decreases when particles' aspect ratio gets away from 1. Moreover, the stratification patterns still exist in small scales, and the triggering mechanism is based on the "static avalanche" instead of void-filling.

For binary mixture of spheres and ellipsoids with same equivalent size, the segregation was found extremely weak, which shows that the size difference is the trigger of segregation while shape difference can only affect segregation intensity.

Chapter 5 Segregation in vibrated systems—rising behavior of single large intruder

5.1 Introduction

Segregation is the most typical unmixed pattern and it plays a significant role in scientific researches on the flow of granular materials. It has been universally acknowledged that segregation is mostly observed in free surface flows and vibrated containers. Therefore the significance to well understand the vibration-induced segregation has motivated researches to extensively investigate this phenomenon through both experiments and simulations.

The basic vibration-induced segregation demonstrates the phenomenon that vibration drives large intruders to move upward within bulk solid of small particles, which is also called “Brazil-nut Effect (BNE)”. Ahmad and Smalley (1973) first conducted physical experiments to study this phenomenon, and the importance of vibration acceleration and density was addressed through their findings. Cooke et al. (1996) did further experiment with the help of advanced high-speed camera, through which they found the motion of the large intruder is largely affected by the size ratio. Many researchers also applied numerical simulations to study this phenomenon due to the reason that simulation methods can easily offer clear profiles within the granular bed. Other researchers adopted Monte Carlo models to investigate the effects of shaking conditions and particle properties under discrete vibrations (Rosato et al.1986, Rosato et al. 1987, Abreu et al. 2003). Poschel and Herrmann (1995) used Molecular Dynamics to study the convection patterns in vibrated granular bed. With the developments of

calculation facilities, the discrete element method (DEM) has been widely used due to its perfect consistency with physical experiments. Moreover, as DEM can offer detailed profiles of velocity, force and position, many researchers have used this method to conduct parameter studies including the effects of particle size ratio, vibration acceleration, initial depth of the large intruders, and particle density ratio (Lan and Rosato 1997, Rosato et al. 2002, Fernando and Wassgren 2003, Yang 2006, Fang and Tang 2007). However, the influence of particle shape and vibration conditions have not been fully understood, especially when vibration amplitude is rather large. In this part, a comprehensive study of vibration conditions and several particle properties were conducted based on a DEM model for ellipsoids. The single intruder was put at the bottom of the granular bed, and harmonious vertical vibrations were input at the base of the cylindrical container. Several interesting features have been observed including a come-back pattern of the large intruder and disappeared BNE at high vibration frequency. More importantly, the granular bed failed to present a convection pattern for cases shown in the simulations.

5.2 Simulation method and conditions

5.2.1 Discrete element method (DEM)

Please refer to Section 4.2.1 in Chapter 4.

5.2.2 Simulation conditions

The simulated problem is shown schematically in Figure 5-1. The dimension of the cylindrical container is 240mm in diameter and unlimited in vertical direction. The granular beds are pre-packed at the base before vibration started, and the single large intruder is set at the bottom in the center of the bed. The vibration imported on the container base follows the pattern of simple harmonious vibrations with amplitude *A* and frequency *f.*

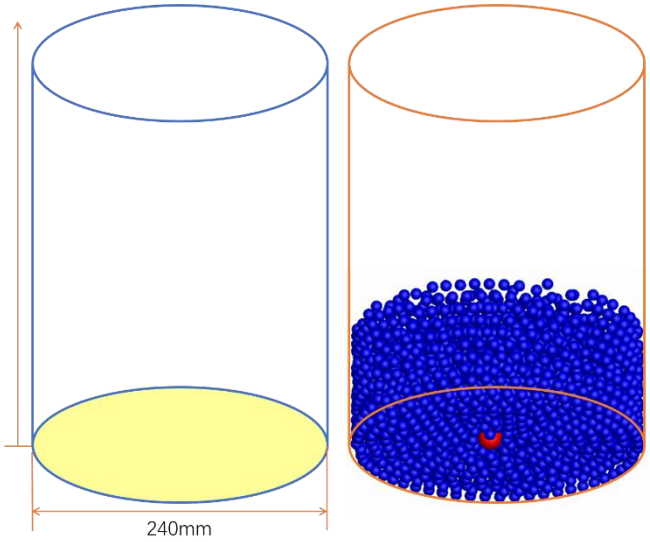

Figure 5-1 Schematic diagram of the simulated cylindrical containers.

The granular materials used in the simulations contain spherical particles and ellipsoids. The exact physical properties of the particles were set to those of glass beads. Details of the physical properties and other input variables are shown in Table 5-1.

Table 5-1 Simulation conditions and related parameters

Input variables	Value
Size of small particles	10mm
Size of large particle	15mm, 20mm, 25mm, 30mm
Number of large/small particles	1/2000
Aspect ratio	0.5, 0.7, 0.9,1, 1.2, 1.5, 1.8, 2, 2.5
Young's module	1×10^8 N/m^2
Poisson's ratio	0.3
Sliding coefficient (P-P)	0.4 (standard)
Sliding coefficient (P-W)	0.4 (standard)
Rolling coefficient (P-P)	0.3 (standard)
Rolling coefficient (P-W)	0.3 (standard)
Particle density	2.7×10^3 kg/m^3
Vibration frequency	5Hz to 80Hz
Vibration amplitude (defined as a dimensionless factor regarding size of small particles)	1mm to 15mm (0.1 small particle diameter – 1.5 small particle diameter)
Simulation Timestep	10^{-3}s

5.3 Results and discussions

To study the vibration-induced segregation, the research has been conducted regarding the vibration conditions and particle properties. More specifically, a phase diagram was constructed in respect to the vibration conditions. And the influence of various factors has been investigated, including vibration frequency

and amplitude, size ratio, and particle shape.

5.3.1 Effects of vibration conditions

5.3.1.1 Phase diagram

The importance of vibration conditions to segregation has been highlighted by many researchers. However, as they mainly focused on vibration acceleration, the individual effects of vibration frequency and amplitude still need further studies. In order to investigate their effects, a phase diagram (Figure 5-2) was first constructed considering the appearance of BNE.

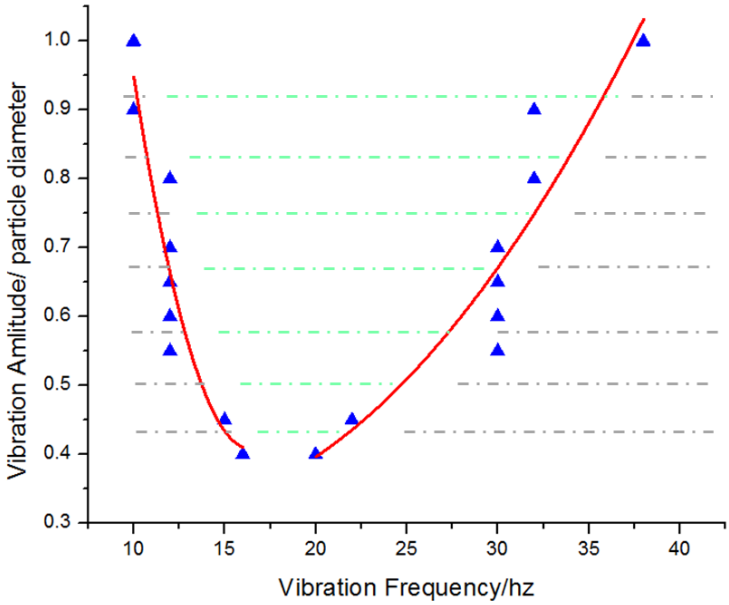

Figure 5-2 Phase diagram of BNE versus vibration frequency and amplitude. The grey area represents the conditions where BNE cannot occur while the green area represents the conditions where BNE can be observed. The used particles are: 20mm large spheres and 10mm small spheres.

Several conclusions can be addressed from the diagram: (1) for fixed vibration amplitude, BNE only occurs within certain ranges of vibration frequencies; (2) increasing vibration amplitude can enlarge the sufficient range of frequency; (3) when amplitude increases, the critical maximum frequency increases and critical minimum frequency decreases. Moreover, the fact that high frequency stops the segregation is against the common sense that higher frequency may induce stronger BNE.

From the simulations, it was also observed that instead of staying on the bed surface, the large intruder tends to present a comeback behavior under specific vibration conditions. The exact patterns are shown in Figure 5-3.

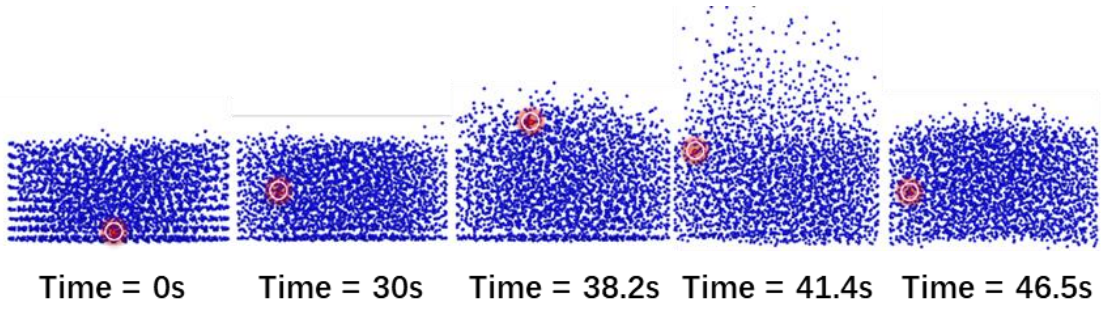

Figure 5-3 Obtained flow patterns showing the intruder's comeback phenomenon.

Vibration frequency: 20Hz; Vibration amplitude: 10mm.

In order to further interpret this phenomenon, it was found that the vertical motion of large intruder is directly decided by its local porosity. More specifically, sharp increase in local porosity can trigger the intruder's downward movement while sharp decrease can make the intruder go upward. The time evolution of the

intruder's position and local averaged coordination number is shown in Figure 5-4. The local averaged coordination number (LACN) describes the time-averaged number of particles in the neighborhood area of the large intruder, which represents the local porosity in particle scale. The obtained figure further interprets the relation between local porosity and intruder's vertical motion, and it also demonstrates that when LACN is at a rather high level, the large intruder will start getting back into the particle bed from the surface, which explains the appearance of the comeback behavior.

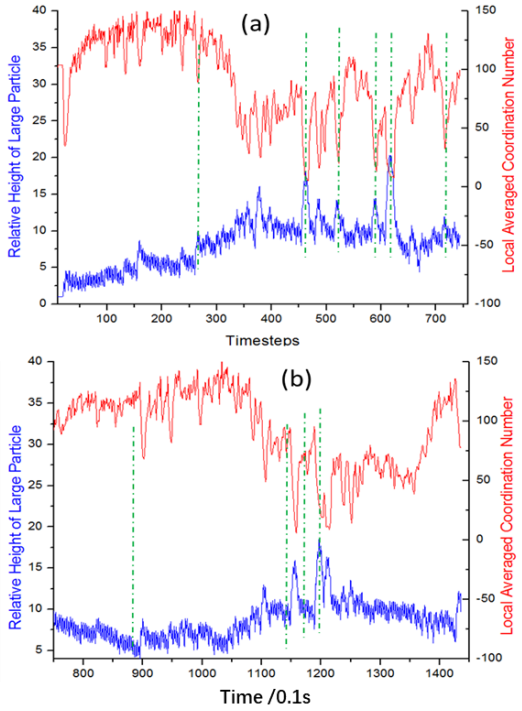

Figure 5-4 Time evolution of the relative height of large particle associated with its LACN. The relative height of large particle describes the distance between the large intruder and the vibrated base. Vibration frequency: 20Hz; Vibration amplitude: 10mm. (a) From 0 to 750 timesteps; (b) from 750 to 1450 timesteps.

Another interesting finding is the disappearing of BNE under high vibration frequencies. As shown in Figure 5-5, when vibration frequency is increased to 50Hz, the motion of the large intruder presents more frequent oscillations. However, as there are not enough sudden decreases in LACN, the uprising motion of the large particle cannot be triggered, which demonstrates the disappearing of BNE in a microscopic view. This finding also shows that as stronger vibration may not result in stronger oscillations in LACN, it is not able to induce greater segregation.

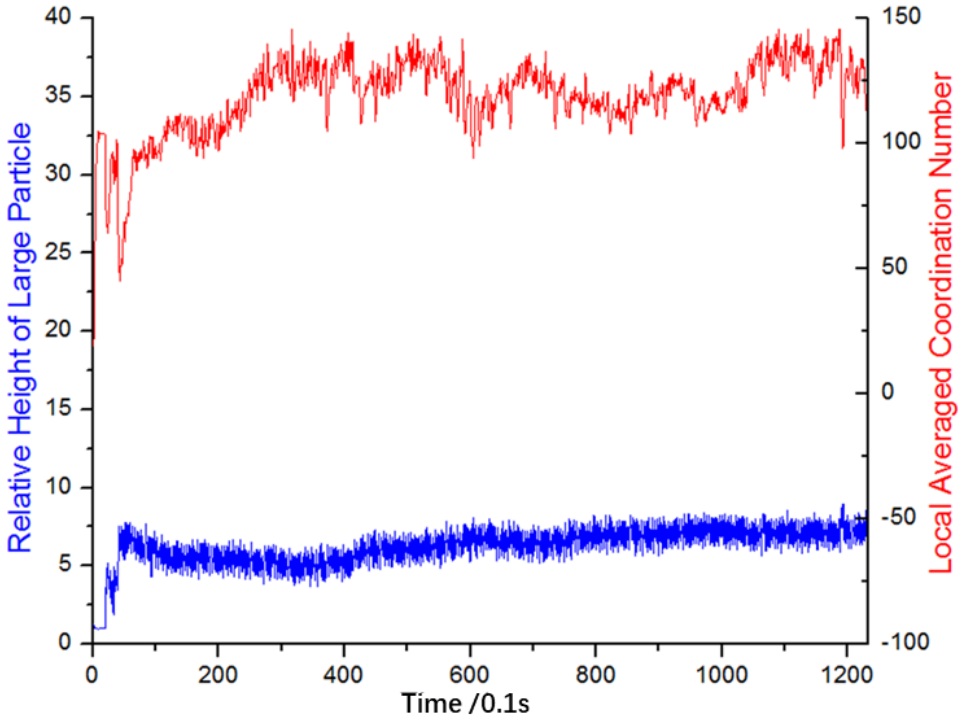

Figure 5-5 Time evolution of the relative height of large particle associated with its LACN. Vibration frequency: 50Hz; Vibration amplitude: 10mm.

5.3.1.2 Effects of vibration frequency

Through further investigation of the frequency effects, it was found that the vertical segregation pattern is largely affected by the overall packing states. Moreover, instead of showing a continuous rising pattern, the motion of the large intruder also presents a discrete vibrated pattern which is largely affected by the overall bed properties. To evaluate the bed properties, the averaged coordination number (ACN) is introduced which defines the averaged contacts within the whole granular bed. After pretreatments of the obtained data, the unrelated noises were eliminated and it was found that the time evolution of ACN shows a harmonious vibrated pattern around a fixed number. The fixed number was found related to the particle shape and will be further talked about in latter chapters. For this case, ACN is vibrating around 5. On the other hand, by adjusting the vibration frequency under 10mm vibration amplitude, the vibration of ACN presents several kinds of loops, which can be used to predict the appearance of BNE.

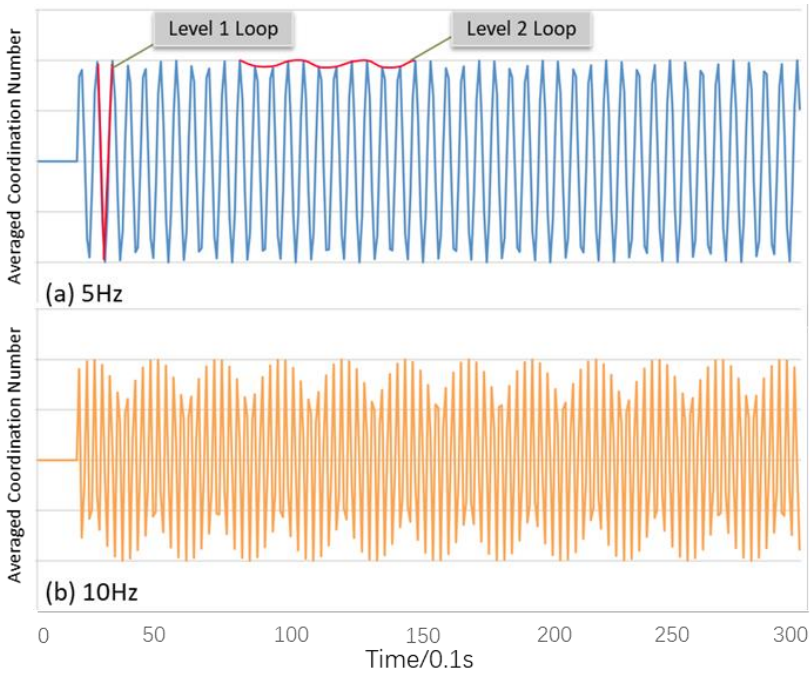

Figure 5-6 Time evolution of ACN. Amplitude:10mm; frequency: (a) 5Hz; (b) 10Hz. Sampling frequency: 100Hz.

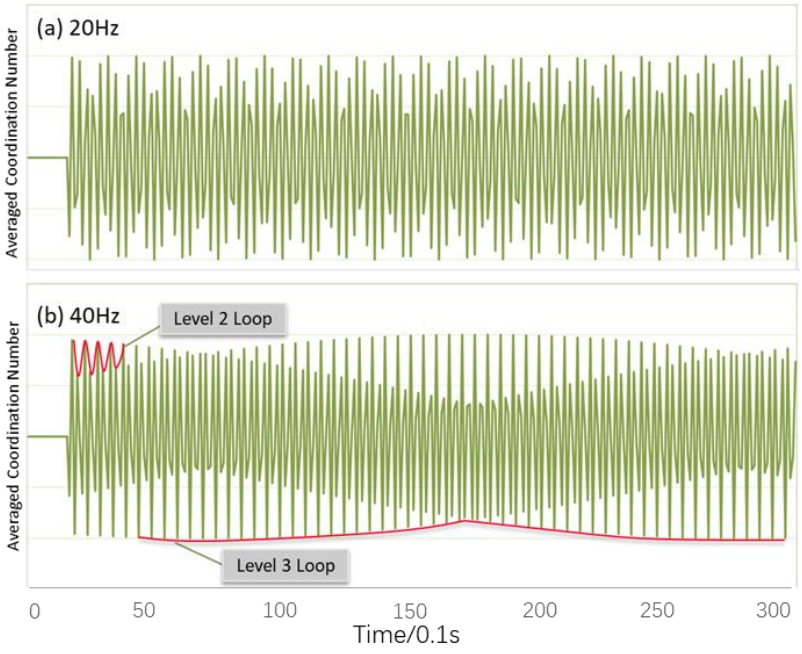

Figure 5-7 Time evolution of ACN. Amplitude:10mm. (a) frequency: 20Hz; (b) frequency: 40Hz. Sampling frequency: 100Hz.

Figure 5-6 and Figure 5-7 present the time evolutions of ACN under different vibration frequencies. The vibration loops with different levels were defined based on different observed patterns. Level 1 loop demonstrates the frequent vibrations from peaks to valleys, which are observed under all vibration conditions. Level 2 loop defines the vibration of peak values in level 1 loop, and the amplitude of level 2 loop was found to be decisive on the appearance of BNE. When vibration frequency increases, the amplitude of level 2 loop also increased, and the discrete jumping effects appeared in flow patterns get stronger. While the amplitude of level 2 loop is large enough, the jumping effects will motivate the large intruder's rising behavior, therefore the BNE can be clearly observed for cases shown in Figure 5-6b (10Hz) and Figure 5-7a (20Hz). With vibration frequency larger than 40Hz, level 3 loop appears as shown in Figure 5-7b. Moreover, the BNE disappeared as level 3 loop presents a weak vibration pattern. This conclusion was further confirmed by simulations under other vibration amplitudes. Therefore, several findings can be summarized through the study of ACN: (1) large amplitude of level 2 loop results in BNE; (2) when frequency is large enough, level 3 loop appears which terminates the BNE.

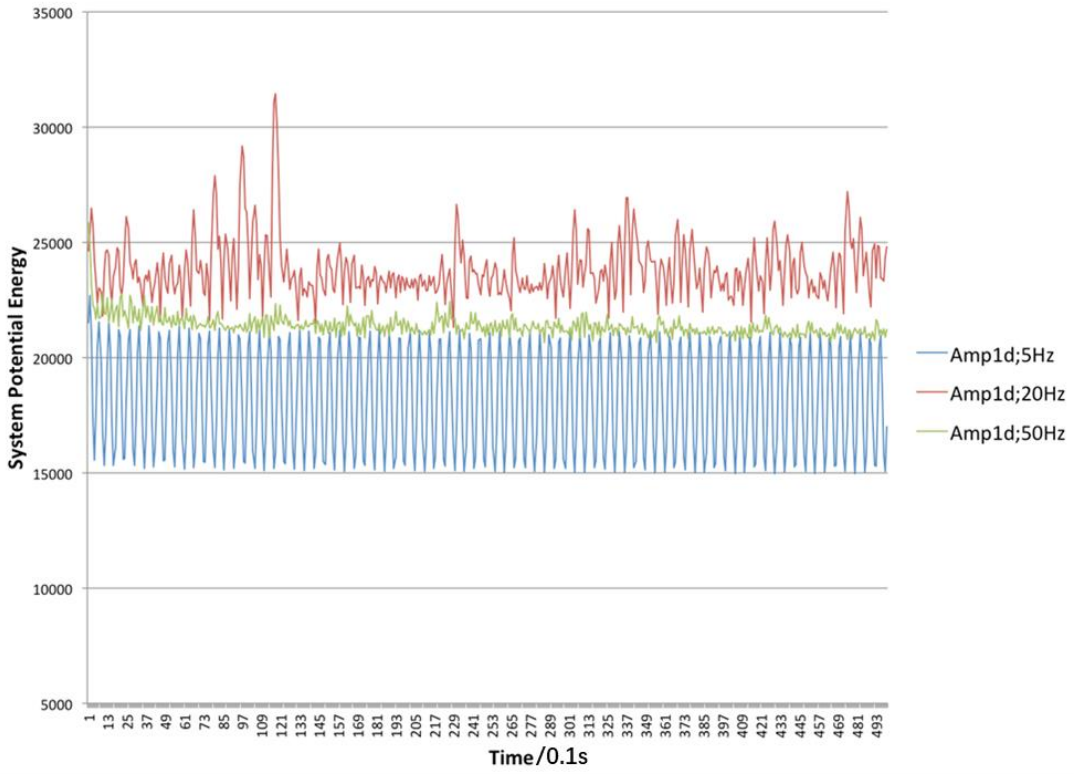

Figure 5-8 Time evolution of the system potential energy (gravitational potential energy only) under different frequencies. Vibration amplitude: 10mm; size ratio 2:1.

On the other hand, the effects of vibration frequency were also studied considering the system potential energy. As shown in Figure 5-8, the energy oscillations can be basically described by two components: oscillation amplitude and oscillation frequency. It was found that higher vibration frequency can directly result in higher oscillation frequency of system energy while oscillation amplitude is highly affected by the motion of large intruder. Then it was concluded that the vertical segregation is cohesively induced by high oscillation amplitude associated with high oscillation frequency.

5.3.1.3 Effects of vibration amplitude

Previous researches have studied effects of vibration amplitude on vertical segregation, the general findings show that larger amplitude can directly result in stronger segregation. The simulations conducted in this work also confirmed this conclusion and further interprets these findings from several views.

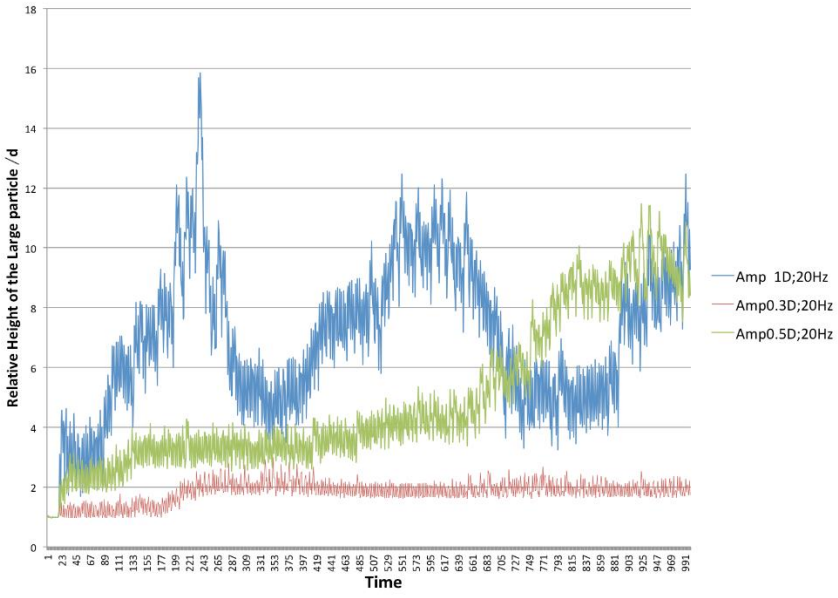

Figure 5-9 Time evolution of the large intruder's vertical position relative to the vibrated base.

To demonstrate the effects of amplitude on large intruder's motion, the time evolution of large particle's vertical position was constructed as shown in Figure 5-9. It can be found that the segregation gets stronger with increasing vibration amplitude. Moreover, when the vibration amplitude is large enough, the comeback behavior of large intruder is also observed. As mentioned in previous section, the comeback behavior is largely decided by the large intruder's local porosity. While

larger amplitude can induce stronger jumping effects of the large intruder, it will indeed extend the upper and lower limitations of the local porosity, which will consequently result in the comeback behavior.

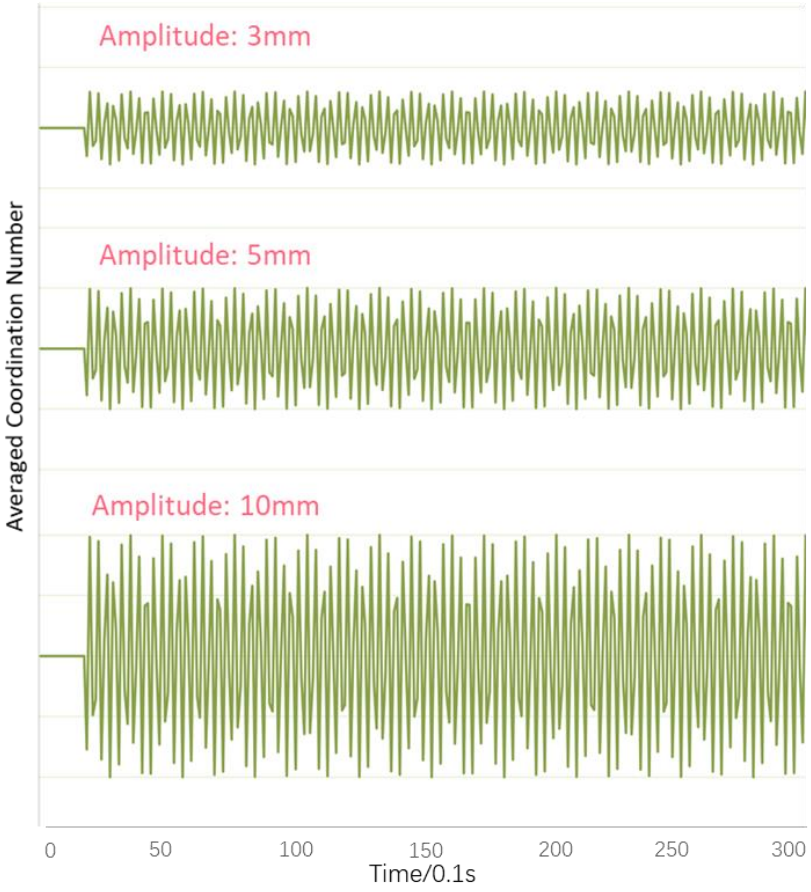

Figure 5-10 Time evolution of CAN with different vibration amplitude. The BNE only occurs in case with 10mm as the amplitude. Vibration frequency: 20Hz. Sampling frequency: 100Hz.

The effects of vibration amplitude were also studied considering the averaged coordination number. As shown in Figure 5-10, the vibration pattern of ACN cannot be affected by changing vibration amplitude. However, the vibration of ACN

can be simply enlarged with increasing vibration amplitude, which also extends the amplitude of level 2 loop. And as previous conclusions have mentioned that BNE appears when the amplitude of level 2 loop is large enough, the increasing amplitude can consequently lead to the occurrence of BNE.

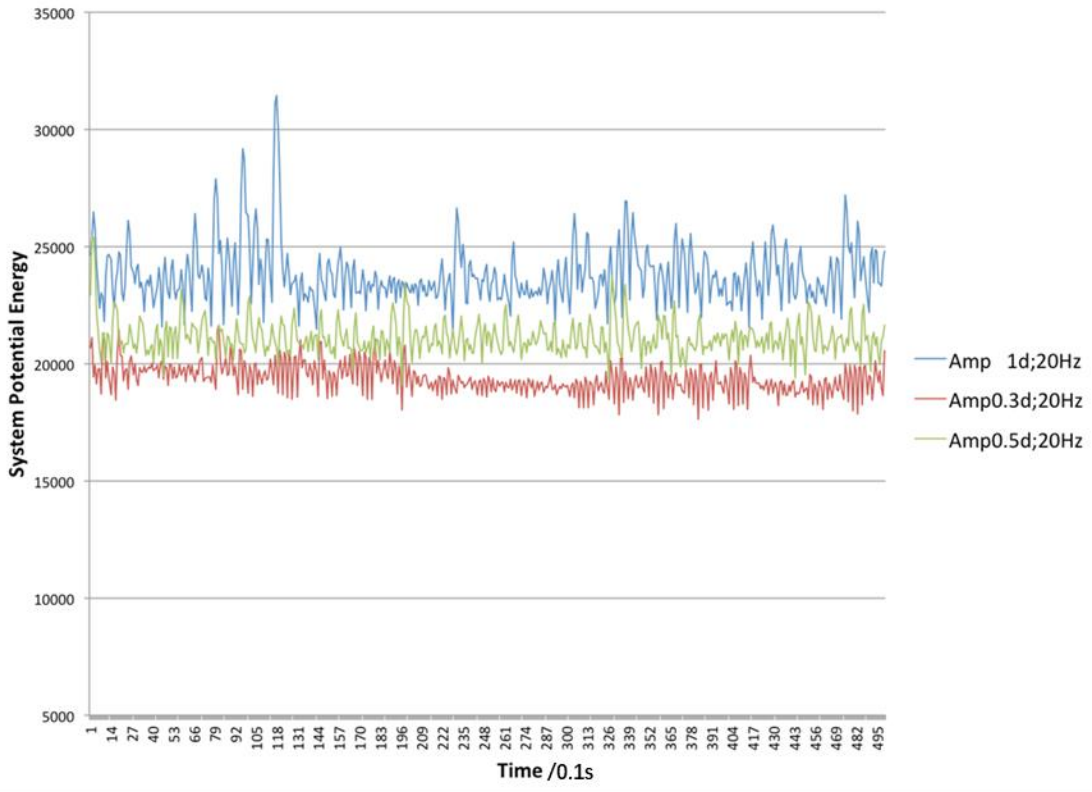

Figure 5-11 Time evolution of the system potential energy (gravitational potential energy only) under different vibration amplitudes. Vibration frequency: 20Hz; size ratio 2:1.

Considering the system potential energy, the influence of vibration amplitude is similar as the study of ACN. Instead of affecting the oscillation patterns shown in system potential energy, increasing vibration amplitude can only enlarge the amplitude of energy oscillations. Then for fixed vibration frequency, larger

vibration amplitude will indeed result in stronger segregation behavior.

5.3.2 Effects of particle properties

5.3.2.1 Effects of particle size

With fixed size (10mm) of small particles, the size of large intruder was changed from 12mm 30mm to investigate the effects of particle size ratio. The motion of the large intruder was recorded in Figure 5-12. Several conclusions can be made based on the simulations. Firstly, the rising behavior of the large intruder is still triggered by vibration conditions which means that BNE can still occur with rather low size ratio under proper vibration conditions. Moreover, as shown in Figure 5-13, the comeback pattern of large intruder exists in all size ratios which also demonstrate the dominating effects of vibration conditions. But through comparisons among different size ratio, it can be clearly found that under same vibration conditions, larger size ratio can enlarge the segregation intensity by accelerating the motion of the large intruder.

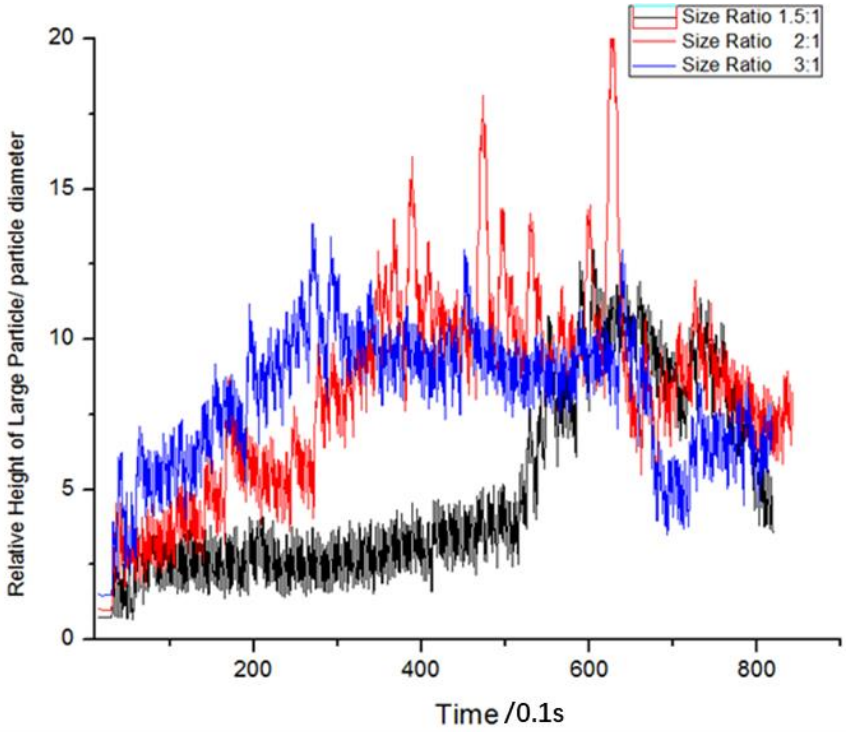

Figure 5-12 Time evolution of the large intruder's vertical position relative to the vibrated base. Vibration frequency: 20Hz; vibration amplitude: 10mm.

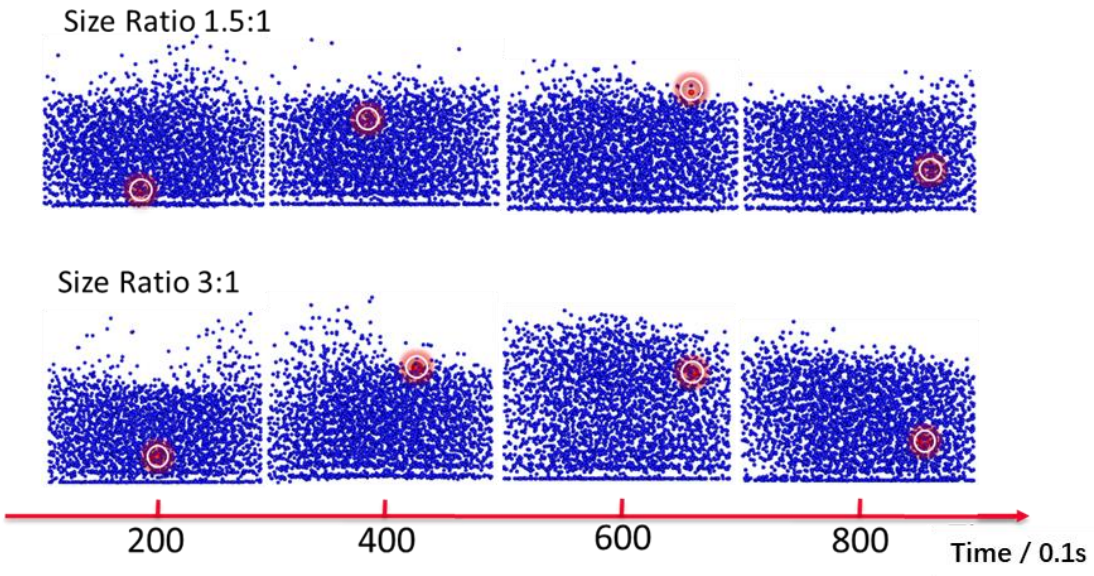

Figure 5-13 Time evolution of the flow patterns under same vibration conditions but different size ratios. Vibration frequency: 20Hz; vibration amplitude: 10mm.

5.3.2.2 Effects of intruder shape

To clearly identify the effects of intruder shape, simulations based on the DEM ellipsoidal model were conducted, and by changing the shape of the large intruder from prolate to oblate, it was found that effect of intruder shape is largely related to the intruder's initial orientation. For ellipsoidal particles, the two extreme particle orientations are shown in Figure 5-14, where Figure 5-14a presents the natural lying pattern while Figure 5-14b shows a unstable standing pattern. From the simulations, the intruder with standing initial orientation was first motivated to a lying-like pattern and then rises through the bed, while the lying-patterned can be directly driven to rise like the motion of spherical intruder.

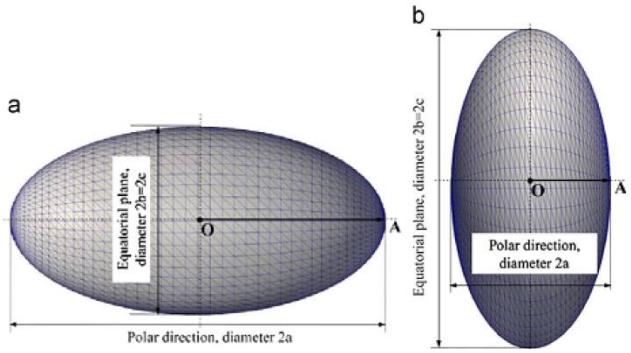

Figure 5-14 Schemes of the two extreme particle orientations for ellipsoidal particles.

Based on the difference of motion patterns between different initial orientations, it was then found that, for fixed aspect ratio, when the intruder's orientation changes from the lying pattern to the standing pattern, the time required to reach the particle surface gets longer. More importantly, if the initial intruder orientation stays as the lying pattern, the shape effects are very weak that there is showing

little difference from the BNE obtained with spherical intruder. The obtained conclusions are also shown in Figure 5-15.

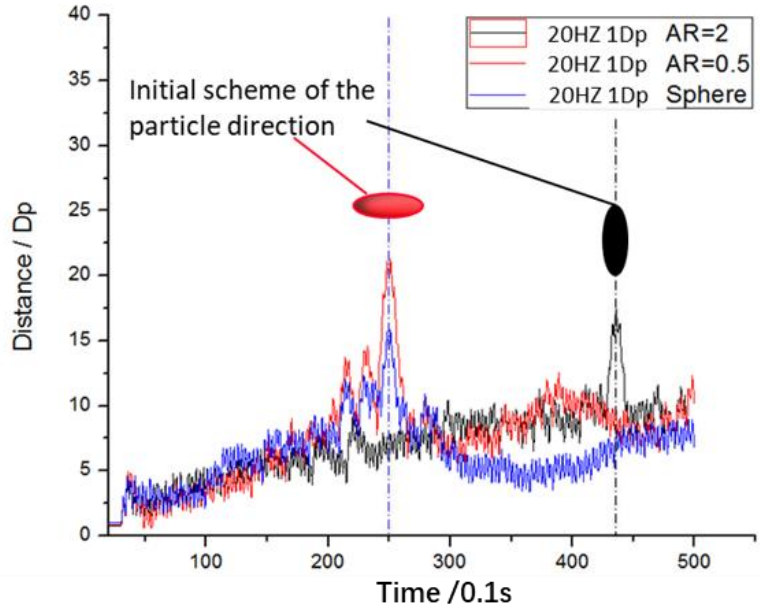

Figure 5-15 Time evolution of the vertical position of the large intruder. Vibration frequency: 20Hz; Vibration amplitude: 10mm. Equivalent size of the large intruder: 20mm.

5.4 Conclusions

In this chapter, the vibration-induced segregation with one intruder has been comprehensively studied considering vibration conditions and particle properties.

Vibration conditions including vibration frequency and vibration amplitude are dominating the occurrence of BNE and a phase diagram was constructed. For fixed vibration amplitude, segregation only occurs when vibration frequency is within a special range, and the critical points of the interval is related to vibration

amplitude while larger vibration amplitude can extend the range of vibration frequency. On the other hand, there is no upper limit for vibration amplitude as larger amplitude can directly induce stronger and faster BNE.

Considering the particle properties, the size ratio and particle shape are studied under certain vibration conditions. By changing the size of the single large intruder, it was found that larger size ratio can enlarge the segregation intensity during the vibration process, but it cannot significantly affect the occurrence of BNE as the segregation is still determined by vibration conditions. For the study of particle shape, the shape of large intruder influences the segregation process by the intruder's initial orientation. More specifically, standing-like initial orientation can increase the time required for the intruder to reach on top while lying-like initial orientation cannot significantly affect the original vertical segregation.

Chapter 6 Vibration-induced segregation in binary mixtures of large and small particles

6.1 Introduction

Granular segregation is mostly a practical concern as it is largely related to various systems in industries. The segregation observed vibrated systems is a typical and fundamental case where the granular behavior is triggered by input motivation. Lots of researches have been conducted to experimentally and numerically understand the fundamental vibration-induced segregation.

The basic vibration-induced segregation demonstrates the phenomenon that vibration drives large intruders to move upward within bulk solid of small particles, which is also called “Brazil-nut Effect (BNE)”. Many researchers have started with the cases with only one large intruder. Ahmad and Smalley (1973) first conducted physical experiments to study this phenomenon, and the importance of vibration acceleration and density was addressed through their findings. Cooke et al. (1996) did further experiment with the help of advanced high-speed camera, through which they found the motion of the large intruder is largely affected by the size ratio. Due to the limitation in physical experiments, this phenomenon was also studied by many researchers through various numerical methods, such as Monte Carlo method (Rosato et al. 1986, Rosato et al. 1987, Abreu et al. 2003), Molecular Dynamics (Pöschel and Herrmann 1995) and discrete element method (DEM) (Lan and Rosato 1997, Rosato et al. 2002, Fernando and Wassgren 2003, Yang 2006, Fang and Tang 2007). The previous part of this thesis also found that the segregation behavior is dominated by vibration

conditions and the shape of intruder can also significantly influence the segregation intensity.

Lots of researches extend the single intruder study to cases with more than one large intruders. Rosato et al. (1987) adopted granular mixture with relative amount of large particles in the simulations, where the influence of vibration acceleration and container geometry (Lan and Rosato 1997) were studied associated with the convection mechanism. Abreu et al. (2003) used 50/50 binary mixtures of spherocylinders, and it was found that the final segregation pattern is largely affected by particle shape when size effects are eliminated. Schroter et al. (2006) summarized the physical mechanisms under different circumstances and also identified the reverse Brazil-nut effect. As the previous researches have extensively studied the cases with intruder, a better understanding of the cases with more than on intruder is comparably lacked and of great need.

In this chapter, the vibration-induced vertical segregation with relative amounts of large particles will be extensively studied considering the vibration conditions and related particle properties. The ellipsoidal DEM model is adopted, and detailed profiles of velocity, force and position were well obtained. Several important conclusions have been made and it was found that the importation of more intruders can largely increase the overall randomness of the particle bed, which will make the vertical segregation easier to occur.

6.2 Simulation method and conditions

6.2.1 Discrete element method (DEM)

Please refer to Section 4.2.1 in Chapter 4.

6.2.2 Simulation conditions

The simulated problem is shown schematically in Figure 5-1. The dimension of the cylindrical container is 170mm in diameter and unlimited in vertical direction. The granular beds are pre-packed at the base before vibration starts, and large intruders are randomly packed at the bottom in the center of the bed. The vibration imported on the container base follows the pattern of simple harmonious vibrations with amplitude *A* and frequency *f*.

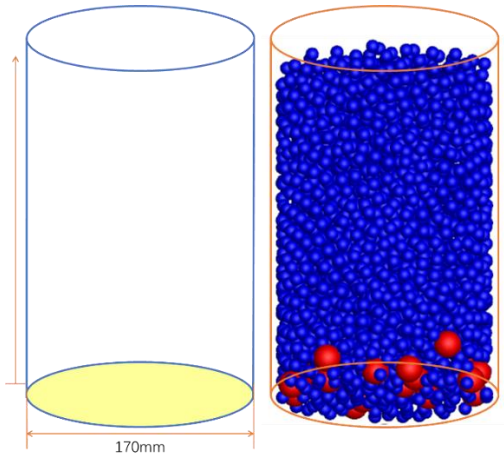

Figure 6-1 Schematic diagram of the simulated cylindrical containers.

The granular materials used in the simulations contain spherical particles and ellipsoids. The exact physical properties of the particles were set to those of glass

beads. Details of the physical properties and other input variables are shown in Table 6-1.

Table 6-1 Simulation conditions and related parameters

Input variables	Value
Size of small particles	10mm
Size of large particle	20mm
Number of large/small particles	(10, 20, 30, 40, …,100)/2000
Aspect ratio	0.5, 0.7, 0.9,1, 1.2, 1.5, 1.8, 2, 2.5
Young's module	1×10^8 N/m^2
Poisson's ratio	0.3
Sliding coefficient (P-P)	0.4 (standard)
Sliding coefficient (P-W)	0.4 (standard)
Rolling coefficient (P-P)	0.3 (standard)
Rolling coefficient (P-W)	0.3 (standard)
Particle density	2.7×10^3 kg/m^3
Vibration frequency	5Hz to 80Hz
Vibration amplitude (defined as a dimensionless factor regarding size of small particles)	1mm to 15mm (0.1 small particle diameter – 1.5 small particle diameter)
Simulation Timestep	10^{-3}s

6.3 Results and discussions

6.3.1 Effects of vibration conditions

The simulations were first conducted to investigate the effects of vibration conditions. As ACN has demonstrated sufficient abilities to help study and predict the vertical segregation phenomenon, it is further applied to study the cases with 20 intruders.

The importance of vibration frequency has been addressed in the study with single large intruder, and it was also found showing dominant effect for cases with more than one large intruders. As shown in Figure 6-2, the obtained patterns of ACN's evolution are almost same as the ones obtained for single intruder cases, which shows that small amounts of large particles cannot affect the overall packing states.

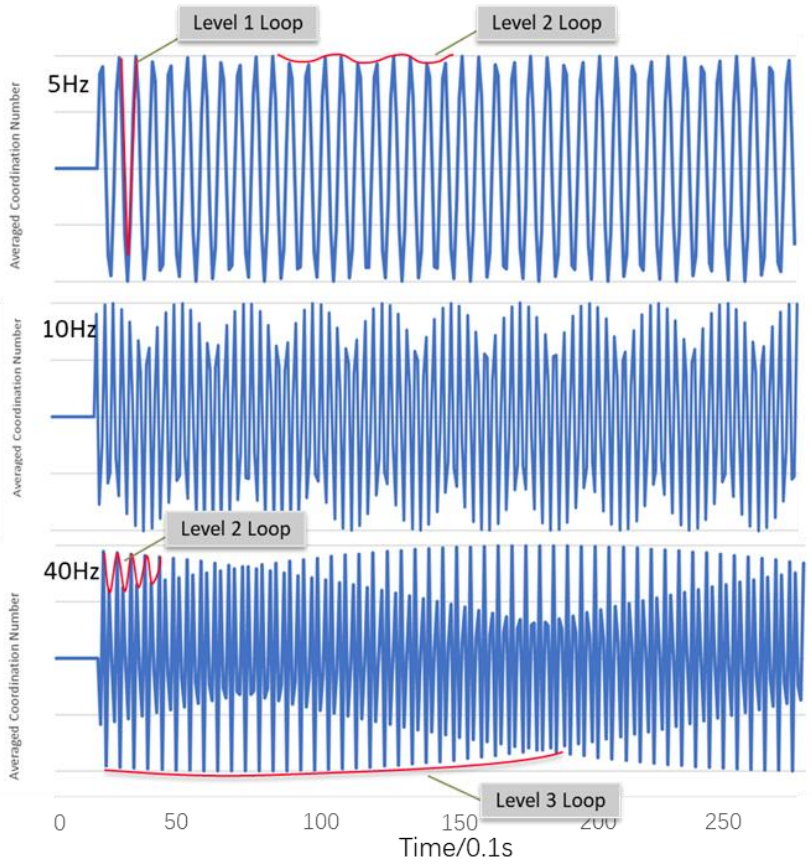

Figure 6-2 Time evolution of ACN under different vibration frequencies. Vibration amplitude: 10mm; size ratio: 2:1; number of large particles: 20. Sampling frequency: 100Hz.

Considering the occurrence of vertical vibration, it also occurs within a certain range of frequencies. When vibration frequency increases, the amplitude of level 2 loop gradually increases which illustrates stronger vibration intensity. The large intruders start to rise while the oscillation amplitude of level 2 loop is large enough, and this is consistent with the findings in single intruder cases. But the situation changes when it comes to the high frequency cases. As level 3 loop can stop the single intruder's rising motion, the Brazil-nut Effects is still observed for

cases with 20 intruders, such as the cases under 40Hz vibration frequency.

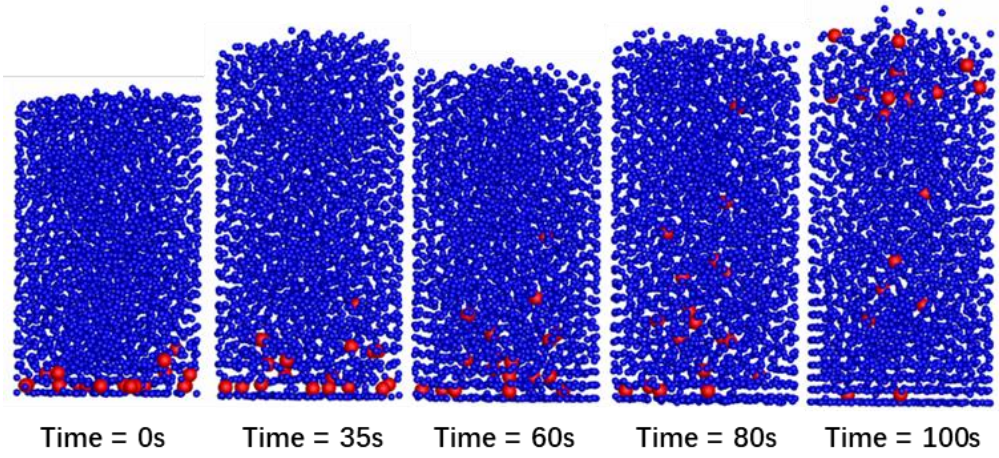

Figure 6-3 Time evolution of flow patterns with 40Hz vibration frequency and 10mm vibration amplitude. Number of large intruders: 20.

To further illustrate the situation happening in 40Hz cases, it was found that a different mechanism is triggering the rising behavior of large intruders. As shown in Figure 6-3, the particles located at the bottom area cannot be instantly driven to rise at the first stage, which is the same as the intruder shown in single intruder cases. But for large particles with higher initial position, the vibration condition can still motivate their rising motions. And even these rising particles cannot largely affect the overall bed properties, they can still influence the local porosity which will motivate rising motion of the neighbor particles in bottom layer. Therefore it can be observed at the beginning stage that the large intruders actually start rising in order instead of staring rising simultaneously. The same regimes were also observed for cases with rather low vibration frequencies. For

instance, when vibration frequency is set to 7Hz, the single intruder case cannot present the BNE while it is successfully observed in multiple intruders simulations.

The effects of vibration amplitude are also studied based on the DEM simulations. The general conclusion is consistent with the results reported in single intruder studies. As shown in Figure 6-4, larger vibration amplitude can induce greater level 2 loop oscillation amplitude which can further induce stronger segregation. And it also shows that intruders' rising behavior only occurs when vibration amplitude is large enough.

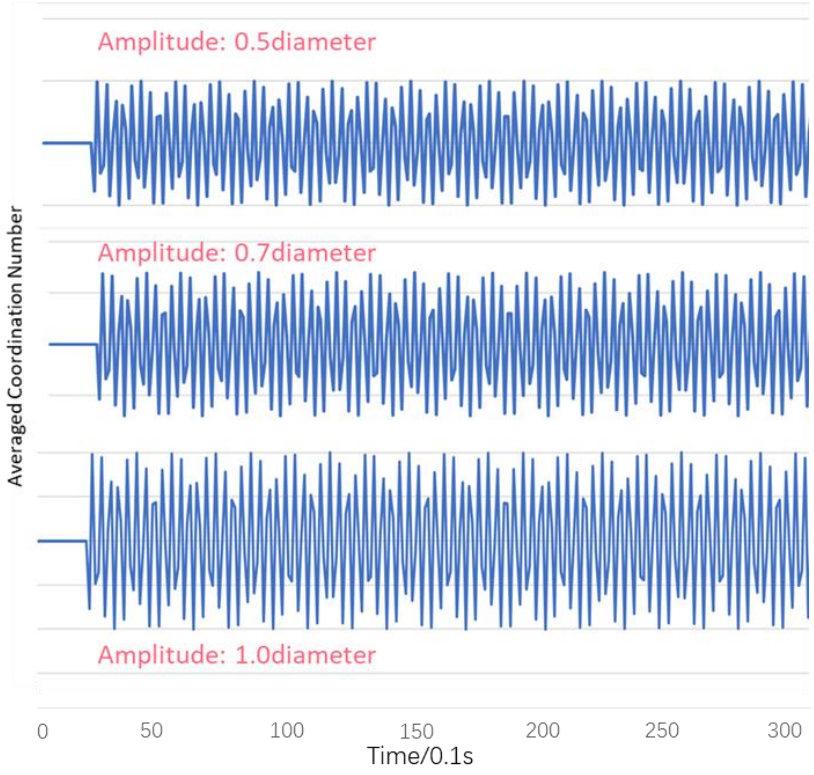

Figure 6-4 Time evolution of ACN under different vibration amplitudes. Vibration frequency: 20Hz; size ratio: 2:1; number of large particles: 20. Sampling frequency: 100Hz.

The general effects of vibration amplitude are further confirmed based on the studies of system potential energy. The system potential energy shows random oscillations with respect to time. These oscillations vary in amplitudes and frequency, and the intensity of oscillations also indicates the pattern evolutions occurring within the particulate bed. Therefore, stronger energy oscillations can directly indicate stronger segregation behavior. As shown in Figure 6-5, under same vibration frequency, the energy oscillations present greater amplitude with larger vibration amplitude. Therefore it can be further concluded that larger vibration amplitude can directly result in greater vertical segregation phenomenon.

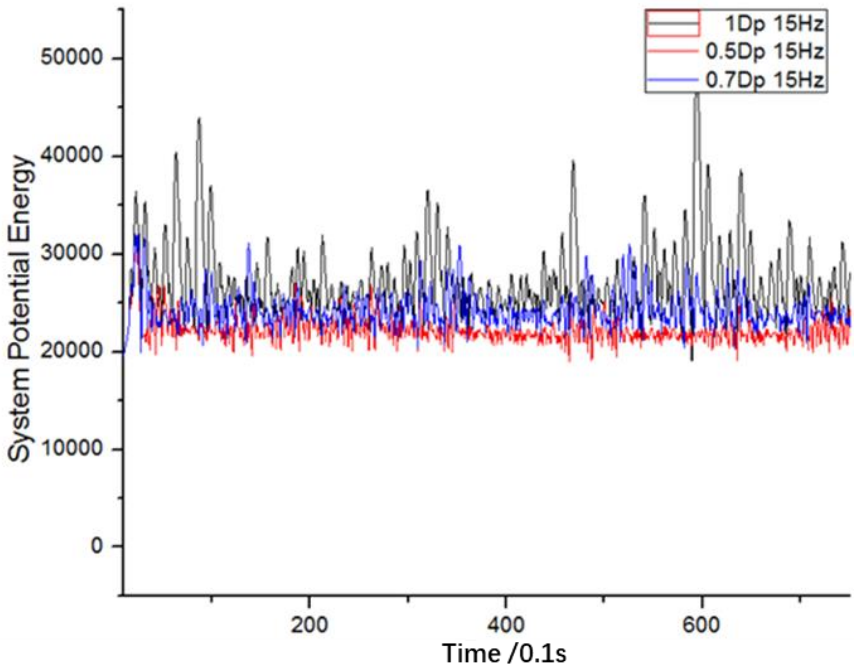

Figure 6-5 Time evolution of the system potential energy under different vibration amplitudes. Vibration frequency: 20Hz; number of large particles: 20.

Even the major effects of vibration amplitude are the same as the findings from single particle cases, the multiple intruder cases still present a different regime when it comes to the cases with rather low vibration amplitude. Figure 6-6 shows the comparison between single intruder results and results obtained with 20 intruders. Under 3mm vibration amplitude and 20Hz vibration frequency, the single intruder failed to rise to the bed surface while multiple intruders present rising behavior. More specifically, the rising regime is similar as the patterns observed in high vibration frequency. While the rather low vibration amplitude still cannot trigger the rising motions of intruders located at the bottom layer, the other intruders with higher vertical positions are successfully motivated to move upwards. These upper layered intruders' moving motions can largely affect the local porosity which can further induce the neighbor intruders in the bottom layer to rise. This ordered chain reaction was found dominant in cases with rather low vibration amplitude. Considering the system potential energy, the multiple intruders cases also present comparably greater oscillations comparted to the single intruder cases, which further confirms the different regimes obtained.

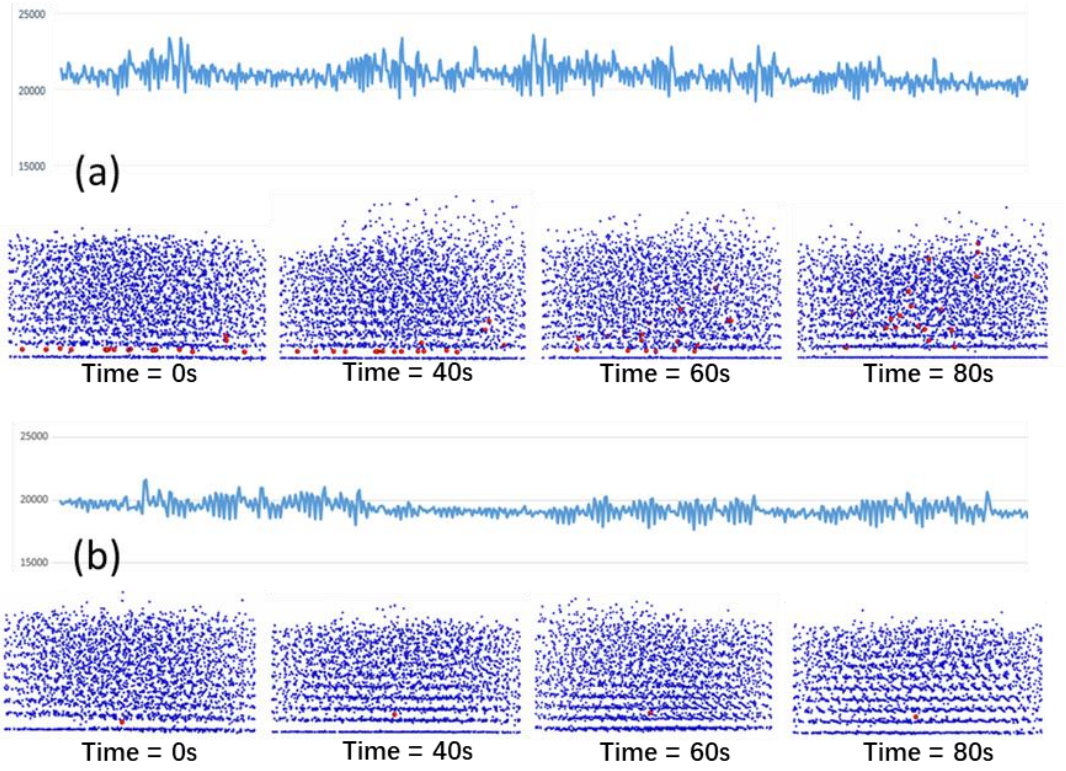

Figure 6-6 Time evolutions of system potential energy and flow patterns. Vibration amplitude: 3mm; vibration frequency: 20Hz. (a) 20 large intruders with 20mm diameter; (b) 1 large intruder.

6.3.2 Effects of particle numbers

By changing the number of large particles, it was found that the particle number can largely influence the flow regimes when BNE occurs.

To identify the exact effects of particle numbers, the simulations were conducted in respect to two specific vibration conditions: (1) vibration condition that is sufficient for inducing intruder's rising behavior in single intruder cases; (2) vibration condition that cannot induce intruder's rising behavior in single intruder

cases while it is sufficient for motivating the vertical segregation happening in cases with multiple intruders.

Figure 6-7 shows the flow patterns obtained under first type of vibration conditions. When the vibration is set to be 10mm in amplitude and 7Hz in frequency, the single intruder cannot be driven to rise while multiple intruders cases can present an ordered rising pattern. By comparing the 10 particles cases and the 40 particles cases, it was found that by increasing the number of large intruders, the vertical segregation gets stronger. More specifically, it takes shorter time for 80% of the large intruders to rise on top when the number of intruders is larger. To further interpret these findings, it was found that, as intruders in the bottom layer cannot be directly motivated by vibrations, the introducing of more intruders can largely increase the chance for them to be influenced by neighbor intruders in higher layers. Therefore, while more intruders can increase the overall uncertainty of the granular bed, it is consequently resulting in higher degrees of vertical vibration.

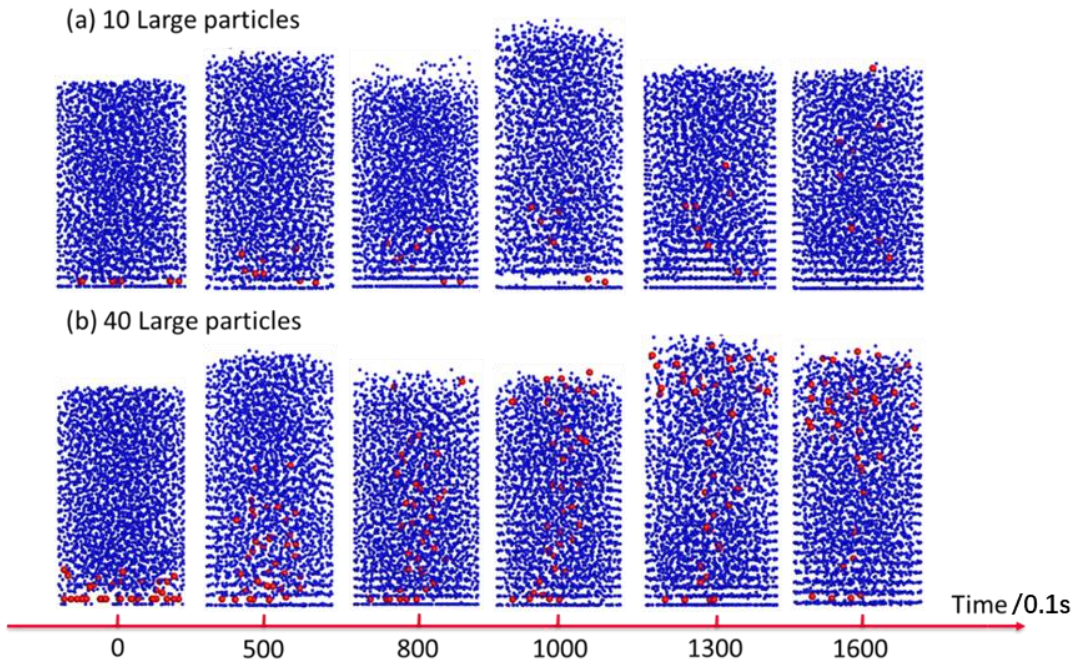

Figure 6-7 The comparison of flow patterns obtained with 10 large intruders and 40 large intruders. Vibration frequency: 7Hz. Vibration amplitude: 10mm.

On the other hand, the effects of particle numbers are also studied under vibration conditions that are sufficient for triggering BNE in single intruder cases. Figure 6-8 shows the comparison of different intruder numbers when vibration frequency is 20Hz and vibration amplitude is 10mm. And two key conclusions were made throughout the simulations. Firstly, while the vibration conditions can directly motivate every intruder's rising motion, it is then observed that all large intruders are rising together regardless of their initial positions. Moreover, as every intruder is rising individually, the overall segregation intensity and rising velocity stay the same when particle number changes. Therefore, it is further concluded that at this type of vibration conditions, the number of large intruders cannot significantly

influence the vertical segregation.

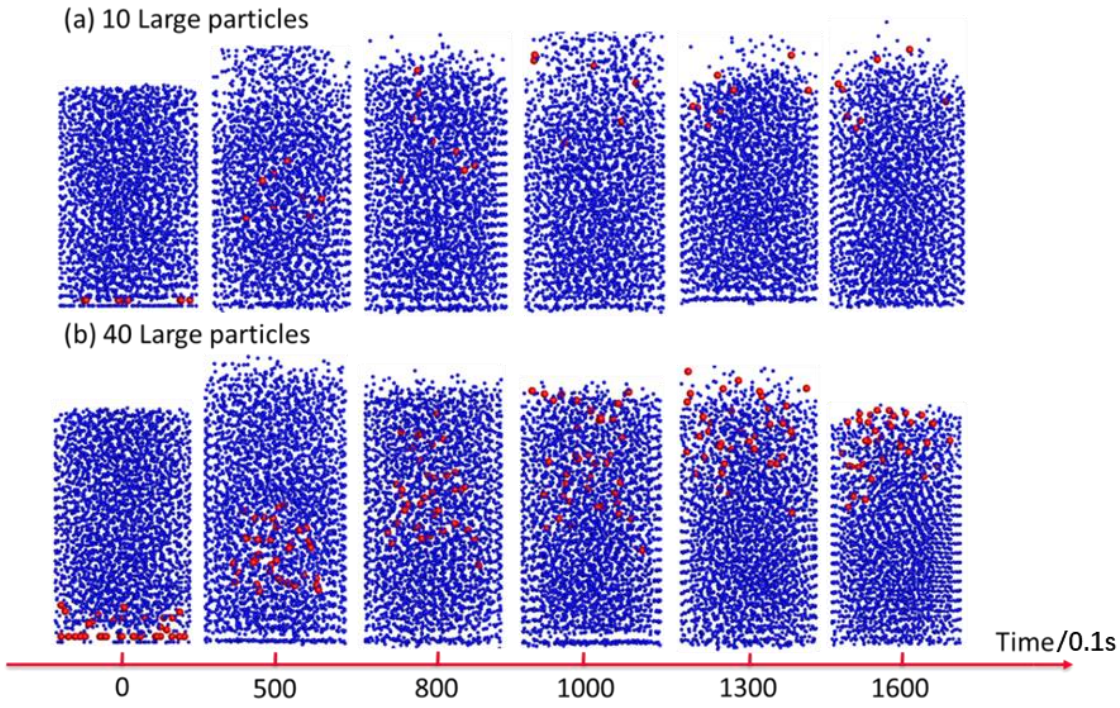

Figure 6-8 The comparison of flow patterns obtained with 10 large intruders and 40 large intruders. Vibration frequency: 20Hz. Vibration amplitude: 10mm.

The studies of system potential energy also confirm the findings through flow patterns. As shown in Figure 6-9, when the vibration conditions are set to be 10mm in amplitude and 20Hz in frequency, the energy oscillations present similar patterns with different averaged energy level. When number of large particles increases, the averaged energy level significantly increases, but the oscillation intensity stays at the same level. So it can be further concluded that vibration-induced segregation is mainly affected by the oscillation intensity of system potential energy while the averaged energy level cannot make a difference.

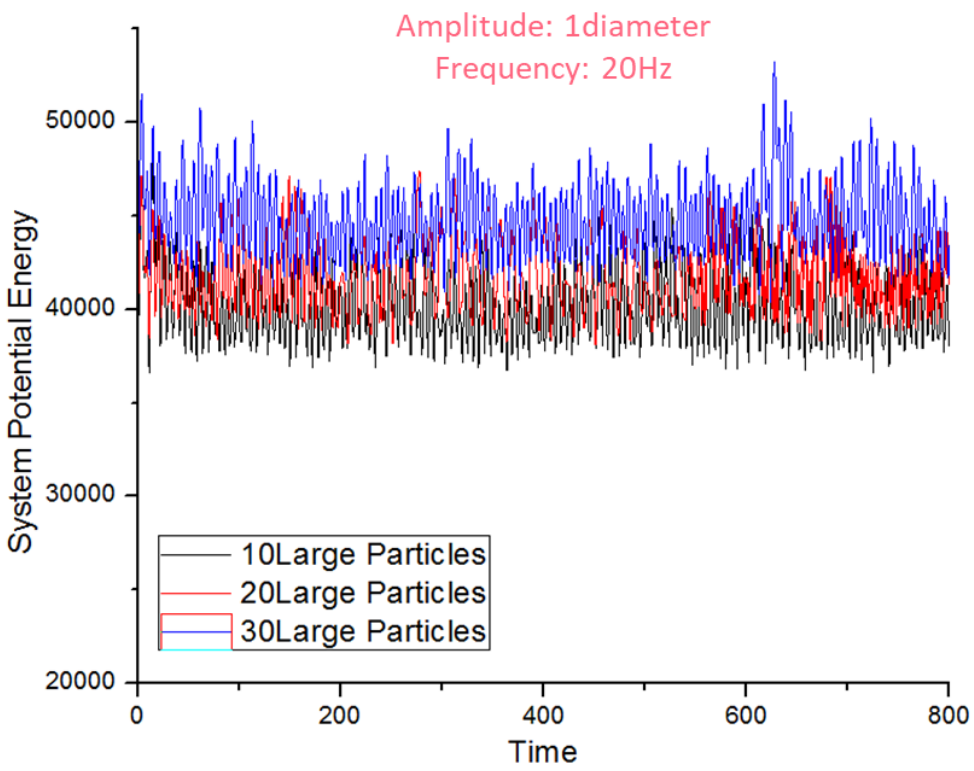

Figure 6-9 Time evolutions of system potential energy when the granular mixtures contain different numbers of large particles. Vibration amplitude: 10mm; vibration frequency: 20Hz.

6.3.3 Effects of particle shape

To clearly identify the shape effects on vibration-induced segregation, the studies were conducted separately in respect to the shape of large intruders and the shape of bulk solids.

6.3.3.1 Shape of large particles

The simulations were conducted based on the ellipsoidal DEM model, and the shape of the large intruders is decided by aspect ratio. By changing the aspect ratio

from 0.2 to 3, the shape of the intruders changes from needle like particles to tablet like particles. The results demonstrate that intruder shape can significantly affect the segregation intensity by influencing the small particles' percolation behavior. Figure 6-10 presents the comparison flow pattern evolutions between several typical cases. It was found that ellipsoidal intruders tend to rise faster compared to spherical intruders. In order to further interpret this finding, it was then found that the small particles' motion has been significantly affected when intruder shape is changed. While the large intruder becomes less spherical, its coordination number increases which shows that more small particles are in contact with the large intruder. This feature will then increase the chance for the neighbor small particles to fill in the voids beneath the large intruder during segregation, therefore the large intruders may rise at a faster velocity.

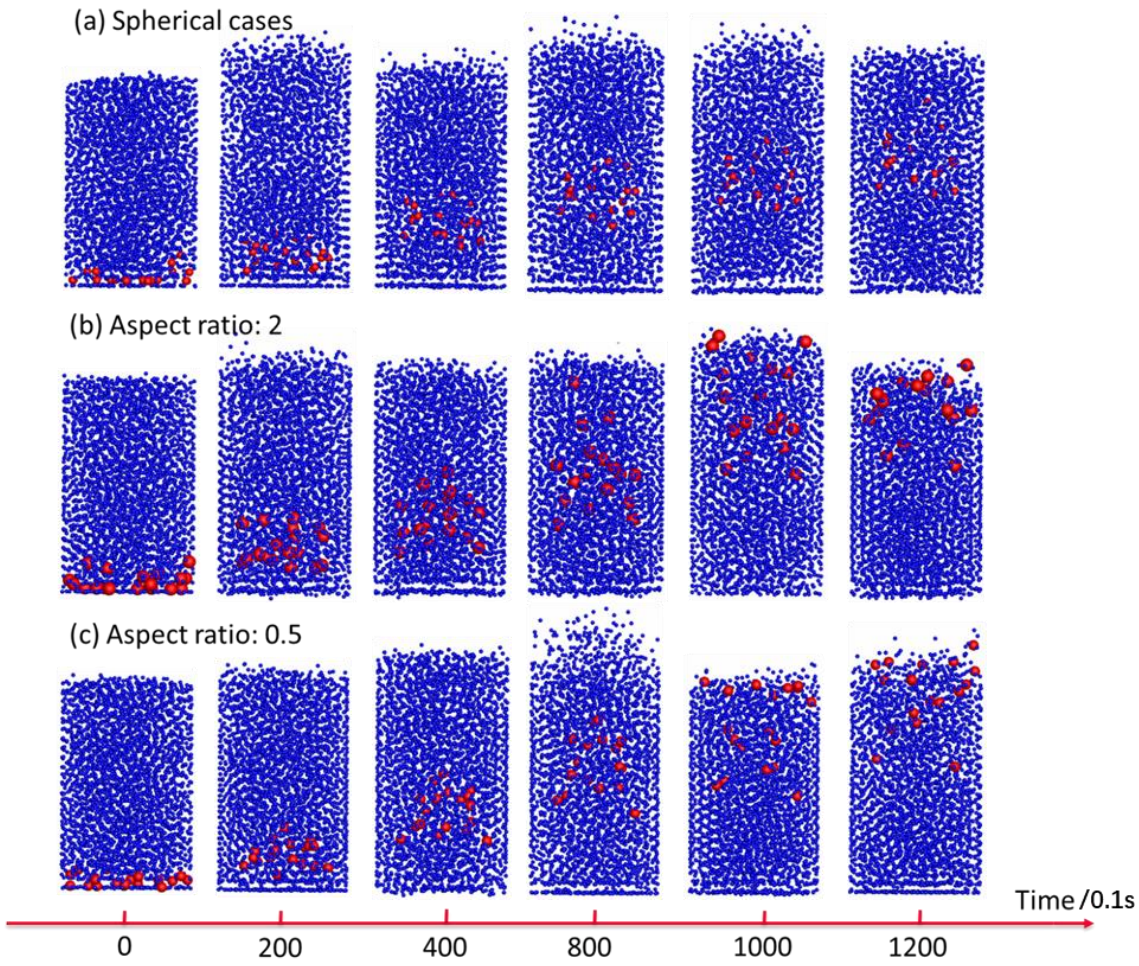

Figure 6-10 The comparison of flow patterns evolutions from several typical cases. Vibration frequency: 20Hz; vibration amplitude: 10mm; number of large particles: 20. (a) spherical intruders; (b) aspect ratio of the large intruders: 2; (c) aspect ratio of the large intruders: 0.5. In (a) and (c), the red spheres are used to represent the ellipsoids.

On the other hand, this phenomenon is also studied based on system potential energy. As shown in Figure 6-11, the oscillations of the system potential energy present similar patterns within different cases.

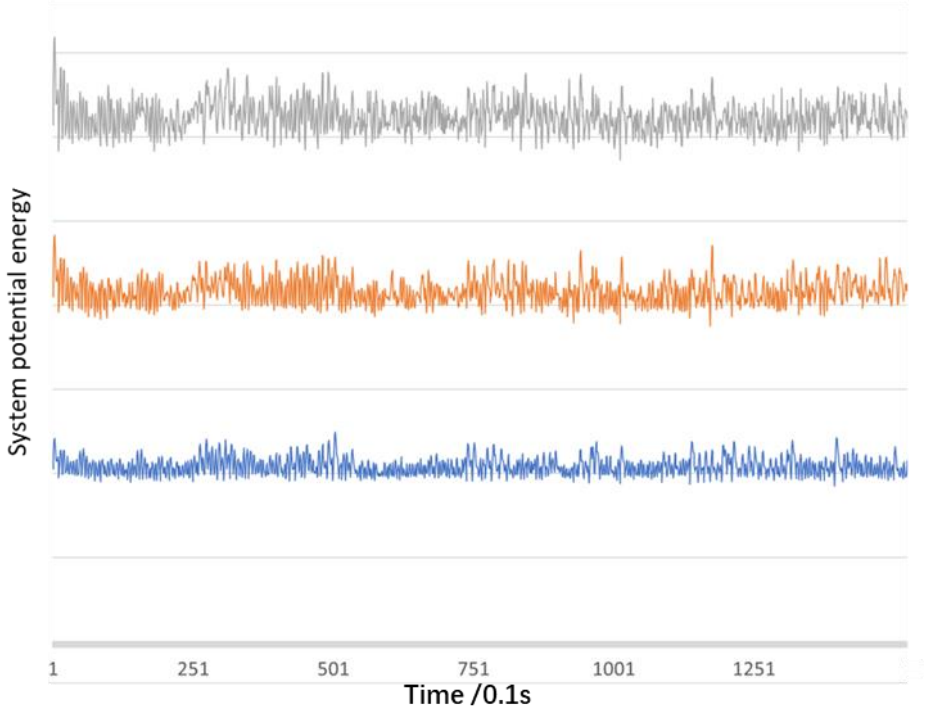

Figure 6-11 The comparison of system potential energy patterns. Vibration frequency: 20Hz; vibration amplitude: 10mm; number of large particles: 20. Grey curves: spherical intruders; Orange curves: large intruders with aspect ratio 2; Blue curves: large intruders with aspect ratio 0.5.

It could be expected that ellipsoidal cases might demonstrate stronger oscillations while stronger vertical segregation has been observed. However, the energy oscillations maintain the same intensity when large intruders get less spherical. In order to explain this phenomenon, it was then found that the intensity of vertical segregation is mainly decided by two effects: the granular bed's discrete jumping behavior and the small particles percolation behavior. Either of these two effects can strengthen the vertical segregation. Moreover, it was also concluded that the

energy oscillations are mainly decided by the discrete jumping effects which are not strengthened by changing the intruders shape. Then it can be consequently summarized that, the intruder shape can decide the segregation intensity by influencing the small particles' percolation behavior, but it cannot affect the discrete jumping phenomenon of the granular bed.

6.3.3.2 Shape of small particles

Different from effects of the large intruders, the properties of small particles can largely affect the overall bed states, which will further dominate the segregation phenomenon.

As the shape of bulk solids can significantly decide the repose angle in stockpile processes, it can also decide the overall contacting states in vibrated containers. More specifically, it was found that, by changing the aspect ratio of the bulk solids, the overall averaged coordination number presents a consistent pattern as shown in Figure 6-12. Several conclusions can be made based on the results: (1) cases with spherical bulk solids have the lowest averaged CN; (2) for prolate particles with increasing aspect ratio, the overall averaged CN increases first and then decreases with the milestone point around 0.5; (3) for oblate particles, the overall averaged CN increases with increasing aspect ratio, but the value of averaged CN maintains around 10 when aspect ratio is greater than 2.

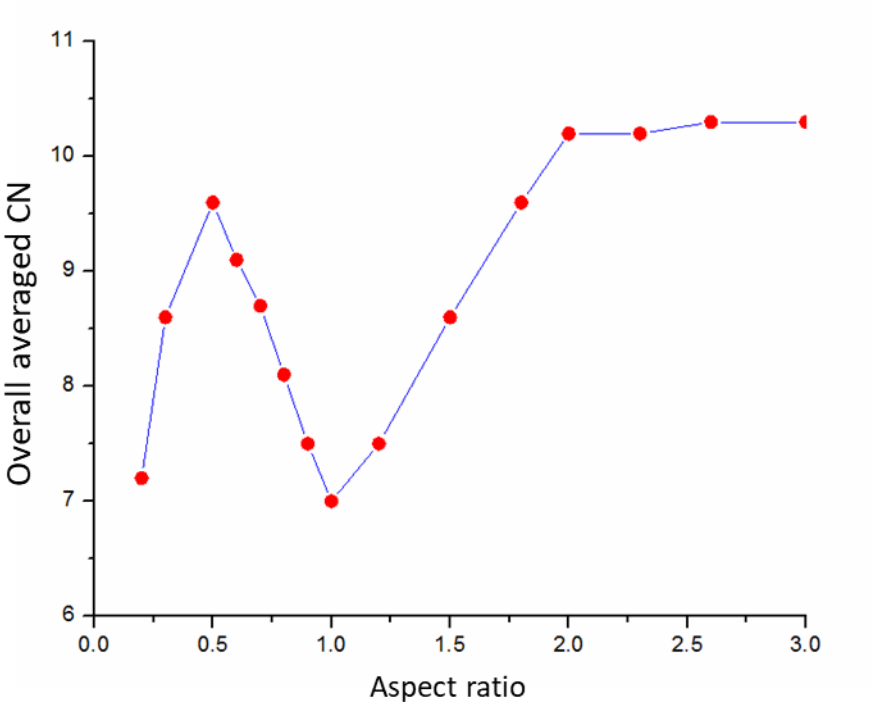

Figure 6-12 Effect of small particles' aspect ratio on overall averaged CN. Vibration frequency: 20Hz; vibration amplitude: 10mm; number of large intruders: 20.

Moreover, it was further found that the overall averaged CN can significantly affect the intruders' rising behavior. The time taken for the first intruder to rise on surface has been recorded in respect to different shapes of small particles, and the results are shown in Figure 6-13. It is obvious that the relation between time and aspect ratio presents an inverse pattern compared to the relation between overall averaged CN and aspect ratio, therefore it can be concluded that lower averaged CN can induce slower rising behavior. In order to further interpret this finding, it was found that the shape of small particles can affect the chance for small particles to percolate underneath the large intruders. More specifically, with larger

averaged CN, more small particles were in contact with the large particles which can strengthen the small particles' percolation behavior, and this will consequently lead to faster rising behavior of the large intruders.

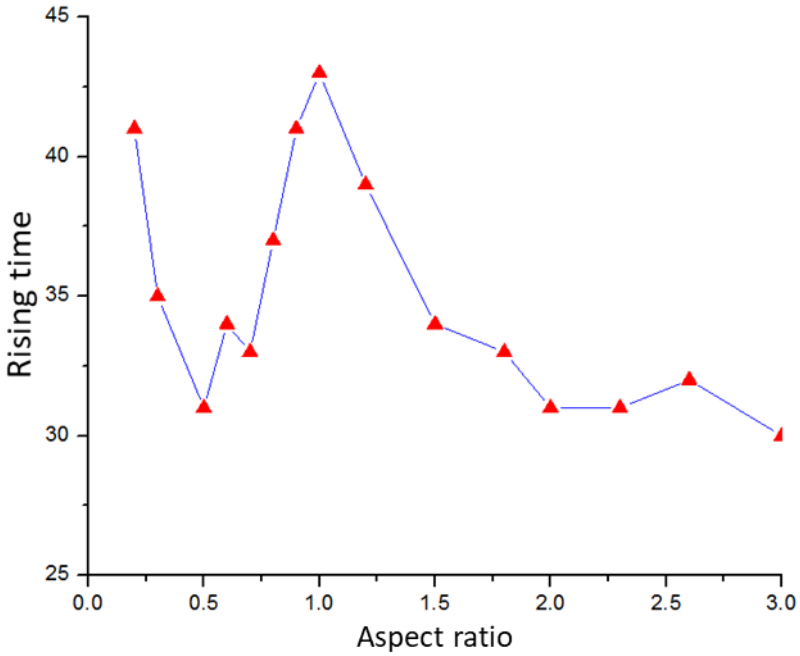

Figure 6-13 Effect of small particles' aspect ratio on the rising time needed for the first large intruder to rise on the granular surface. Vibration amplitude: 10mm; vibration frequency: 20Hz; number of large intruders: 20.

6.4 Conclusions

In this chapter, a DEM based study on vibration-induced size segregation has been conducted. The granular mixtures used are binary mixtures of bulk solids of small particles and large intruders, and the number of large intruders varies from 10 to 100. As the cases investigated in this part contains more than one large intruders,

the results further upgrade the studies from the cases with only one large intruder and several significant conclusions have been made.

The effects of vibration conditions have been well studied considering the vibration frequency and vibration amplitudes. For fixed vibration amplitude, the vertical segregation still occurs within a certain range of the vibration frequency, but the critical values of the range have been extended compared to the single intruder cases. For fixed vibration frequency, higher vibration amplitude can directly result in stronger vertical segregation, and the introduction of more intruders also lower the lowest amplitude required for the occurrence of BNE. The changes observed in effects of vibration conditions were found related to the initial location of large intruders. More specifically, under extreme vibration conditions, the intruders at higher layer can still rise and they can affect the neighbor intruders at the bottom layer, which will consequently trigger the overall segregation pattern.

The effects of particle number and particle shape have also been comprehensively studied. By changing the number of large intruders, it was found the effects of particle number is largely related to vibration conditions. For vibration conditions that can trigger the segregation in single intruder cases, the number of large intruders cannot largely affect the segregation behavior. But for vibration conditions that cannot trigger the segregation in single intruder cases, if they are sufficient for the occurrence of BNE in cases with multiple intruders, the

segregation gets stronger when number of large particles increases.

Considering the effects of particle shape, the exact effects vary from shape of large intruders and shape of bulk solids. The shape of large intruders can affect the small particles' percolation behavior and further influence the rising pattern of intruders. And it was concluded that intruders with less spherical shape can consequently result in stronger segregation. The shape of small particles can largely decide the overall packing states, and it was found the particle shape can affect the segregation by deciding the overall mean coordination number. Finally, it was concluded that smaller averaged coordination number can slower the rising velocity of large intruders.

Chapter 7 Conclusions and future work

7.1 Conclusions

This thesis focuses on the segregation phenomena occurs in piling process and vibrated systems. With the help of the ellipsoidal DEM model, a comprehensive study of the segregation process has been obtained from both microscopic and macroscopic views. In order to better interpret the observed granular behavior, various factors have been studied in association with the processing methods. And the detailed conclusions are divided into four parts and are listed below:

1) For piling process with binary mixtures of spherical particles, the stratification phenomenon occurs associated with segregation under certain conditions. It was found these two phenomena are cohesively triggered by a void-filling mechanism which can differentiate the moving patterns of small particles and large particles. The associated parameter studies were also conducted, and it was found that larger size ratio, lower injection height and comparably smaller R can induce stronger segregation. And friction coefficient including sliding coefficient and rolling coefficient were also found significant to the segregation intensity.

2) The stockpile segregation was further investigated considering the effects of particle shape. While the shape of the granular matters were changed to ellipsoids, the flowability of the surface flow gets worse and a “static avalanche” appears. This phenomenon illustrates that pre-piled ellipsoids tend to

maintain their positions instead of reconstructing the local pattern with upcoming particles. Based on this interpretation, it can be then demonstrated that worse flowability can induce weaker segregation, which also shows granular mixtures with less spherical shapes can weaken the segregation phenomenon. On the other hand, it was found that the segregation is still dominated by size effects while particle shape can affect the intensity of the size segregation.

3) The vibration-induced segregation was first studied with granular mixtures with only one large intruder. The vibration conditions were found dominant in the occurrence of the intruder's rising behavior, and a phase diagram was well constructed. Under fixed vibration, segregation only occurs within a special range of vibration frequency, and the critical points of the interval is related to vibration amplitude while larger vibration amplitude can extend the interval range. The effect of particle size was also investigated, and it was found that larger size ratio can induce stronger segregation, but the occurrence of segregation is still decided by vibration conditions. It was also found that the temporal evolution of averaged coordination number can be applied to illustrate the overall state of the vibration system. Moreover, the intruder shape was also studied and its effect was found largely related to the initial orientation.

4) The studies of vibration-induced segregation were upgraded to contain

multiple intruders instead of single intruder. The vibration conditions are still dominant to the occurrence of vertical segregation, while the introduction of more large intruders have extended the range of sufficient conditions needed for segregation to be observed. The effects of intruder number are also studied and it was concluded that more intruders can induce stronger segregation. Moreover, a comprehensive study on the particle shape has been made and it was found the particle shape can influence the segregation behavior by affecting the small particles percolation behavior.

7.2 Future work

Through the work presented in this thesis, several research gaps have been solved, but there are still problems remain unsolved. The future work may focus on the issues listed below:

1) For segregation issues in piling process, the current research only focuses on studies of binary or ternary mixtures, but the real industries majorly apply more complex mixtures. Therefore, it is of great significance to use granular mixtures which follows a size or shape distribution. This may largely increase the difficulty in reaching, but it can also provide a completely new view on the segregation issue.

2) The vibration-induced segregation has been well studied considering simple

harmonious vibrations, while the discrete vibration pattern may largely change the story. Other researchers have applied the discrete vibrations in their studies, but considering the work conducted in this thesis, the adoption of discrete vibration might offer a different understanding.

3) Most of the vibration-induced segregation studies have used binary granular mixture which regard the large particle as the intruder. However, if complex mixture with a distribution of particle size is adopted, the segregation pattern can be much more complicated as the local porosity properties can be more difficult the predict. As most industrial vibrated systems use complex mixtures instead of simple binary mixtures, it is of great significance to extend the study in this area.

4) The work conducted in this thesis only uses dry particles while many microscopic forces are not considered. By upgrading the particles to wet particles, the effects studied might be completely different and are of great significance to be further studied. And while the capillary forces still remain a big problem in DEM researches, it is of great need to better understand the effects of moisture content through numerical simulations.

5) In this thesis, the validation results from experiments remain in qualitative state, further physical experiments with more quantitative analysis might be conducted to better support the simulation results.

This page is intentionally blank

LIST OF REFERENCES

Abreu, C. R., F. W. Tavares and M. Castier (2003). "Influence of particle shape on the packing and on the segregation of spherocylinders via Monte Carlo simulations." Powder Technology **134**(1-2): 167-180.

Ahmad, K. and I. Smalley (1973). "Observation of particle segregation in vibrated granular systems." Powder Technology **8**(1-2): 69-75.

Ahmad, K. and I. J. Smalley (1973). "Observation of particle segregation in vibrated granular systems." Powder Technology **8**(1): 69-75.

Akiyama, T., M. Kimura, H. Tanimura and G. Yokoyama (2001). "Inverse density segregation of binary particle mixtures subjected to vertical tappings and vibration." Advanced Powder Technology **12**(1): 105-116.

An, X., R. Yang, K. Dong, R. Zou and A. Yu (2005). "Micromechanical simulation and analysis of one-dimensional vibratory sphere packing." Physical review letters **95**(20): 205502.

An, X., R. Yang, R. Zou and A. Yu (2008). "Effect of vibration condition and inter-particle frictions on the packing of uniform spheres." Powder Technology **188**(2): 102-109.

Arshad, K. (2004). "Size separation in vibrated granular matter." Reports on Progress in Physics **67**(3): 209.

Baxter, J., U. Tüzün, J. Burnell and D. M. Heyes (1997). "Granular dynamics

simulations of two-dimensional heap formation." Physical Review E **55**(3): 3546-3554.

Baxter, J., U. Tüzün, D. Heyes, I. Hayati and P. Fredlund (1998). "Stratification in poured granular heaps." Nature **391**(6663): 136-136.

Benito, J. G., I. Ippolito and A. M. Vidales (2013). "Novel aspects on the segregation in quasi 2D piles." Powder Technology **234**: 123-131.

Benito, J. G., R. O. Uñac, A. M. Vidales and I. Ippolito (2014). "Influence of geometry on stratification and segregation phenomena in bidimensional piles." Physica A: Statistical Mechanics and its Applications **396**: 19-28.

Benito, J. G., R. O. Uñac, A. M. Vidales and I. Ippolito (2015). Influence of geometry on stratification and segregation phenomena in bidimensional piles.

Boutreux, T. and P. De Gennes (1996). "Surface flows of granular mixtures: I. General principles and minimal model." Journal de Physique I **6**(10): 1295-1304.

Brone, D. and F. Muzzio (1997). "Size segregation in vibrated granular systems: A reversible process." Physical Review E **56**(1): 1059.

Brown, R. (1939). "The fundamental principles of segregation." The Institute of Fuel **13**: 15-23.

Chandratilleke, G., A. Yu, J. Bridgwater and K. Shinohara (2012). "A particle-scale index in the quantification of mixing of particles." AIChE Journal **58**(4): 1099-1118.

Cizeau, P., H. A. Makse and H. E. Stanley (1999). "Mechanisms of granular spontaneous stratification and segregation in two-dimensional silos." Physical Review E **59**(4): 4408-4421.

Cooke, W., S. Warr, J. Huntley and R. Ball (1996). "Particle size segregation in a two-dimensional bed undergoing vertical vibration." Physical Review E **53**(3): 2812.

Cundall, P. A. and O. D. Strack (1979). "A discrete numerical model for granular assemblies." Geotechnique **29**(1): 47-65.

De Silva, S. (1997). "Mixing and segregation in industrial processes." IFPRI Report SAR: 12-20.

de Silva, S. R., A. Dyrøy and G. G. Enstad (2000). Segregation Mechanisms and Their Quantification Using Segregation Testers, Dordrecht, Springer Netherlands.

Di Renzo, A. and F. P. Di Maio (2004). "Comparison of contact-force models for the simulation of collisions in DEM-based granular flow codes." Chemical Engineering Science **59**(3): 525-541.

Drahun, J. A. and J. Bridgwater (1983). "The mechanisms of free surface segregation." Powder Technology **36**(1): 39-53.

Fan, L., S. Chen and C. Watson (1970). "Annual review solids mixing." Industrial & Engineering Chemistry **62**(7): 53-69.

Fan, Y., Y. Boukerkour, T. Blanc, P. B. Umbanhowar, J. M. Ottino and R. M. Lueptow (2012). "Stratification, segregation, and mixing of granular materials in quasi-two-dimensional bounded heaps." Physical Review E **86**(5): 051305.

Fang, X. and J. Tang (2007). "A numerical study of the segregation phenomenon in granular motion." Journal of Vibration and Control **13**(5): 711-729.

Feng, Y. Q., B. H. Xu, S. J. Zhang, A. B. Yu and P. Zulli (2004). "Discrete particle simulation of gas fluidization of particle mixtures." AIChE Journal **50**(8): 1713-1728.

Fernando, D. and C. Wassgren (2003). "Effects of vibration method and wall boundaries on size segregation in granular beds." Physics of Fluids **15**(11): 3458-3467.

Grasselli, Y. and H. J. Herrmann (1998). "Experimental study of granular stratification." Granular Matter **1**(1): 43-47.

Gray, J. M. N. T. and C. Ancey (2009). "Segregation, recirculation and deposition of coarse particles near two-dimensional avalanche fronts." Journal of Fluid Mechanics **629**: 387-423.

Gray, J. M. N. T. and C. Ancey (2011). "Multi-component particle-size segregation in shallow granular avalanches." Journal of Fluid Mechanics **678**: 535-588.

Gray, J. M. N. T. and V. A. Chugunov (2006). "Particle-size segregation and diffusive remixing in shallow granular avalanches." Journal of Fluid Mechanics **569**:

365-398.

Gray, J. M. N. T. and K. Hutter (1997). "Pattern formation in granular avalanches." Continuum Mechanics and Thermodynamics **9**(6): 341-345.

Gray, J. M. N. T. and B. P. Kokelaar (2010). "Large particle segregation, transport and accumulation in granular free-surface flows." Journal of Fluid Mechanics **652**: 105-137.

Harnby, N. (2000). "An engineering view of pharmaceutical powder mixing." Pharmaceutical science & technology today **3**(9): 303-309.

Harris, J. F. and A. M. Hildon (1970). "Reducing segregation in binary powder mixtures with particular reference to oxygenated washing powders." Industrial & Engineering Chemistry Process Design and Development **9**(3): 363-367.

Harwood, C. F. (1977). "Powder segregation due to vibration." Powder Technology **16**(1): 51-57.

Hertz, H. (1882). "Über die Berührung fester elastischer Körper." Journal für die reine und angewandte Mathematik **92**: 156-171.

Hsiau, S.-S. and W.-C. Chen (2002). "Density effect of binary mixtures on the segregation process in a vertical shaker." Advanced Powder Technology **13**(3): 301-315.

Hsiau, S. S., P. C. Wang and C. H. Tai (2002). "Convection cells and segregation in

a vibrated granular bed." AIChE Journal **48**(7): 1430-1438.

Huerta, D. A. and J. C. Ruiz-Suárez (2004). "Vibration-Induced Granular Segregation: A Phenomenon Driven by Three Mechanisms." Physical Review Letters **92**(11): 114301.

Johanson, J. (1996). "Predicting segregation of bimodal particle mixtures using the flow properties of bulk solids." Pharmaceutical technology **20**(5): 46-57.

Jullien, R. and P. Meakin (1990). "A mechanism for particle size segregation in three dimensions." Nature **344**(6265): 425-427.

Knight, J. B., H. M. Jaeger and S. R. Nagel (1993). "Vibration-induced size separation in granular media: The convection connection." Physical review letters **70**(24): 3728.

Koeppe, J., M. Enz and J. Kakalios (1998). "Phase diagram for avalanche stratification of granular media." Physical Review E **58**(4): R4104.

Lacey, P. (1997). "The mixing of solid particles." Chemical Engineering Research and Design **75**: S49-S55.

Lacey, P. M. C. (1954). "Developments in the theory of particle mixing." Journal of applied chemistry **4**(5): 257-268.

Lan, Y. and A. D. Rosato (1997). "Convection related phenomena in granular dynamics simulations of vibrated beds." Physics of Fluids **9**(12): 3615-3624.

Langston, P., U. Tüzün and D. Heyes (1994). "Continuous potential discrete particle simulations of stress and velocity fields in hoppers: transition from fluid to granular flow." Chemical Engineering Science **49**(8): 1259-1275.

Lawrence, L. and J. K. Beddow (1969). "Powder segregation during die filling." Powder Technology **2**(5): 253-259.

Liao, C., M. Hunt, S. Hsiau and S. Lu (2014). "Investigation of the effect of a bumpy base on granular segregation and transport properties under vertical vibration." Physics of Fluids **26**(7): 073302.

Liffman, K., K. Muniandy, M. Rhodes, D. Gutteridge and G. Metcalfe (2001). "A segregation mechanism in a vertically shaken bed." Granular Matter **3**(4): 205-214.

Liffman, K., M. Nguyen, G. Metcalfe and P. Cleary (2001). "Forces in piles of granular material: an analytic and 3D DEM study." Granular Matter **3**(3): 165-176.

Liu, J., Q. Sun and F. Jin (2011). "The influence of flow rate on the decrease in pressure beneath a conical pile." Powder Technology **212**(1): 296-298.

Lumay, G., F. Boschini, R. Cloots and N. Vandewalle (2013). "Cascade of granular flows for characterizing segregation." Powder Technology **234**: 32-36.

Makse, H. A. (1997). "Stratification instability in granular flows." Physical Review E **56**(6): 7008.

Makse, H. A. (1998). "Kinematic Segregation of Flowing Grains in Sandpiles."

Makse, H. A., P. Cizeau and H. E. Stanley (1997). "Possible Stratification Mechanism in Granular Mixtures." Physical Review Letters **78**(17): 3298-3301.

Makse, H. A., P. Cizeau and H. E. Stanley (1998). "Modeling stratification in two-dimensional sandpiles." Physica A: Statistical Mechanics and its Applications **249**(1–4): 391-396.

Makse, H. A., S. Havlin, P. R. King and H. E. Stanley (1994). "Spontaneous stratification in granular mixtures." Science **265**: 1850-1852.

Makse, H. A. and H. J. Herrmann (1998). EPL (Europhysics Letters) **43**(1): 1.

Makse, H. A. and H. J. Herrmann (1998). "Microscopic model for granular stratification and segregation." EPL (Europhysics Letters) **43**(1): 1.

Meakin, P. (1990). "A simple two-dimensional model for particle segregation." Physica A: Statistical Mechanics and its Applications **163**(3): 733-746.

Meakin, P. and R. Jullien (1992). "Simple models for two and three dimensional particle size segregation." Physica A: Statistical Mechanics and its Applications **180**(1): 1-18.

Mindlin, R. D. and H. Deresiewica (2013). "Elastic spheres in contact under varying oblique forces." Journal of applied mechanics **20**.

Mosby, J. (1996). "Investigations of the segregation of particulate solids with emphasis on the use of segregation testers." Dr. Ing. Thesis, Telemark

College/Norwegian University of Science & Technology.

Mosby, J. (1996). "Investigations of the segregation of particulate solids with emphasis on the use of segregation testers." Dr. Ing. Thesis, Norwegian University of Science and Technology/Telemark University College.

Ottino, J. M. and D. V. Khakhar (2000). "Mixing and segregation of granular materials." Annual Review of Fluid Mechanics **32**: 55-91.

Perschin, V. (1990). The mixing and segregation of particulate solids of different particle size. International congress of chemical equipment and automatics,«CHISA-90», Praha, Czechoslovakia.

Pöschel, T. and H. J. Herrmann (1995). "Size segregation and convection." EPL (Europhysics Letters) **29**(2): 123.

Puri, V. M. (2004). "Methods for Minimizing Segregation: A Review AU - TANG, P." Particulate Science and Technology **22**(4): 321-337.

Rodríguez, D., J. G. Benito, I. Ippolito, J. P. Hulin, A. M. Vidales and R. O. Uñac (2015). "Dynamical effects in the segregation of granular mixtures in quasi 2D piles." Powder Technology **269**: 101-109.

Rosato, A., F. Prinz, K. J. Standburg and R. Swendsen (1986). "Monte Carlo simulation of particulate matter segregation." Powder Technology **49**(1): 59-69.

Rosato, A., K. J. Strandburg, F. Prinz and R. H. Swendsen (1987). "Why the Brazil

nuts are on top: Size segregation of particulate matter by shaking." Physical Review Letters **58**(10): 1038-1040.

Rosato, A. D., D. L. Blackmore, N. Zhang and Y. Lan (2002). "A perspective on vibration-induced size segregation of granular materials." Chemical Engineering Science **57**(2): 265-275.

Salter, G. F., R. J. Farnish, M. S. A. Bradley and A. J. Burnett (2000). "Segregation of binary mixtures of particles during the filling of a two-dimensional representation of a hopper." Proceedings of the Institution of Mechanical Engineers **214**(3): 197.

Savage, S. and C. Lun (1988). "Particle size segregation in inclined chute flow of dry cohesionless granular solids." Journal of Fluid Mechanics **189**: 311-335.

Schröter, M., S. Ulrich, J. Kreft, J. B. Swift and H. L. Swinney (2006). "Mechanisms in the size segregation of a binary granular mixture." Physical Review E **74**(1): 011307.

Shi, Q., G. Sun, M. Hou and K. Lu (2007). "Density-driven segregation in vertically vibrated binary granular mixtures." Physical Review E **75**(6): 061302.

Shimokawa, M., Y. Suetsugu, R. Hiroshige, T. Hirano and H. Sakaguchi (2015). "Pattern formation in a sandpile of ternary granular mixtures." Physical Review E **91**(6): 062205.

Shinohara, K. and B. Golman (2002). "Particle segregation of binary mixture in a moving bed by penetration model." Chemical Engineering Science **57**(2): 277-285.

Sleppy, J. A. and V. Puri (1996). "Size-segregation of granulated sugar during flow." Transactions of the ASAE **39**(4): 1433-1439.

Smith, L., J. Baxter, U. Tüzün and D. M. Heyes (2001). "Granular Dynamics Simulations of Heap Formation: Effects of Feed Rate on Segregation Patterns in Binary Granular Heap." Journal of Engineering Mechanics **127**(10): 1000-1006.

Smith, W., P. D. Foote and P. Busang (1931). "Capillary rise in sands of uniform spherical grains." Physics **1**(1): 18-26.

Sommier, N., P. Porion, P. Evesque, B. Leclerc, P. Tchoreloff and G. Couarraze (2001). "Magnetic resonance imaging investigation of the mixing-segregation process in a pharmaceutical blender." International journal of pharmaceutics **222**(2): 243-258.

Tai, C. H., S. S. Hsiau and C. A. Kruelle (2010). "Density segregation in a vertically vibrated granular bed." Powder Technology **204**(2): 255-262.

Tang, P., V. Puri and P. Patterson (2003). Size segregation analysis of poultry mash feed. 2003 ASAE Annual Meeting, American Society of Agricultural and Biological Engineers.

Tang, P. and V. M. Puri (2004). "Methods for Minimizing Segregation: A Review." Particulate Science and Technology **22**(4): 321-337.

Thornton, C. (1997). "Coefficient of restitution for collinear collisions of elastic-

perfectly plastic spheres." Journal of Applied Mechanics **64**(2): 383-386.

Thornton, C. and K. Yin (1991). "Impact of elastic spheres with and without adhesion." Powder technology **65**(1-3): 153-166.

Tsuji, Y., T. Tanaka and T. Ishida (1992). "Lagrangian numerical simulation of plug flow of cohesionless particles in a horizontal pipe." Powder technology **71**(3): 239-250.

Urbanc, B. and L. Cruz (1997). "Order parameter and segregated phases in a sandpile model with two particle sizes." Physical Review E **56**(2): 1571-1579.

Vallance, J. W. and S. B. Savage (2000). Particle segregation in granular flows down chutes. IUTAM Symposium on Segregation in Granular flows, Springer.

Vandewalle, N. (1999). "Phase segregation and avalanches in multispecies sandpiles." Physica A: Statistical Mechanics and its Applications **272**(3–4): 450-458.

Vu-Quoc, L. and X. Zhang (1999). An elastoplastic contact force–displacement model in the normal direction: displacement–driven version. Proceedings of the Royal Society of London A: Mathematical, Physical and Engineering Sciences, The Royal Society.

Walton, O. R. (1993). "Numerical simulation of inclined chute flows of monodisperse, inelastic, frictional spheres." Mechanics of materials **16**(1-2): 239-247.

Walton, O. R. and R. L. Braun (1986). "Viscosity, granular-temperature, and stress calculations for shearing assemblies of inelastic, frictional disks." Journal of Rheology **30**(5): 949-980.

Williams, J. (1963). "The segregation of powders and granular materials." Fuel Soc. J **14**: 29-34.

Williams, J. C. (1968). "The mixing of dry powders." Powder Technology **2**(1): 13-20.

Williams, J. C. (1976). "The segregation of particulate materials. A review." Powder Technology **15**(2): 245-251.

Williams, J. C. and G. Shields (1967). "The segregation of granules in a vibrated bed." Powder Technology **1**(3): 134-142.

Yan, X., Q. Shi, M. Hou, K. Lu and C. Chan (2003). "Effects of air on the segregation of particles in a shaken granular bed." Physical review letters **91**(1): 014302.

Yang, S. (2006). "Density effect on mixing and segregation processes in a vibrated binary granular mixture." Powder Technology **164**(2): 65-74.

Yi, H., B. Mittal, V. Puri, F. Li and C. Mancino (2001). "Measurement of bulk mechanical properties and modeling the load-response of rootzone sands. Part 1: Round and angular monosize and binary mixtures." Particulate science and technology **19**(2): 145-173.

Yu, A. B., R. P. Zou and N. Standish (1992). "Packing of ternary mixtures of nonspherical particles." Journal of the American Ceramic Society **75**(10): 2765-2772.

Yu, Y., J. Zhang, J. Zhang and H. Saxén (2018). "DEM and experimental studies on pellet segregation in stockpile build-up." Ironmaking & Steelmaking **45**(3): 264-271.

Zhou, Y. C., B. D. Wright, R. Y. Yang, B. H. Xu and A. B. Yu (1999). "Rolling friction in the dynamic simulation of sandpile formation." Physica A: Statistical Mechanics and its Applications **269**(2–4): 536-553.

Zhou, Z. Y., R. P. Zou, D. Pinson and A. B. Yu (2014). "Angle of repose and stress distribution of sandpiles formed with ellipsoidal particles." Granular Matter **16**(5): 695-709.

Zhu, H. P., Z. Y. Zhou, R. Y. Yang and A. B. Yu (2007). "Discrete particle simulation of particulate systems: Theoretical developments." Chemical Engineering Science **62**(13): 3378-3396.

Zhu, J., Y. Liang and Y. Zhou (2013). "The effect of the particle aspect ratio on the pressure at the bottom of sandpiles." Powder Technology **234**: 37-45.

Zou, R. and A. Yu (2003). "Porosity calculation of mixtures of fibrous particles." China particuology **1**(1): 27-32.

Zuriguel, I. and T. Mullin (2008). "The role of particle shape on the stress distribution in a sandpile." Proceedings of the Royal Society of London A: Mathematical, Physical and Engineering Sciences **464**(2089): 99-116.